International Energy Agency

IEA District Heating and Cooling

Programme of Research, Development and Demonstration on District Heating and Cooling

Optimisation of Operating Temperatures and an Appraisal of the Benefits of Low Temperature District Heating

Published by

Netherlands agency for energy and the environment

Novem

Acting as operating agent for the IEA District Heating and Cooling project

1999: T1

International Energy Agency

IEA District Heating and Cooling

Programme of Research, Development and Demonstration on District Heating and Cooling

The Optimisation of District Heating Operating Temperatures and an Appraisal of the Benefits of Low Temperature District Heating

Paul Woods, Rebecca Gunning,
Chris Snoek, Tom Onno, Libing Yang,
Markku Ahonen,
Robin Wiltshire

Merz Orchard Ltd - 4 Roger St, London, WC1N 2JX, UK
CANMET - 555 rue Booth Street, Ottawa, K1A 0G1, CANADA
VTT - Lämpömiehenkuja 3 Espoo, PO Box 1804, FIN 02044 VTT, FINLAND
BRECSU, Building Research Establishment, Garston, Watford, WD2 7JR, UK

Preface

The IEA was established in 1974 within the framework of the OECD to implement an International Energy Programme. One of the main aims of the IEA is to foster co-operation among the 21 IEA participating countries to increase energy security through energy conservation, development of alternative energy sources and energy research, development and demonstration (RD&D).

As an element of the International Energy Programme, the participating countries undertake co-operative activities in energy RD&D.

District heating is seen by the IEA as a means by which countries may reduce their dependence on oil and improve their energy efficiency. It involves the increased use of indigenous or abundant fuels, the utilisation of waste energy and combined heat and power production.

IEA's programme of Research, Development and Demonstration on district heating was established in 1983 at a meeting in Stockholm. In the first phase (Annex I) 10 countries took part in the programme: Belgium, Canada, Denmark, Germany, Finland, Italy, The Netherlands, Norway, Sweden and the USA. Later, Annexes II, III and IV were prepared.

This project has been carried out under Annex V and 9 countries have participated: Canada, Denmark, Finland, Germany, Republic of Korea, The Netherlands, Norway, Sweden and the United Kingdom.

Annex V comprises the following technical areas:

Cost effective district heating networks
Optimal operation, operational availability and maintenance in district heating systems
Optimisation of district heating operating temperatures and an appraisal of the benefits of low temperature district heating
District heating and cooling in future buildings
Combined heating and cooling, balancing the production and demand in CHP
Fatigue analysis of district heating systems
Handbook on plastic pipe systems

NOVEM, the Netherlands Agency for Energy and the Environment, has been acting as the Operating Agent for Annex V.

General information on the IEA District Heating Project may be obtained from:

IEA Sectretariat
Mr Mel Kliman
9 Rue de la Federation
F-75775 Paris Cedex 15
France

Tel: +33-1-40576785
Fax: +33-1-40576759

or

Novem, Netherlands Agency for Energy and the Environment
Mr Frank van Bussel
P O Box 17
NL-6130 AA Sittard
The Netherlands

Tel: +33-46-4202202
Fax: +33-46-4528260

The study team for this project comprised four organisations:

Merz Orchard Ltd, 4, Roger St, London WC1N 2JX, UK, +44-171-242-1980, contact Paul Woods
CANMET, 1, Haanel Drive, Ottawa, Ontario, Canada, +1-613-992-1832, contact Chris Snoek
VTT, Lämpömiehenkuja 3 Espoo, PO Box 1804, FIN 02044 VTT, FINLAND, +358 0 456 4724
BRECSU, Building Research Establishment, Garston, Watford, WD2 7JR, UK, +44-1923-664534 contact Robin Wiltshire

Acknowledgements

The work carried out for this project has been monitored by an Experts Group and the authors would like to thank all the members for their very valuable guidance and advice. The members of the Experts Group were:

Arnold Sijben - NOVEM - The Netherlands
Svend Frederiksen - Technical University of Lund - Sweden
Rune Volla - Energi Konsult - Norway
Jacob Stang - University of Trondheim - Norway
Nick Andersen - DTI Energy - Denmark

We would also like to thank many other colleagues in the CHP and District Heating industry who have given freely of their advice.

Summary

One of the most fundamental decisions to be made by a designer of a new district heating system is the selection of design operating temperatures. Lower operating temperatures will reduce the cost of heat production from CHP plant but to achieve lower temperatures requires additional investment in the heating systems within the buildings. The cost of the district heating network is reduced if the temperature difference between flow and return is maximised. There is therefore a need to establish the optimum design temperatures to achieve the most cost-effective scheme.

In order to identify the optimum design temperatures, a series of case studies based on notional groups of buildings were developed and comparative economic analyses produced. The case studies comprised combinations of:

- three types of built form: apartment blocks, row houses and commercial buildings;
- two sample climates : London and Toronto;
- three types of CHP plant: extraction-condensing steam turbine, back pressure combined cycle gas turbine and spark-ignition gas-engine.

The analysis of the heating systems within the buildings was carried out by CANMET who developed simulation models using the Simulink software. This enabled hour by hour heat demands, district heating flow rate and return temperatures to be calculated for each case. These heat demand patterns were then used as the basis for the spreadsheet models developed by Merz Orchard to simulate the operation of a CHP plant over the year and hence calculate the cost of heat production. Designs for the district heating network were produced using System RORNET by Merz Orchard and the capital cost was estimated. Finally, costs were obtained from manufacturers for district heating substations, radiators and air heating coils required within the buildings. All of these cost elements were calculated for a range of design operating temperatures, from 90°C to 70°C flow and from 55°C to 30°C return.

The results are presented in a series of graphs for each case study analysed showing the cost of heat against the design temperature difference for different flow temperatures. It was found that, for all cases, it was not worthwhile to reduce the design flow temperature below 90°C as this leads either to a smaller temperature difference and therefore higher network costs or, if the temperature difference is maintained, additional costs for larger radiators. Both of these cost penalties are more significant than the small reduction in heat production cost obtained with using lower flow temperatures.

For a peak flow temperature of 90°C the optimum temperature difference was found to be about 35°C (55°C return temperature) in all cases, although the cost curves are relatively flat and a variation in return temperature of +/- 10°C about the optimum resulted in a cost variation of less than 3%.

There are many other potential benefits from using lower temperatures, in particular the ability of the district heating network to utilise low grade heat sources available from industry, solar heat and heat pumps. The cost penalty from selecting a 70°C temperature instead of 90°C was found to result in an overall increase in the cost of heat of between 4% and 6% of a typical heat selling price. It is possible that, in some circumstances, this relatively small increase is justifiable given the potential environmental benefits in the longer term of maximising the use of waste heat and renewable energy by means of district heating. However, in many cases, the low grade heat sources will contribute only part of the energy supply and will effectively pre-heat the return water. A reduction of return water temperatures will therefore be the more important requirement.

Table of Contents

Preface

Acknowledgements

Summary

1 Introduction 1
2 General Approach and Definition of Case Studies 3
2.1 The buildings and their heating systems 3
2.1.1 Size and layout 3
2.1.2 Heat demand profile 4
2.1.3 Type of heating system 4
2.1.4 Types of building connection 5
2.2 The District Heating Network 5
2.2.1 Spacing of Buildings 5
2.2.2 Types of pipe system 5
2.2.3 Ground Condition 6
2.3 The Heat Supply Plant 6
2.3.1 Plant Options 6
2.3.2 Steam Turbine CHP 7
2.3.3 Spark-Ignition gas-engine CHP 7
2.3.4 Combined Cycle CHP 7
2.4 Combinations for analysis 7
2.5 Economic Analysis 8
3 Climatic Data 10
4 Description of Building Models 13
4.1 Introduction 13
4.2 Specifications of Building Types 14
4.2.1 General Approach 14
4.2.2 Apartment building 15
4.2.3 Commercial Building 19
4.2.4 Directly and indirectly connected 2-stage heating systems in the apartment building 19
4.2.5 Directly and indirectly connected parallel heating systems in the row-house 21
4.2.6 Directly and indirectly connected heating systems in the commercial building 23
4.2.7 Assumptions Applied in the Building Heating System Simulations 24
4.3 Results of the building heating system simulations 26
4.4 Capital cost of building heating system 33
4.4.1 Cost Elements 33
4.4.2 Radiators 33
4.4.3 Air-coils 34
4.4.4 Capital cost of domestic water heating systems 34
4.4.5 Capital cost of building connections 34
4.5 Operating costs of building heating systems 35
5 The Network Models 36
5.1 District Heating Network Costs 36
5.2 The Apartment Blocks Model 37
5.3 The Row Houses Model 39
5.4 The Commercial Building Model 41
5.5 Direct and Indirect Connections 43
6 The Heat Production Models 45
6.1 General Description 45
6.1.1 Typical Operating Days 45
6.1.2 Input to the Model 46
6.1.3 Other assumptions 46

6.1.4 Outputs from the model 47
6.2 Heat Production Model with Spark-Ignition Gas-Engine CHP 48
6.2.1 Capital Cost 48
6.2.2 CHP Performance 48
6.3 Extraction-Condensing Steam Turbine CHP Plant 49
6.3.1 Capital Cost 49
6.3.2 CHP Performance 49
6.4 Combined Cycle Gas Turbine Plant 50
6.4.1 Capital Cost 50
6.4.2 CHP Performance 51
6.5 Summary of the influence of DH operating temperatures on heat production costs 51
7 Apartment Block Case Studies Results 52
7.1 Presentation of the results 52
7.2 Spark-Ignition Gas-Engine CHP Cases 52
7.3 Steam Turbine CHP Cases 55
7.4 Combined Cycle CHP Cases 57
8 Row-house Case Studies Results 59
8.1 Spark-Ignition Gas-Engine CHP Cases 59
8.2 Steam Turbine CHP Cases 60
8.3 Combined Cycle CHP Cases 61
9 Downtown Area Case Studies Results 62
9.1 Spark-Ignition Gas-Engine CHP Cases 62
9.2 Steam Turbine CHP Cases 63
9.3 Combined Cycle CHP Cases 64
10 Interpretation of Results 65
10.1 General 65
10.2 The Apartment Blocks Model 65
10.3 Row Houses Model 66
10.4 Commercial Buildings Model 66
10.5 The influence of climate on the optimum operating temperatures 66
10.6 The influence of the heat density of the buildings supplied on the optimum operating temperatures 66
10.7 The benefits of reducing operating temperatures in relation to external air temperature 67
10.8 The differences between indirect and direct connection 67
11 Discussion 68
11.1 Practical Cases and Existing Schemes 68
11.2 General Observations 68
11.3 Implications of alternative sources of heat 69
11.4 Environmental benefits of lower operating temperatures 69
11.5 The use of 120°C flow temeperatures 70
12 Sensitivity Analysis 71
12.1 Sensitivity to Economic Parameters 71
12.2 Sensitivity to boiler efficiency 71
12.3 Sensitivity to electricity prices 72
12.4 Sensitivity to Heat Density 72
13 Conclusions 74
14 References 76

List of Tables

Table 2.1 Types of Built Form 3
Table 2.2 - Case Studies Analysed 8
Table 2.3 - Comparison of financing assumptions 9
Table 3.1 - Comparison of climates for capital cities 10
Table 4.1 Specification of building, heating system, connections, climate and supply temperature levels. 14
Table 4.2 Variables used in building simulations. 15
Table 4.3 Peak heat losses and heat loss factors at design conditions. 15
Table 4.4 - Energy use predictions from Simulink models 27
Table 4.5 - Cost of installed radiator capacity (US$/kW) 33
Table 4.6 - Cost of air heating coils (US$ /kW) based on a 150kW coil 34
Table 4.7 - Cost of indirect connection substations US$/kW (heating and hot water) 34
Table 5.1 - Characteristics of apartment block network 37
Table 5.2 - Characteristics of rowhouses network 39
Table 5.3 - Characteristics of commercial building network 41
Table 6.1 Definition of Typical Days 45
Table 6.2 Heat Output in kW from Wartsila W16V25SG 48
Table 6.3 Heat Output expressed as a ratio to the heat output at 90°C flow, 50°C return 48
Table 6.4 Heat Production Model – Spark-Ignition Engine HCP – Assumptions 49
Table 6.5 z-factor calculated for a range of operating temperatures 50
Table 6.6 Lost electricity expressed as a ratio to the electricity lost at 90°C flow, 50°C return (Winkens formula) 50
Table 6.7 Heat Production Model – Combined Cycle CHP (<100MW) – Assumptions 51
Table 12.1 Variation in boiler efficiency with DH return temperatures 72

List of Figures

Figure 3.1 - Average Daily Temperatures in London 11
Figure 3.2 – Average solar radiation in London 11
Figure 3.3 – Comparison of average temperatures in Helsinki and Toronto 12
Figure 3.4 – Comparison of average solar radiation in Helsinki and Toronto 12
Figure 4.1 Layout and outside wall of one apartment unit 16
Figure 4.2 Domestic hot water consumption (including diversification) for one apartment. 17
Figure 4.3 First and second floor layout of a row-house 18
Figure 4.4 Domestic hot water consumption for one row-house. 19
Figure 4.5 Diagram of a directly connected heating system for the apartment building. 20
Figure 4.6 Diagram of an indirectly connected heating system for the apartment building. 21
Figure 4.7 Diagram of a directly connected heating system for the row-house 22
Figure 4.8 Diagram of an indirectly connected parallel heating system for the row house 22
Figure 4.9 Diagram of a directly connected heating system for the commercial building. 23
Figure 4.10 Diagram of an indirectly connected heating system for the commercial building. 24
Figure 4.11 - Variation of DH supply temperature with outside air temperature for London 25
Figure 4.12 - Variation of DH supply temperature with outside air temperature for Toronto 26
Figure 4.13 - Results for apartment blocks in London - winter - direct connection 28
Figure 4.14 - Results for apartment blocks in London - summer - direct connection 28
Figure 4.15 - Results for apartment blocks in Toronto - winter - direct connection 29
Figure 4.16 - Results for apartment blocks in Toronto - summer - direct connection 29
Figure 4.17 - Results for row houses in London - winter - direct connection 30
Figure 4.18 - Results for row houses in London - summer - direct connection 30
Figure 4.19 - Results for row houses in Toronto - winter - direct connection 31
Figure 4.20 - Results for row houses in Toronto - summer - direct connection 31
Figure 4.21- Results for the winter 3 months for apartment buildings in London 32
Figure 4.22 - Results for the winter three months for apartment buildings in Toronto 32
Figure 5.1 - Optimisation of Pipe Sizes in the Apartment Block Network (London) 36

Figure 5.2 - Average of Installed Costs of District Heating Pipes from UK Canada Sweden and Germany 37
Figure 5.3 - The apartment block network 38
Figure 5.4 Cost of District Heating Networks – Apartments 39
Figure 5.5 - The rowhouses network 40
Figure 5.6: Cost of District Heating Networks - Rowhouses 41
Figure 5.7 - The commercial building network 42
Figure 5.8 - Cost of District Heating Networks - Commercial 43
Figure 6.1 Typical variation in electricity prices form UK Pool Prices 46
Figure 6.2 Example of heat production model output for an Autumn day for a Spark-Ignition gas-engine CHP plant and a thermal store 47
Figure 7.1- Spark-Ignition Gas-Engine CHP - Apartment Blocks in London - Direct Connection 53
Figure 7.2- Spark-Ignition Gas-Engine CHP - Apartment Blocks in Toronto - Direct Connection 53
Figure 7.3- Spark-Ignition Gas-Engine CHP - Apartment Blocks in London - Indirect Connection 54
Figure 7.4- Spark-Ignition Gas-Engine CHP - Apartment Blocks in Toronto - Indirect Connection 54
Figure 7.5- Steam Turbine CHP - Apartments in London - Direct Connection 55
Figure 7.6 - Steam Turbine CHP - Apartment blocks in Toronto - Direct connection 55
Figure 7.7 Steam Turbine CHP - Apartment blocks in London -indirect connection 56
Figure 7.8 Steam Turbine CHP - Apartment blocks in Toronto - indirect connection 56
Figure 7.9- Combined Cycle CHP - Apartment Blocks in London - Direct Connection 57
Figure 7.10- Combined Cycle CHP - Apartment Blocks in Toronto - Direct Connection 57
Figure 7.11- Combined Cycle CHP - Apartment Blocks in London - Indirect Connection 58
Figure 7.12- Combined Cycle CHP - Apartment Blocks in Toronto - Indirect Connection 58
Figure 8.1: Spark Ignition Gas-engine CHP - Row houses in London 59
Figure 8.2: Spark Ignition Gas-engine CHP - Row houses in Toronto 59
Figure 8.3: Steam Turbine CHP - Row houses in London 60
Figure 8.4: Steam Turbine CHP - Row houses in Toronto 60
Figure 8.5- Combined Cycle CHP - Row houses in London 61
Figure 9.1- Spark-Ignition Gas-Engine CHP - Commercial Buildings in London 62
Figure 9.2- Spark-Ignition Gas-Engine CHP - Commercial Buildings in Toronto 62
Figure 9.3- Steam Turbine CHP - Commercial Buildings in London 63
Figure 9.4- Steam Turbine CHP - Commercial Buildings in Toronto 63
Figure 9.5- Combined Cycle CHP - Commercial Buildings in London 64
Figure 9.6- Combined Cycle CHP - Commercial Buildings in Toronto 64
Figure 12.1 Economic Sensitivity of Steam Turbine CHP – Apartment Blocks in London 71
Figure 12.2 Boiler efficiency sensitivity on Steam Turbine CHP – London Apartment Blocks 72
Figure 12.3 Heat Density sensitivity on Steam Turbine CHP – London Apartment Blocks 73

Annex A - The Use of Simulink for Building Heating Simulations

1 Introduction

One of the first decisions that a designer of a district heating system needs to make is the flow and return design temperatures. These will determine:

- the flow rates in the pipe network and hence the pipe sizes
- the design of the central plant and in some cases the type of Combined Heat and Power (CHP) plant
- the selection and sizing of the heating equipment within the buildings

The temperatures to be decided are not only a maximum flow and return temperature but also: the temperatures of primary, secondary and perhaps tertiary systems, different return temperatures for different types of heating application and the variation of temperature with external weather conditions.

Once the temperatures have been determined a second important aspect is the type of building connection. If temperatures are below 90°C then a direct connection to smaller buildings may be used to avoid the need for heat exchangers, provided the pressures in the network are compatible with the design of the building's heating system.

In many countries, particularly Scandinavia and Eastern and Central Europe there are large well established district heating schemes and the designer will have limited scope for selecting temperatures in any extension to the scheme. Even where district heating has not been established a new scheme will probably be connecting existing buildings and the operating temperatures which are already used by the building heating system will be a major constraint. The context of this research is the situation facing designers of new district heating systems perhaps in countries where the technology is not so well established with the aim of providing guidance on the most economic temperatures to select and where new heating equipment is to be installed within the buildings. It is commonly the case that in countries where district heating does not have a large market share the economic case for CHP/DH is marginal and there is no strong government policy for its implementation. Consequently, the improvement of the economics of CHP/DH is of major concern and the optimisation of operating temperatures is one element for ensuring the economic returns from investment in CHP/DH are maximised.

The Range of CHP/DH Projects

There is a very wide range of possible district heating developments but each will consist of three main components: the buildings to be supplied and their heating systems, the heat distribution system and the heat production plant. Within these components there are significant variations:

- The buildings to be supplied:

  -size of each building and total size of scheme
  -heat demand profile, over 24 hours and over a year
  -type of heating system, whether existing or new
  -type of connection to the district heating system

- The DH network layout:

  -spacing of buildings, linear heat density
  -type of pipe system
  -ground conditions

- The heat supply plant:

  -boilers, conventional or condensing
  -waste-fired boilers
  -open cycle gas-turbine

-combined cycle gas-turbine
-steam turbine back-pressure
-steam turbine extraction- condensing
-compression-ignition reciprocating engine
-spark-ignition gas-engine
-heat pumps
-solar
-geothermal

When the number of possible combinations of these factors are considered there is clearly scope for enormous variation and all of these factors will have a bearing on the selection of optimum temperatures. Consequently in order to limit the scope of the research project to affordable and manageable proportions it was necessary to draw up a list of the particular combinations to be analysed as a series of design case studies. The following section discusses each of the above components and defines the case studies which were agreed with the Experts Group.

2 General Approach and Definition of Case Studies

2.1 The buildings and their heating systems

2.1.1 Size and layout

The size of each building is the major factor in determining the relative importance of the connection cost to the district heating system. Small buildings are relatively expensive to connect particularly using an indirect connection method. At the connection point there will be a control interface to provide for flow limitation, differential pressure control, secondary side temperature control if indirect connection, metering if installed and perhaps central time control.

The nature of buildings varies between urban, suburban and rural areas and styles and the thermal quality of buildings vary considerably between countries. A useful categorisation is provided in (IEA 1996: N3) which defines 11 different types of built form:

Table 2.1 Types of Built Form

Type	Description
1	patchwork, rural isolated buildings
2	detached residential in suburban areas
3	village centre in rural areas
4	row houses in suburban areas
5	apartment buildings 3-5 storeys
6	high rise buildings peripheral to urban areas
7	urban development close to downtown/city centres
8	downtown/city centre high density from turn of century
9	historic town centre
10	large complexes e.g. hospital, university
11	industrial and warehouse buildings

The report concludes that types 6, 7 and 8 are most suited to district heating. Types 1 to 4 are normally uneconomic because of the low heat density. Type 9, the historic city centre, may also be uneconomic because of the difficulty of installing heat mains. Type 10 can be considered as a special case and may well be suited for a small-scale CHP plant sized for the particular building or group of buildings. The report makes the point that an economic analysis is required in most cases as it is difficult to immediately judge the viability of a scheme simply by examining its type using the above system.

The most useful categories to examine in this research are therefore:

Type 6 - high rise and medium rise apartment buildings peripheral to urban areas e.g. satellite towns
Type 7 - urban development, multi-family dwellings on a regular grid layout of streets
Type 8 - downtown/city centre areas high density, assumed to be mix of commercial and retail with some residential apartment blocks
Type 11 - industrial and warehouse buildings

For this research project we have taken Types 6 and 7 and a high density development which assumes a number of commercial buildings each with a mix of office space and industrial production space i.e. elements of Types 8 and 11. Clearly the last category could involve a wide variety of buildings and it is difficult to make a representative selection.

The district heating schemes could have a large range in total size, from a peak demand of say 5 MW to 500 MW. Large cities may have networks in excess of this size but we would expect the optimisation of these very large schemes to be similar to multiples of a smaller unit size.

2.1.2 Heat demand profile

The heat demand profile will depend on a number of factors:

- space heating will depend on the local climate, the building fabric and the times the building is occupied
- hot water heating will depend on use patterns and type of water using appliances
- process heating will depend on the business concerned, patterns of working etc.
- the demand profiles will also be influenced by the mechanism for charging for heat, the structure of the heat sales tariff, the level of customer control installed and individual customer choice.

The most important influence is the climate and it was decided to examine two different climatic types, a continental climate such as found in Central Europe and North America, and a western maritime climate such as found in Western Europe.

2.1.3 Type of heating system

Space heating

The most common heating system in the housing sector is steel panel radiators although underfloor heating systems are popular in some countries (particularly Germany) and in Canada air heating is normally used. In commercial buildings a wide range of systems may be employed, typically perimeter radiators or fan-coil units together with heating of a central fresh air supply by means of a finned heating coil in an air-handling unit.

This research project has assumed that steel panel radiators will be used for the housing sector and a mixed system with perimeter radiators and an air heating system for the commercial buildings.

Water heating

There are a number of different types of system available:

1. Storage calorifiers at point of use
2. Storage calorifiers centrally
3. Instantaneous heat exchangers at point of use
4. Instantaneous heat exchangers centrally
5. Combination of instantaneous heat exchangers and storage with the storage capacity on the primary circuit
6. Combination of instantaneous heat exchangers and storage with the storage capacity on the secondary circuit

The point of use systems predominate in linear housing, but central systems are more likely to be used in larger commercial buildings and possibly also in apartment blocks. After discussion within the Experts Group the following selection was made for the analysis:

- Apartment blocks would have a centralised hot water system using a two-stage heat exchanger system as described in detail in section 4 below. This system was also analysed in IEA, 1996 N5.
- Individual houses would have instantaneous heat exchangers connected in parallel with the space heating radiator circuit.
- Commercial buildings are assumed to have a very small hot water demand which can be ignored

An important aspect of the use of district heating to provide domestic hot water is the need to maintain a minimum flow temperature of 70 °C to enable stored domestic hot water to be maintained at 60°C to avoid the growth of the legionella bacterium (IEA, 1996 N5).

2.1.4 Types of building connection

There are three methods of connecting a building heating system to a district heating network, depending on the compatibility of temperatures and pressures of the network and the building heating system:

- Direct connection when both temperatures and pressures are compatible
- Mixing connection when pressures are compatible but temperatures are not
- Indirect connection when the pressures are not compatible

We can assume that temperature compatibility is obtained if the network temperature is less than 90°C. Pressure compatibility depends on the equipment installed but most building systems would be designed to at least a 6 bar limit and possibly 10 bar. Although total pressures can be reduced by means of distributed pumping stations, for larger systems and where there is significant variation in ground levels and building height across the scheme a primary network operating at up to 16 bar is often needed. This means that indirect connection of buildings is required or there needs to be local heat exchanger substations supplying smaller secondary networks which are directly connected to the buildings.

2.2 The District Heating Network

2.2.1 Spacing of Buildings

The greatest influence on network cost is the density of buildings. This may be expressed as a 'linear heat demand density' i.e. the kW peak diversified heat demand per metre of trench length with the trench distance assumed to be up to the building entry point. Typical figures for linear heat density are:

High density housing in apartment blocks in the UK : 5.3 kW/m
Low density suburban housing in the UK : 0.8 kW/m
Helsinki District Heating System (central area) : 2.0 kW/m
Helsinki District Heating System (suburban area) : 1.5 kW/m

After discussion with the Experts Group it was agreed to use a linear heat density of 3.5 kW/m for the western maritime climate and apartment blocks model and 1.5 kW/m for the western maritime climate and the row houses model. A decision was also needed as to whether the heat density should be kept constant for the continental climate which generally will mean moving the buildings further apart or whether the building density should be kept constant so that with the harsher climate the linear density increases. It was decided that the built form density is more likely to be a constant between the various IEA countries than artificially attempting to keep the same heat density.

2.2.2 Types of pipe system

A determining factor on cost is the type of pipe system. There are three main categories:

- Ducted, mineral-fibre insulation
- Pre-insulated steel to EN253
- Pre-insulated cross-linked polyethylene (PEX) or polybutylene (PB)

These each have temperature limits for a 30 year design life: ducted mains are suitable for any practical district heating temperature, pre-insulated steel is suitable up to 130°C and pre-insulated PEX or PB is limited to a 90°C constant temperature at 6 bar.

Although there is still a case in some applications for ducted mains and some cost benefits can be realised with the all-plastic systems the majority of pipe systems installed now are of the pre-insulated steel EN253 type. With this type of system the cost will be determined mainly by the pipe diameter, although a small additional cost associated with expansion provision will occur as the operating temperatures increase. For maximum design temperatures less than 90 °C the savings associated with expansion provision are negligible as a cold laying technique or single action compensators are viable techniques and comprise only a small element of the total cost. It is possible that if lower temperatures are used then the thickness of insulation could be reduced. The use of a smaller casing size, less insulation and a correspondingly narrower trench is estimated to reduce the total network cost by 2.5% (Ramboll, 1998). This was considered negligible in the context of this study however, in absolute terms it is still an appreciable potential cost saving and one that could be investigated by designers of low temperature systems. It would also be possible to consider reducing further the insulation on the return pipeline or even omitting the insulation completely although with steel systems a form of protection to prevent external corrosion would still be needed.

When considering the potential costs and benefits of using temperatures above 90 °C the potential advantages of PEX or PB pipes would be lost and the costs associated with provision for expansion will increase. These factors may influence the overall network cost and should be taken into account in a temperature optimisation where temperatures above 90°C are being considered. For the purposes of this research however the pre-insulated steel system has been assumed throughout as we have concentrated on temperatures below 90 °C and in this operating region there are no major step changes in cost associated with technological choices.

2.2.3 Ground Condition

Assuming the pre-insulated system to be directly buried in the ground there will be further cost variations depending on the nature of the ground surface and the complexity of other buried services. In most cases the district heating mains will be installed under roads or footpaths however and it is this type of ground that has been assumed throughout the study.

2.3 The Heat Supply Plant

2.3.1 Plant Options

The range of heat supply plants listed in section 1 above is large and can of course be at many different sizes. The geothermal and solar supply plants are considered too specialised to be considered in this project. Geothermal heat may be limited in temperature although heat pumps may be used to upgrade it. Solar heating is likely to have a varying temperature available over a year and at times is a relatively low temperature heat source. Of the remaining plant options there are two broad categories: those where the cost of heat is strongly dependent on the temperature at which the heat is required and those where the cost of heat is only slightly influenced by temperature:

Plant where cost of heat is strongly influenced by temperatures:

Steam turbine CHP whether extraction/condensing or back-pressure
Combined Cycle CHP
Heat pumps

Plant where cost of heat is slightly influenced by temperature:

Reciprocating engine CHP (assuming return temperatures are low enough for heat recovery from jacket cooling circuit)
Condensing boilers and non-condensing boilers.
Gas-turbine single cycle CHP
Waste-fired boilers

In most CHP/DH schemes the CHP plant only supplies part of the load with peak and standby plant consisting of boilers.

After discussion within the Experts Group, three types of CHP plant were selected to be incorporated in the optimisation analysis:

- Steam turbine plant: extraction condensing type, electrical output c50-100MWe.
- Reciprocating engine CHP, electrical output 5-10MWe
- Gas-turbine combined cycle, electrical output c 30-50MWe, back-pressure steam turbine and district heating economiser

For each case, conventional boilers will also be used to meet the peak demands and as standby plant.

2.3.2 Steam Turbine CHP

The steam turbine plant would be a typical system for a central power station or a turbine linked to waste incineration where the high investment costs and the need to continuously burn the fuel means that an extraction condensing turbine would be used. Higher district heating operating temperatures will result in steam being extracted at a higher pressure and the electrical production will fall resulting in effectively a higher cost for the heat produced.

2.3.3 Spark-Ignition gas-engine CHP

Gas engines have been found to be the most economic choice for smaller schemes and although there are step changes in heat output for different district heating operating temperatures there is no effect on the electrical output. If flow temperatures are less than 90 °C then the heat and electricity is nearly independent of district heating temperatures, the only factors being the ability to recover heat from the aftercooler and the amount of cooling of the exhaust gases.

2.3.4 Combined Cycle CHP

A combined cycle gas turbine CHP plant can take two principal forms: using an extraction/condensing steam turbine so that electrical production can be maintained even if there is no heat demand or a back-pressure steam turbine where the electricity production is linked to the heat demand. Examples of both these types of plant have been constructed in Europe in recent years and it is the electricity and gas prices that determine which is the more economic option. For example, if periods of low heat demand (e.g. in the summer and at night) coincide with periods of low electricity price and if gas prices are relatively high then the simpler back-pressure plant will be more economic. This appears to be the case for several northern European countries where there is significant hydro or nuclear plant on the system. However, larger plant utilising more complex steam cycles are more likely to be operated as base load plant using extraction-condensing steam turbines. Recent designs have also incorporated a district heating economiser which extracts additional heat from the exhaust gases, heat that otherwise could not be utilised in the steam cycle. This enables exhaust gases to be rejected at temperatures as low as 75 °C. On falling heat demand, this economiser can be taken out of the circuit to maintain a demand on the steam circuit and hence maintain electrical output.

It was concluded that the back-pressure combined cycle plant with district heating economiser would be the most appropriate plant for comparison with the steam turbine and reciprocating engine types.

2.4 Combinations for analysis

Having selected particular types of building, heating systems, climate, heat distribution systems and CHP plant it is possible to put together combinations which can be analysed as a series of design case studies. These are formed from:

- three building types with typical heating systems defined above and corresponding district heating densities, direct connection used for smaller schemes and for row houses
- two climatic conditions,
- three CHP heat production plant types.

Combining these gives a total of 18 cases which are listed in Table 2.2.

Table 2.2 - Case Studies Analysed

Ref No.	Building type	Climate	Heat supply plant
1	Apartment blocks in peripheral areas	Continental	Steam turbine
2	Apartment blocks in peripheral areas	Continental	Combined Cycle
3	Apartment blocks in peripheral areas	Continental	Reciprocating engine
4	Apartment blocks in peripheral areas	Maritime	Steam turbine
5	Apartment blocks in peripheral areas	Maritime	Combined Cycle
6	Apartment blocks in peripheral areas	Maritime	Reciprocating engine
7	High density linear housing	Continental	Steam turbine
8	High density linear housing	Continental	Combined Cycle
9	High density linear housing	Continental	Reciprocating engine
10	High density linear housing	Maritime	Steam turbine
11	High density linear housing	Maritime	Combined Cycle
12	High density linear housing	Maritime	Reciprocating engine
13	Downtown/city centre	Continental	Steam turbine
14	Downtown/city centre	Continental	Combined Cycle
15	Downtown/city centre	Continental	Reciprocating engine
16	Downtown/city centre	Maritime	Steam turbine
17	Downtown/city centre	Maritime	Combined Cycle
18	Downtown/city centre	Maritime	Reciprocating engine

Direct connection was assumed for the row houses as this is generally more economic. Both indirect and direct connections were analysed for the apartment blocks and the commercial buildings.

2.5 Economic Analysis

The aim of this project is to perform an economic optimisation and the principles by which this analysis has been carried out are set out below.

In order to derive an overall cost of heating it is necessary to convert the capital cost of the building heating systems into an annualised figure. This has been carried out using a discounted cashflow analysis assuming a time horizon of 20 years and a real discount rate of 10%. These assumptions are considered realistic for a private sector led CHP/DH industry as in the UK. Smaller schemes may be analysed over 15 years with a 12% discount rate whereas larger, government-backed schemes may be based on a 30 year period and a 5% discount rate. A sensitivity analysis with respect to these economic parameters for one of the case studies has been carried out (see section 12.1). The importance of these assumptions is illustrated in Table 2.3 below by calculating the annual cost that needs to be recovered from heat sales for a given investment of say £1m under different assumptions.

Table 2.3 - Comparison of financing assumptions

Assumptions	Annual charge for £1m capital investment	Factor on base case assumption
	£ p.a.	
10% over 20 years	117,500	1.0
12% over 15 years	146,800	1.25
5% over 30 years	65,060	0.55

Hence an assumption of 5% over 30 years results in a cost of capital nearly half that assumed in the base case.

In the discounted cashflow analysis we have excluded inflation so all discount rates given are in real terms. This in effect assumes that fuel and electricity prices will rise in accordance with general inflation. In the longer term it is possible that real increases in fuel and electricity prices will be seen but in the shorter term many countries are likely to see prices falling in real terms if deregulation and greater competition is introduced. An examination of the future price levels in different countries is beyond the scope of this study.

3 Climatic Data

To compare the optimisations in different climate regions it was agreed with the Experts Group to consider a typical western maritime climate and a typical continental climate.

After discussion with the Experts Group, London was selected to represent the maritime climate. The temperature and solar radiation data for an average year in London, (obtained from BRESCU, Building Research Establishment, UK), are shown in Figures 3.1 and 3.2. Both sets of data are shown for the time period of 8 months between September 1st and April 30th, defined in this report as the 'heating season'.

Figure 3.1 shows the temperature variation over a typical heating season in London, UK. Figure 3.2 shows the London radiation data. The radiation values are for a one square metre vertical surface, facing south. The figure indicates that the radiation is fairly substantial during the autumn and spring, but rather low during the winter months. In London, a south-facing window would receive 403 kWh/m2 for the 8 month heating season. The number of degree-days in London is equal to 2495 (18°C base, see Table 3.1).

The data consists of "20-year average" temperature and solar radiation data. The calculation of the "average" has been accomplished by taking months with a degree-day accumulation equal to the 20-year average, and using their exact hourly average temperature and solar radiation measurements. The normal temperature and radiation variability is therefore included in the data. To avoid showing the high fluctuations of the hourly and daily temperatures in the graphs shown in this section, the raw data was put through a filter which averaged each data point over a two week period. The graphs therefore show a smooth two-week running average. The simulations however were performed with the hourly data.

To select an appropriate city for the continental climate, meteorological data from Helsinki, Finland, and Toronto, Canada were compared. The Helsinki weather data was obtained from the Finnish Meteorological Institute, while the Toronto data was obtained from the University of Waterloo WATSUN laboratory.

The two-week running average temperatures in Helsinki and Toronto are shown in Figure 3.3. The Toronto temperatures are generally higher than those of Helsinki, except during some periods in the winter. The degree-days for Helsinki and Toronto are 4479 and 3844, respectively (see Table 3.1).

The two-week running average radiation values for Helsinki and Toronto are shown in Figure 3.4. Again, the values are computed for a vertical, one square meter surface, facing south. The amount of radiation received in Toronto is substantially higher than that in Helsinki. The total amount of radiation received for the 8 month heating season in Helsinki is 519 kWh/m2 and the radiation received in Toronto is about 30% higher at 687 kWh/m2.

With regards to both solar radiation and temperature, it is evident that Toronto's climate is milder than that of Helsinki. Although there may be a number of Northern European cities better represented by Helsinki, Toronto's weather was more representative of the majority of continental European cities as well as cities in the northern parts of the United States and Canada. It was therefore decided to use the Toronto weather data to model a continental climate in the building heating system simulations.

Table 3.1 - Comparison of climates for capital cities

City	Design Temp	Degree days	Solar Radiation (heating season)
	°C		kWh/m2
London	-5	2495	403
Toronto	-17	3844	687
Helsinki	-26	4479	519

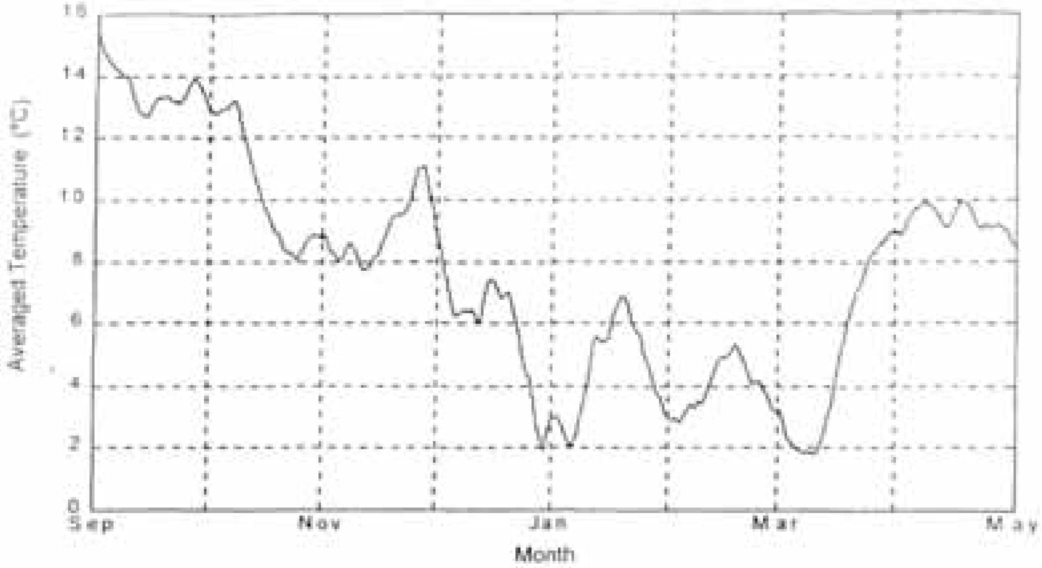

Figure 3.1 - Average Daily Temperatures in London

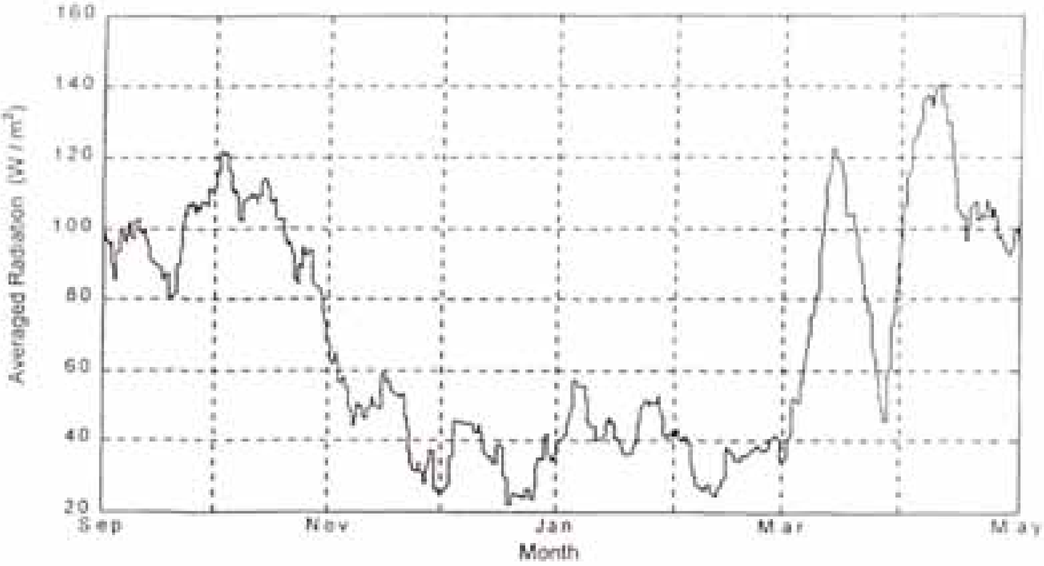

Figure 3.2 – Average solar radiation in London

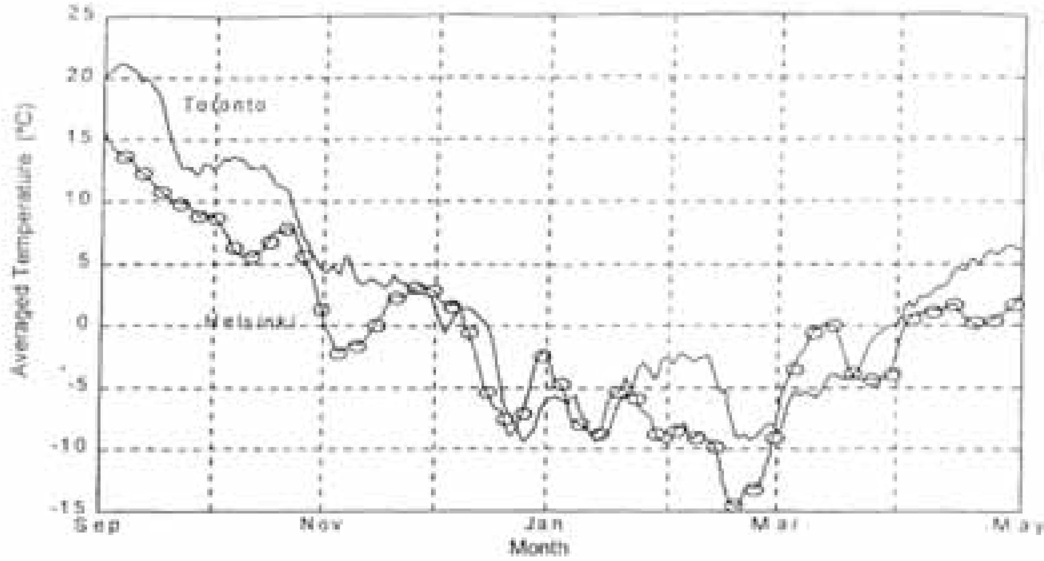

Figure 3.3 – Comparison of average temperatures in Helsinki and Toronto

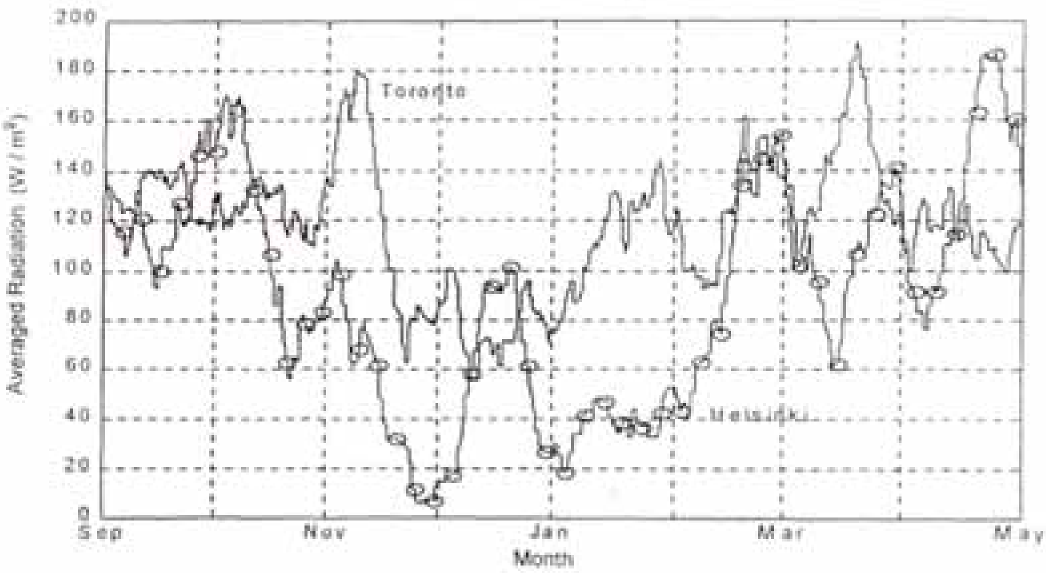

Figure 3.4 – Comparison of average solar radiation in Helsinki and Toronto

4 Description of Building Models

4.1 Introduction

Section 2 above describes three different types of building and a typical heating system for each as follows:

- apartment blocks: radiators, two-stage hot water heating (non-storage)
- row houses: radiators, parallel hot water heating (non-storage)
- commercial buildings: air heating and radiators, no hot water

In order to optimise the whole CHP/DH system with respect to operating temperatures it is necessary to establish for a range of design operating temperatures:

- how the capital cost of the heating installation changes
- how the flow rate and operating temperatures vary over a year

The latter information enables an accurate assessment to be made of the costs of heat production, district heating network heat losses and pumping costs. Although approximations can be made to derive this information, e.g. by taking annual or monthly averages, the development of advanced software simulation tools (SIMULINK - The Math Works Inc.) enables hour by hour variations in flow rates and temperatures to be calculated for each building for subsequent use in the heat production models (see section 6).

The three building types and the two climates result in 6 models where both design flow and return temperatures can be varied.

After discussion within the Experts Group it was agreed to consider the following variations in flow temperatures:

For direct connection:

- constant 70 °C
- varying temperature from 80 °C to 70 °C with external air temperature
- constant 90 °C
- varying temperature from 90 °C to 70 °C with external air temperature

For indirect connection:

- constant primary 70 °C, constant secondary 60 °C
- constant primary 80 °C, constant secondary 70 °C
- constant primary 90 °C, constant secondary 80 °C

Table 4.1 summarises the simulations for the types of building, heating system and connections, as well as climate and supply temperature levels.

Table 4.1 Specification of building, heating system, connections, climate and supply temperature levels.

Building Type		Apartment Bldg.		Row-House		Commercial Bldg.	
Climate		Toronto	London	Toronto	London	Toronto	London
Direct Connection		2-stage	2-stage	Parallel	Parallel		
Primary							
70°C (constant)		✓	✓	✓	✓	✓	✓
80-70°C (variable)		✓	✓	✓	✓	✓	
90-70°C (variable)		✓	✓	✓	✓	✓	
90°C (constant)		✓	✓				
Indirect Connection		2-stage	2-stage	Parallel	Parallel		
Primary	Secondary						
70°C (constant)	60°C (constant)	✓	✓			✓	✓
80°C (constant)	70°C (constant)	✓	✓	✓	✓	✓	✓
90°C (constant)	80°C (constant)	✓	✓				
90°C (variable)	80°C	✓					

Higher temperatures than 90°C were not considered as these systems would not be classed as low temperature systems (for a discussion of temperatures higher than 90°C see section 11.5).

For each of the above cases, the heat emitter (radiator) size was then increased in stages to give 6 different design return temperatures. This resulted in a total of 180 output files each containing hourly demand simulation results.

The following sections describe the assumptions made for each of the building models in more detail (Appendix A provides additional information on the SIMULINK models for the building heating systems, as well as the detailed model description for different components). This is followed by a discussion on the capital cost relationships with operating temperatures.

4.2 Specifications of Building Types

4.2.1 General Approach

A modular approach was used to design the buildings. For example, a single, nine storeys high, 18-unit "slice" of an apartment building was simulated. By multiplying the number of slices, an apartment building with almost any load can be modelled. The same can be applied to the row-houses and commercial buildings where the number of units can be multiplied up.

All buildings were modelled with two thermal masses. However, since the temperature set-points were constant, these thermal masses did not affect the simulation to a great extent.

The selection of variables to simulate each building type was carefully considered. Although the most realistic system would simulate all variables for each building type, such an approach would result in overly complex and lengthy simulations. Table 4.2 summarises the variables which have been taken into account in each of the building types.

Table 4.2 Variables used in building simulations.

	Forced Ventilation Losses	Natural Ventilation Losses	DHW	Solar Gain	Internal Gain
Apartment		✓	✓	✓	
Row-House		✓	✓	✓	
Commercial	✓				✓

Solar gain was calculated by assuming that, on average, the buildings were oriented so that they received 45% of the radiation of a south-facing building and using a glass transmittance factor of 0.7.

Table 4.3 shows the peak heat losses and heat loss factors for corresponding design outdoor temperatures and room temperature set-points for the three types of buildings in Toronto, Ontario, Canada and London, United Kingdom.

Table 4.3 Peak heat losses and heat loss factors at design conditions.

Building Type	City	Peak Heat Loss (kW)	Heat Loss Factor (kW/°C)	Design Outdoor Temperature (°C)
Apartment	Toronto	77.6	2.14	-17.2
	London	52.8	2.14	-5
Row-House	Toronto	7.30	0.201	-17.2
	London	4.82	0.201	-5
Commercial	Toronto	1000	27.62	-17.2
	London	663	27.62	-5

The room temperature has been selected at 19°C for all cases which is slightly lower than the average internal temperature to take account of some internal gains from occupants and electrical equipment. It is expected that room temperature set points will also vary according to the external temperature, higher temperatures being needed in cold climates. However this additional complexity in the simulations was not considered worthwhile.

The solar gain was not considered in the commercial building as this is assumed to have a deep plan and limited window area being partly office and partly an industrial space.

The layout and characteristics of the buildings are described below:

4.2.2 Apartment building

The apartment building is a medium-rise building. One "slice" of the apartment building is 9 storeys high, one unit wide and two units deep. This gives the flexibility needed to provide a wide range of loads while not oversimplifying the situation. The layout of one unit is shown in Fig. 4.1. Approximately 46% of the outside wall consists of window area.

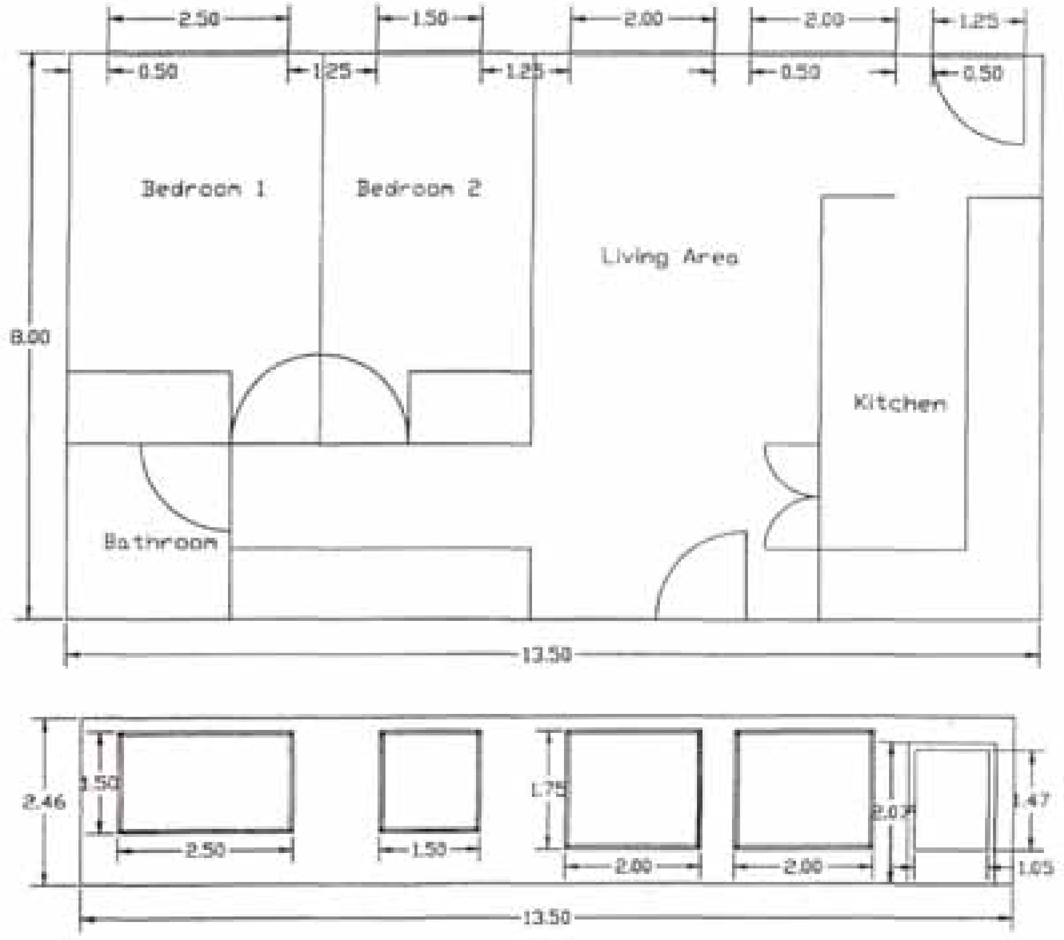

Figure 4.1 Layout and outside wall of one apartment unit

The heat loss factor for one slice of the apartment building is 2.14 kW/°C. This heat loss factor results in peak design loads of 77.6 kW and 51.4 kW in Toronto and London respectively. It is assumed that there is no heat transfer from the sidewalls. This is a reasonable assumption if the apartment building is made up of many slices. The breakdown of the heat losses at design condition is:

- 31% natural ventilation
- 10% envelope losses through wall
- 59% envelope losses through windows

The DHW consumption was 208.3 l/day/apartment according to the profile shown in Figure 4.2. This consumption value was derived from a demand curve for a 24-unit apartment building, taken from Yang (1994). DHW consumption diversification in the 18 units of the "slice" has been taken into account.

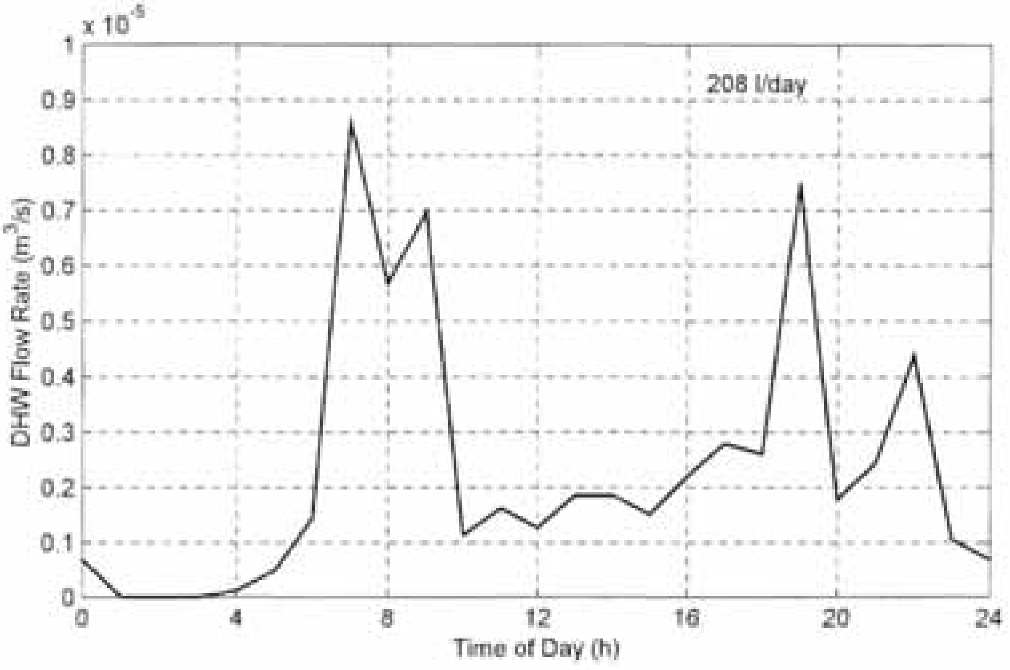

Figure 4.2 Domestic hot water consumption (including diversification) for one apartment.

Row-House

The row house has two storeys and a full basement. The layout of the first and second floor is shown in Fig. 4.3. The simulations were carried out for one unit, assumed to be located between similar units.

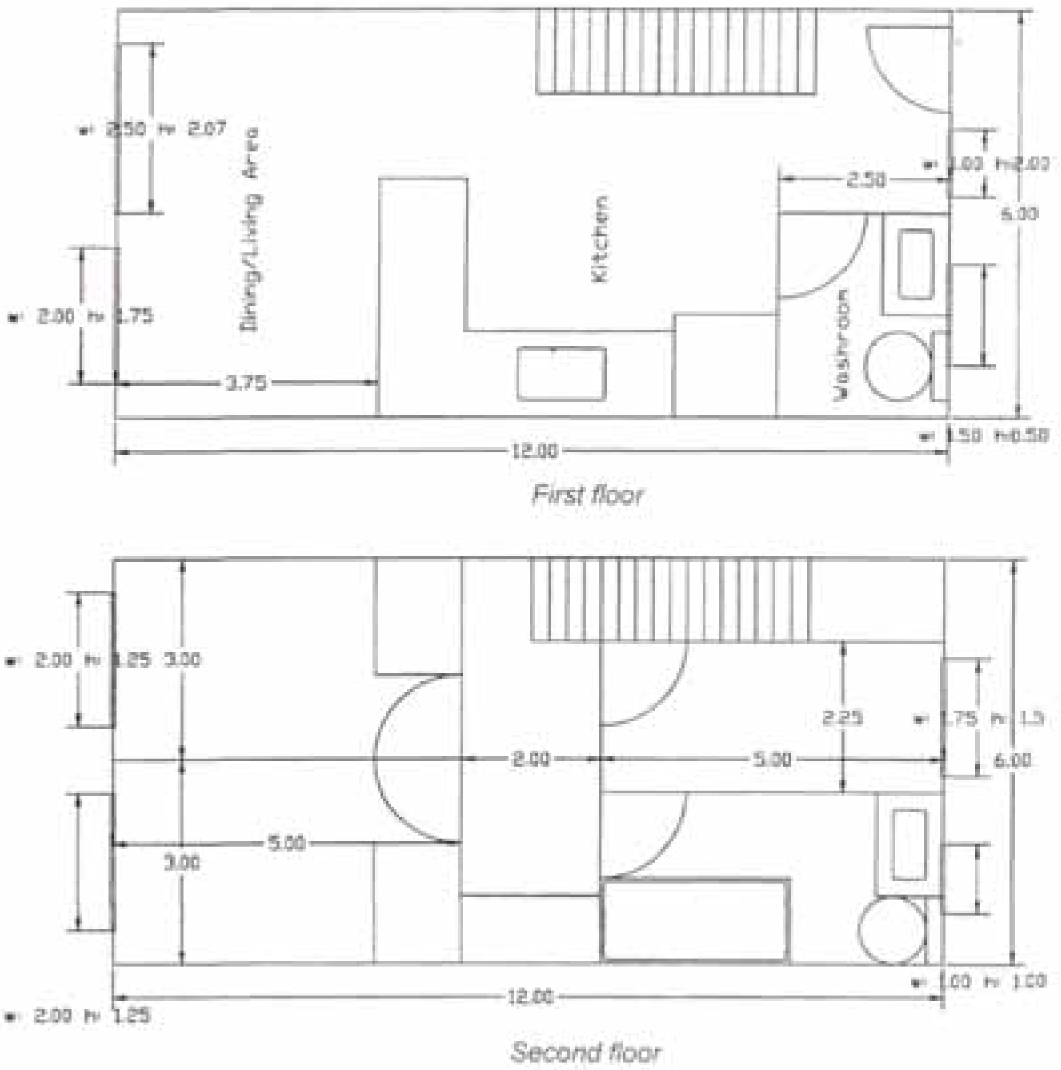

Figure 4.3 First and second floor layout of a row-house

The heat loss factor for one row house is 0.201 kW/°C. This leads to a design load of 7.3 kW in Toronto and 4.82 kW in London. The breakdown of the heat losses at design condition is listed in the following:

- 40% natural ventilation
- 18% envelope losses through walls
- 35% envelope losses through windows
- 7% envelope losses through ceiling

From the DHW consumption study by Lawaetz (1985), the DHW consumption in this study was assumed at 238 l/day/house (assumes 2 adults and 2 children per dwelling). The consumption profile is shown in Figure 4.4. This profile allows for a diversity factor of 0.27 on a peak demand of 63kW (assuming a peak load from a single bath tap at 0.3 l/s with a temperature rise from 5°C to 55°C), and therefore represents a typical demand profile for a group of say 10 row-houses. The simulation output is based on providing hourly average demands and this effectively increases the diversity factor to about 0.04.

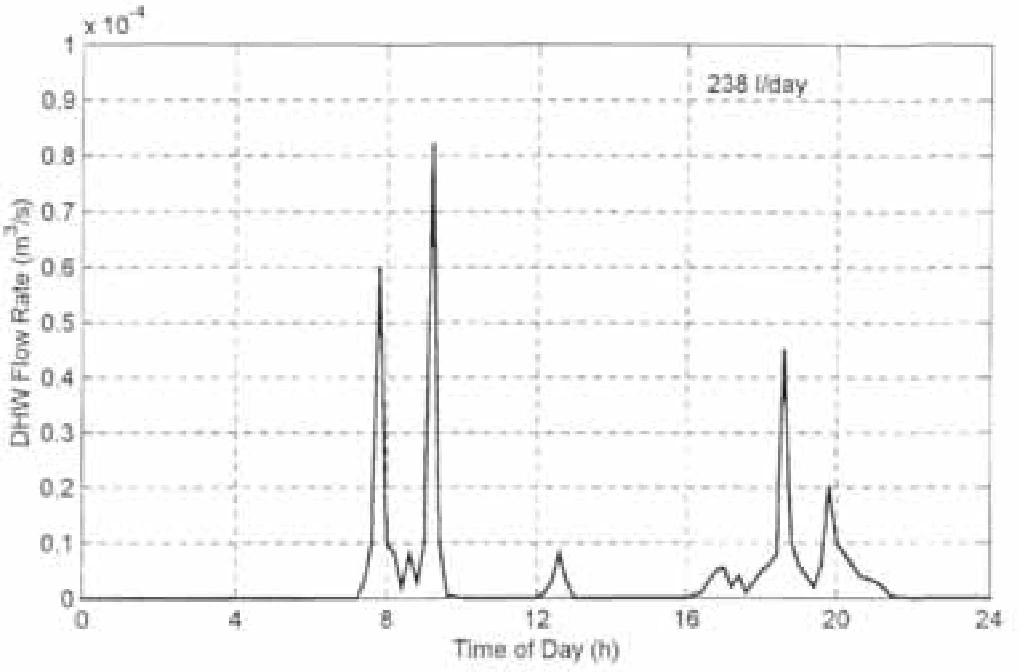

Figure 4.4 Domestic hot water consumption for one row-house.

4.2.3 Commercial Building

The commercial building has dimensions of 104 metres long by 104 metres wide and 8 metres high. There are two main sections: office and workshop area. The office area occupies one half of the volume of the building and consists of two floors (each 4 metres high ceilings). The workshop area occupies the remaining half and has 8-metre high ceilings.

The heat loss factor for the commercial building is 27.62 kW/°C. The resulting design loads are 1000 kW and 663 kW for Toronto and London respectively. The breakdown of the heat losses is:

36% forced ventilation
64% envelope losses

Internal gain of 15W/m² for both floors of the office area and 10W/m² for the workshop area (total of 216.32 kW) are considered in the building model for lighting, workshop machines, etc., from 8:00 to 18:00 on weekdays.

Domestic hot water was assumed to be heated electrically, and was not part of these simulations.

4.2.4 Directly and indirectly connected 2-stage heating systems in the apartment building

The diagram of the directly connected heating system of the apartment building is shown in Figure 4.5. It includes a space heating system and a domestic hot water system. It should be stressed that the diagram shown in the figure is simplified in that it omits a number of components, essential to safe operation in practice, but not to thermodynamic performance.

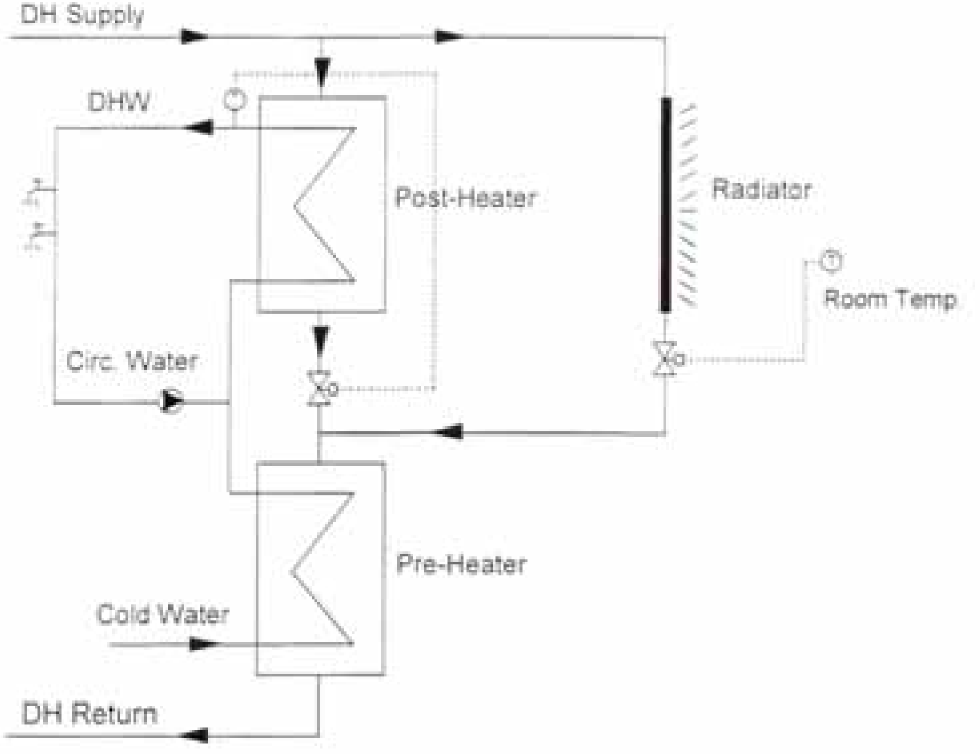

Figure 4.5 Diagram of a directly connected heating system for the apartment building

The DH water is directly fed to the radiators in the space heating system. There are two heat exchangers (pre-heater and post-heater) for domestic hot water heating. The pre-heater further cools the DH water coming from the radiators and pre-heats the cold water mains when the domestic hot water (DHW) is being drawn off. The post-heater of the second stage heats the DHW to set-point temperature.

The room temperature is controlled by a temperature sensor in the room. The DH flow through the radiators is adjusted by comparing the actual room temperature to the set-point. The domestic hot water temperature control is similar to the space heating control except the temperature sensor is placed in the outlet of the post-heater.

The diagram of the indirectly connected heating system of the apartment building is shown in Fig. 4.6. The system is similar to the direct connection except that the space heating system is supplied with hot water via a heat exchanger. The supply temperature to the radiators is regulated by a control valve in the DH return line.

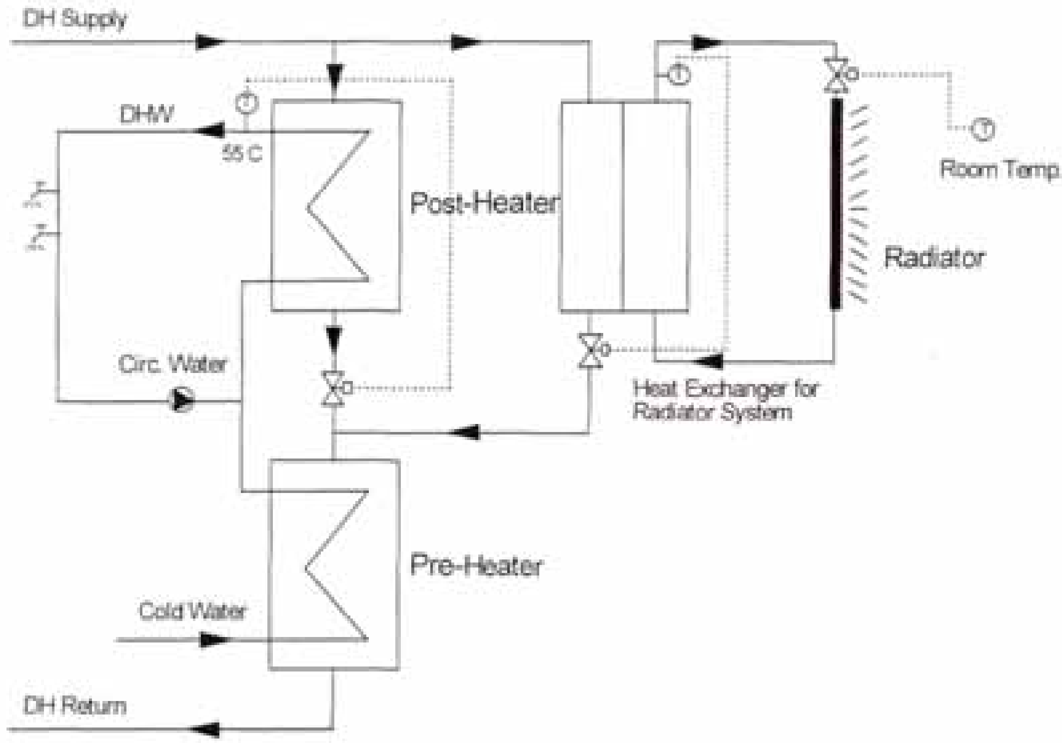

Figure 4.6 Diagram of an indirectly connected heating system for the apartment building.

The DHW circulation water flow (both in the direct and indirect connections) is assumed to be constant. The circulation line has an assumed average heat loss of 100 W/apartment and a resulting temperature drop around the loop of 8°C. The heat loss from the circulation line is considered as a constant heat gain in the building model.

4.2.5 Directly and indirectly connected parallel heating systems in the row-house

The diagram of the directly connected heating system of the row-house is shown in Figure 4.7. It includes a space heating system and a DHW system with one heat exchanger. The temperature controls are identical to those for the directly connected 2-stage heating system in the apartment building.

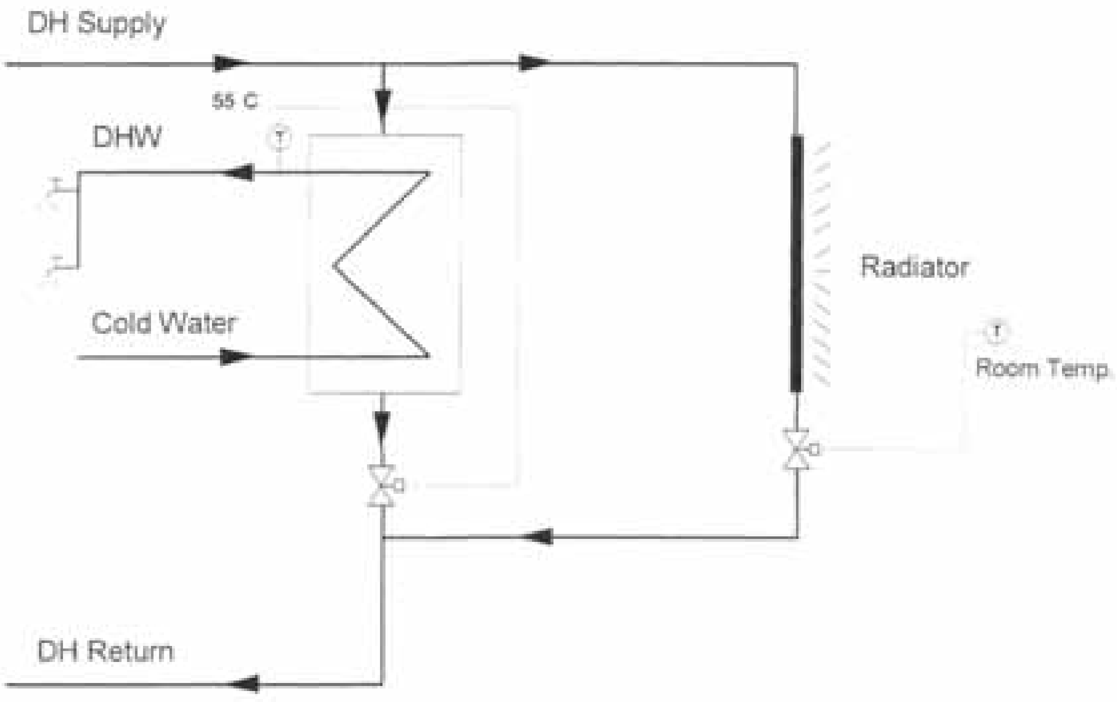

Figure 4.7 Diagram of a directly connected heating system for the row-house.

The diagram of the indirectly connected heating system of the row-house is shown in Fig. 4.8. There are two heat exchangers in the system, one for space heating and one for DHW. The temperature controls are identical to those used for the indirectly connected 2-stage heating system in the apartment building.

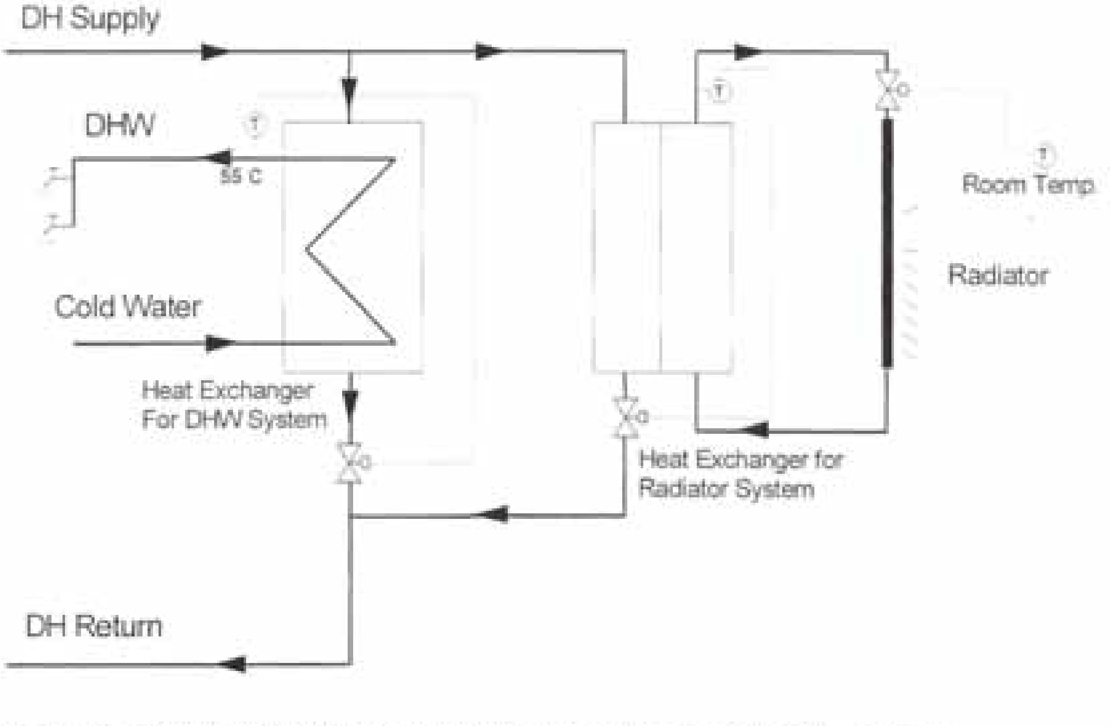

Figure 4.8 Diagram of an indirectly connected parallel heating system for the row house.

4.2.6 Directly and indirectly connected heating systems in the commercial building

The directly connected heating system of the commercial building is shown in Fig. 4.9. It includes a radiator system and a ventilation air coil system. The connection of the ventilation air coil system is based on the "System 3" in Volla et al. (1996). The ventilation air coil is connected in series with the outlet of the radiator system. Water to the heating coil is drawn from the DH system (if necessary) from a two-way valve and from a three-way valve which mixes the return water coming from the heating coil and the return water coming from the radiators.

The indirectly connected heating system for the commercial building is shown in Fig. 4.10. It also includes a radiator system and a ventilation air coil system. The ventilation air coil is connected on the primary side to the outlet of the radiator heat exchanger. A three-way valve mixes the return water from the coil and the return water from the radiator heat exchanger. If required, supplementary hot water to the heating coil is drawn from the DH system.

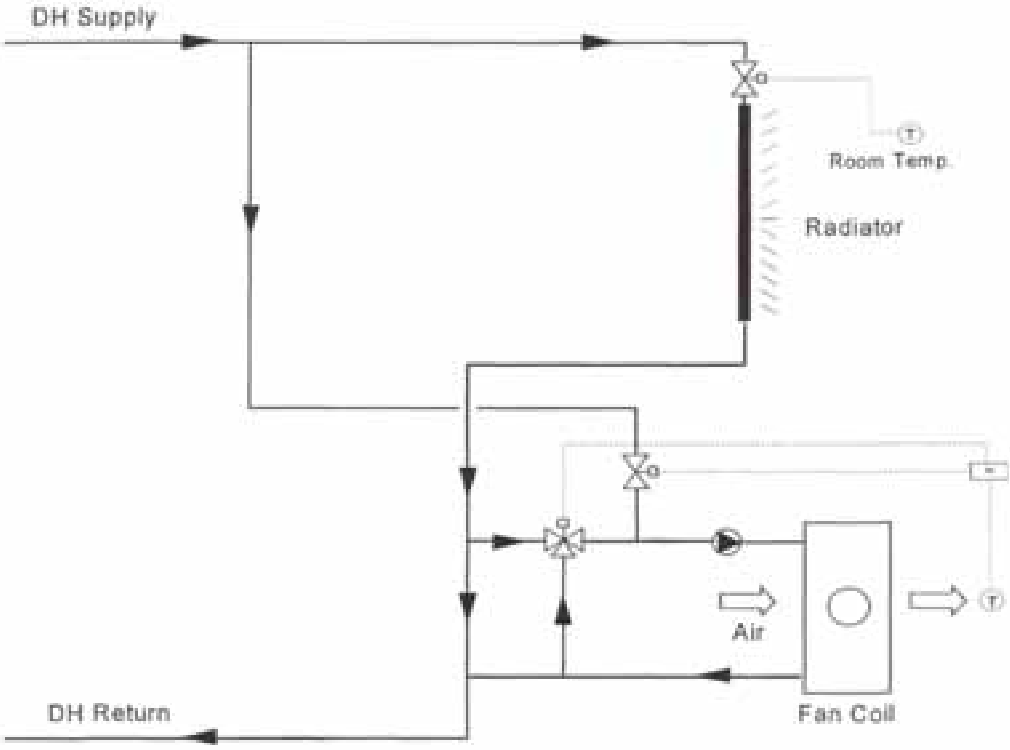

Figure 4.9 Diagram of a directly connected heating system for the commercial building.

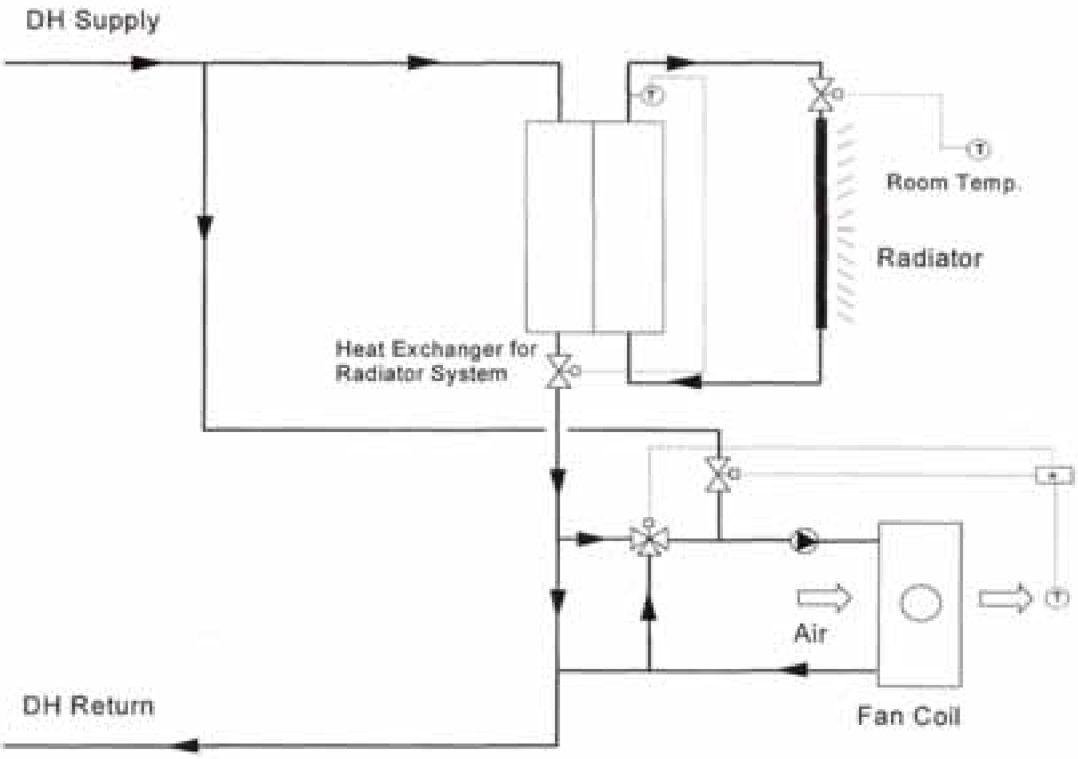

Figure 4.10 Diagram of an indirectly connected heating system for the commercial building.

4.2.7 Assumptions Applied in the Building Heating System Simulations

Some assumptions applied to the dynamic simulations, common to all building types, are listed below:

- In some simulation cases, the DH supply temperature is varied with the outdoor temperature. In these cases, the supply temperature increased linearly from the 70°C base temperature when the outdoor temperature dropped below 0°C in Toronto and below 5°C in London, see Figures 4.11 and 4.12. As the outdoor temperature dropped, the system supply temperature change was rate-limited to no more than 2°C/h. Conversely, as the outdoor temperature increased, the supply temperature could not decrease by more than 0.5°C/h.

- For indirectly connected space heating systems, the heat exchangers for the radiators were designed based on the primary and secondary side temperatures shown below:

Primary Side	Secondary Side
70°C / 55°C	60°C / 50°C
80°C / 55°C	70°C / 50°C
90°C / 55°C	80°C / 50°C

  The heat exchanger size was further oversized by 20%.

- The heat transfer area of the radiators was designed so that the return temperature from the radiator was 55°C for the direct connection and 50°C for the indirect connection at design load. Six different radiator surface areas, A1.00, A1.15, A1.25, A1.35, A1.50 and A1.75, were applied in each case study to get six different return temperatures. A1.00 is the base case, A1.15 denotes a 15% increase of radiator surface area above the A1.00 base case, etc.

- Room temperature set-point was 19°C.

- The heat exchanger for the DHW system was designed on a 9°C logarithmic mean temperature difference basis (primary side 70°C /10°C and secondary side 5°C /55°C), with 20% oversizing. Primary side is 70°C for all cases as for the variable cases the demand must be satisfied for the summer operation. Hence there is a small additional oversizing element in the design for the constant 90°C and constant 80°C cases. The additional cost of the heat exchanger surface is relatively low however and has negligible effect on the economic comparisons.

- The DHW temperature set-point was 55°C.
- The domestic cold water supply temperature was varied between 5°C and 12°C, depending on the season.

Several additional assumptions applied to the commercial building heating system simulations are outlined in the following:

- The radiator heating system was designed to cover 64% of the building heat loss at design conditions.
- The ventilation air coil system was designed to cover 36% of the building heat loss at design conditions. The inlet air temperature was at outdoor temperature (i.e. no re-circulated air). The outlet air temperature was 19°C. The fresh air supply rate was a constant 8.4 m^3/s. At design conditions, the water temperature to the inlet of the fan coil was 10°C lower than the DH supply temperature. This temperature level was achieved by mixing the outlet water from the radiators/radiator heat exchanger with fresh DH water. The fan coil outlet water temperature was 30°C at design conditions.
- The heat transfer areas of the fan coils were increased by the same ratio as the radiator areas, i.e. 0%, 15%, 25%, 35%, 50% and 75%.

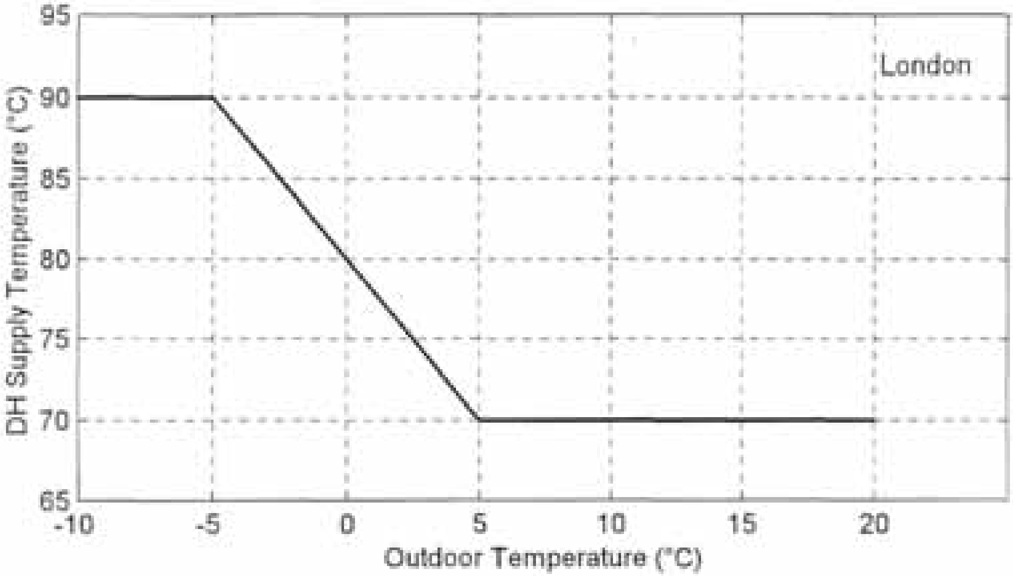

Figure 4.11 - Variation of DH supply temperature with outside air temperature for London

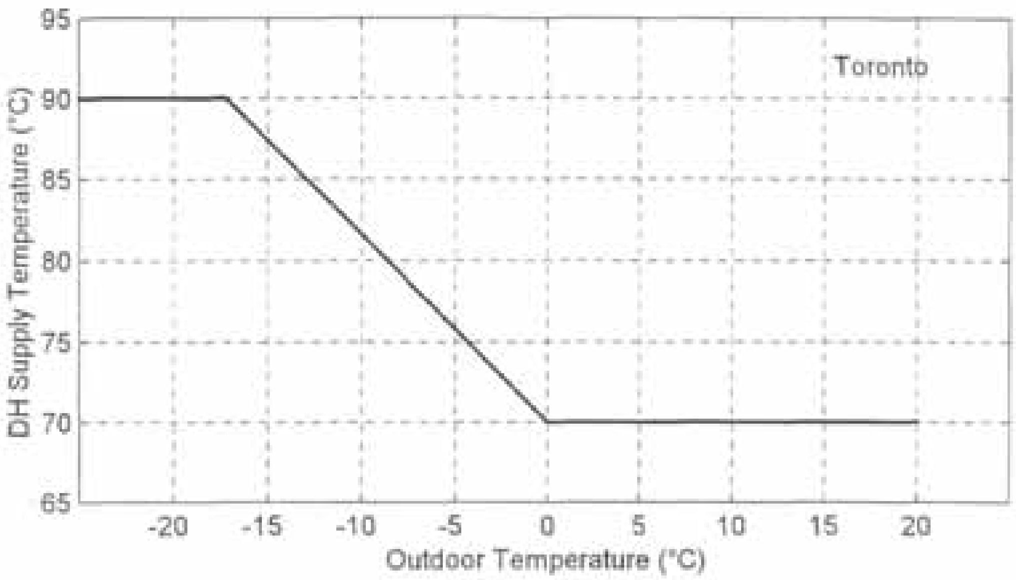

Figure 4.12 - Variation of DH supply temperature with outside air temperature for Toronto

4.3 Results of the building heating system simulations

The results of the simulations for each temperature case were contained in a file listing the DH flow rate, DH supply temperature and DH return temperature for each hour of the year. Figures 4.13 to 4.20 illustrate the 24 hour profiles for typical summer and winter days for the apartment blocks and the row houses in London and Toronto for the variable DH supply temperature and direct connection cases.

The Figures 4.13 to 4.20 illustrate that consistently lower return temperatures can be obtained with the double heat exchanger system as used in the apartment block model during the winter period, compared to the row houses model, as the return water from the radiators is used to preheat the cold feed to the hot water system. In the summer night period the heat demand is only required to compensate for heat losses from the domestic hot water distribution circuit. As there is minimal cold water draw off in this period the return water temperature rises nearer to the domestic hot water recirculation temperature. This rising temperature characteristic does not occur with the row houses as there is no hot water recirculation.

The Figures also illustrate the difference in demand over 24 hours between London and Toronto. The much larger swings in flow rate and return temperature in Toronto arise from the greater temperature range in a typical winter day and the influence of higher solar radiation.

The results of the simulation can also be presented as an annual energy use prediction for heating and hot water as shown in Table 4.4. Although the climate is much colder in Toronto the load factor is only slightly less than in London

Table 4.4 - Energy use predictions from Simulink models

Building	Climate	Peak Heating Demand	Annual Heat Energy Used	Load Factor
		kW	kWh	%
Apartment Blocks	London	72.5	198626	31.3
	Toronto	102.8	253347	28.1
Row houses	London	7.5	18367	28.0
	Toronto	10.5	23956	26.0

Note: the load factor = 100 x annual energy/(peak demand x 8760). The peak demands are the maximum demand that occurs during the average year that has been modelled.

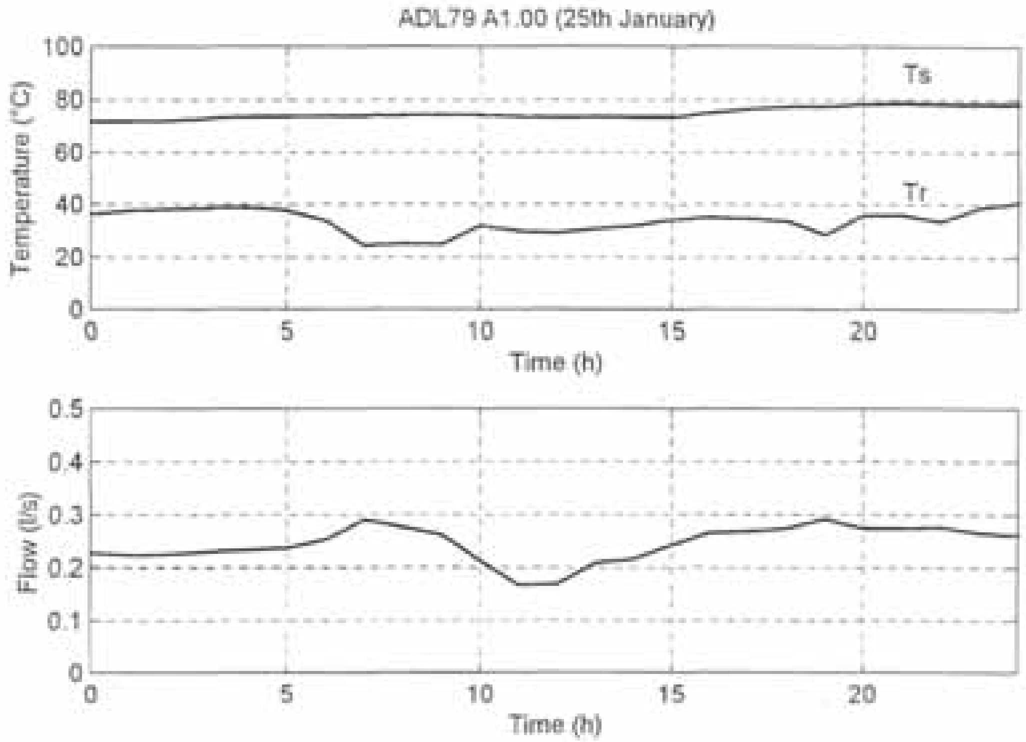

Figure 4.13 - Results for apartment blocks in London - winter - direct connection

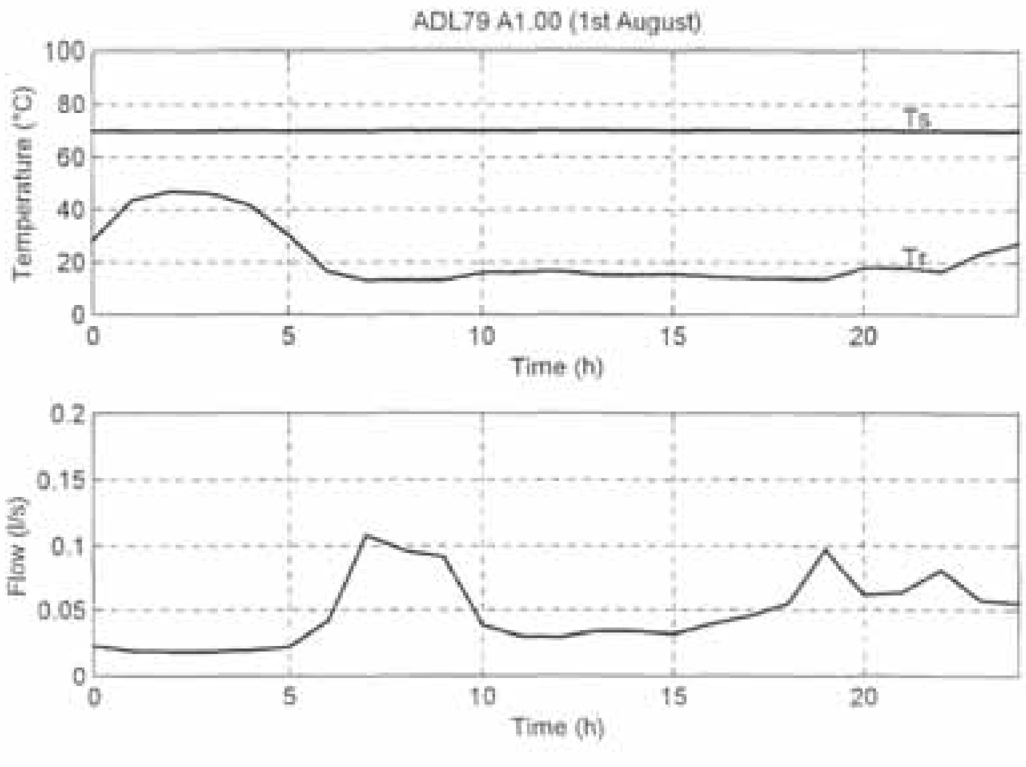

Figure 4.14 - Results for apartment blocks in London - summer - direct connection

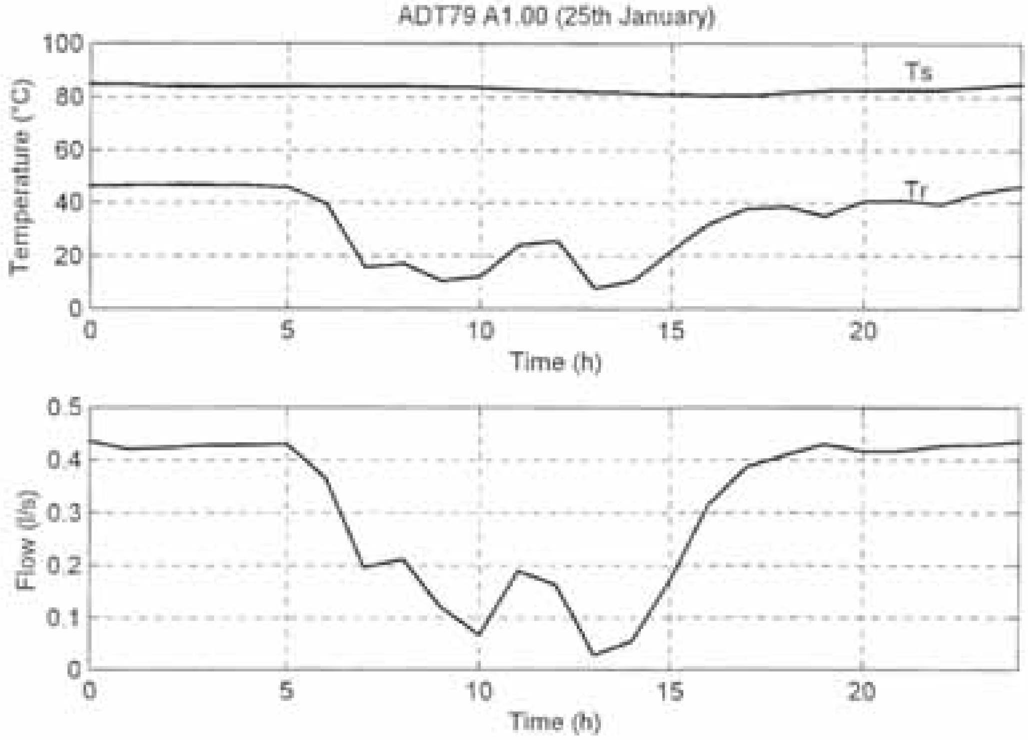

Figure 4.15 - Results for apartment blocks in Toronto - winter - direct connection

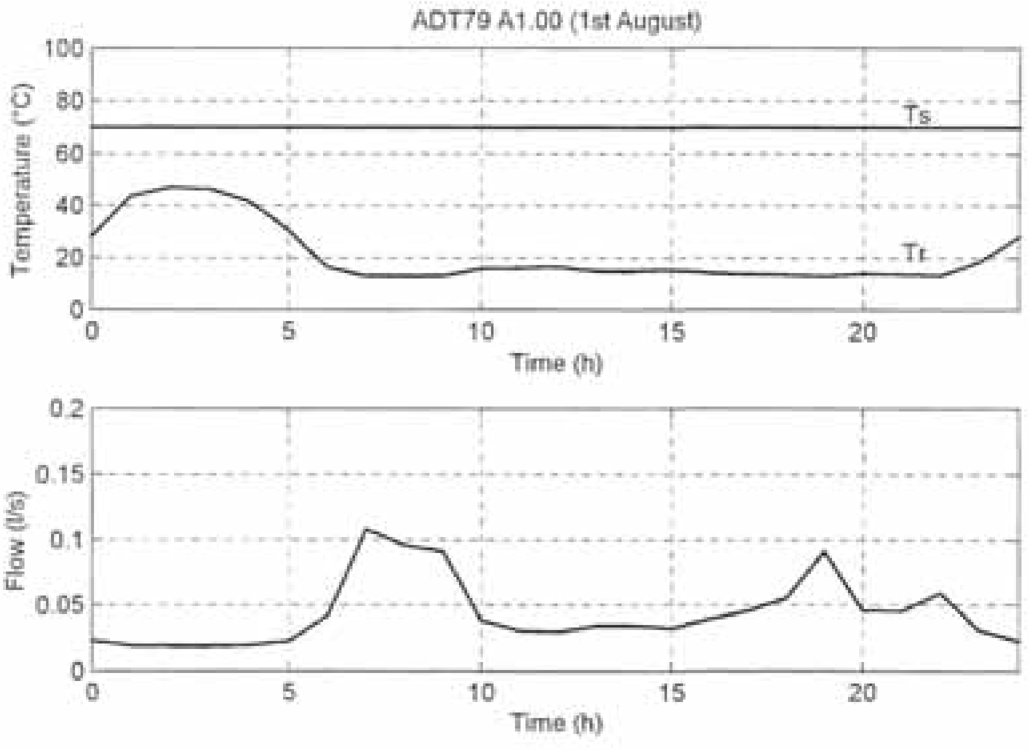

Figure 4.16 - Results for apartment blocks in Toronto - summer - direct connection

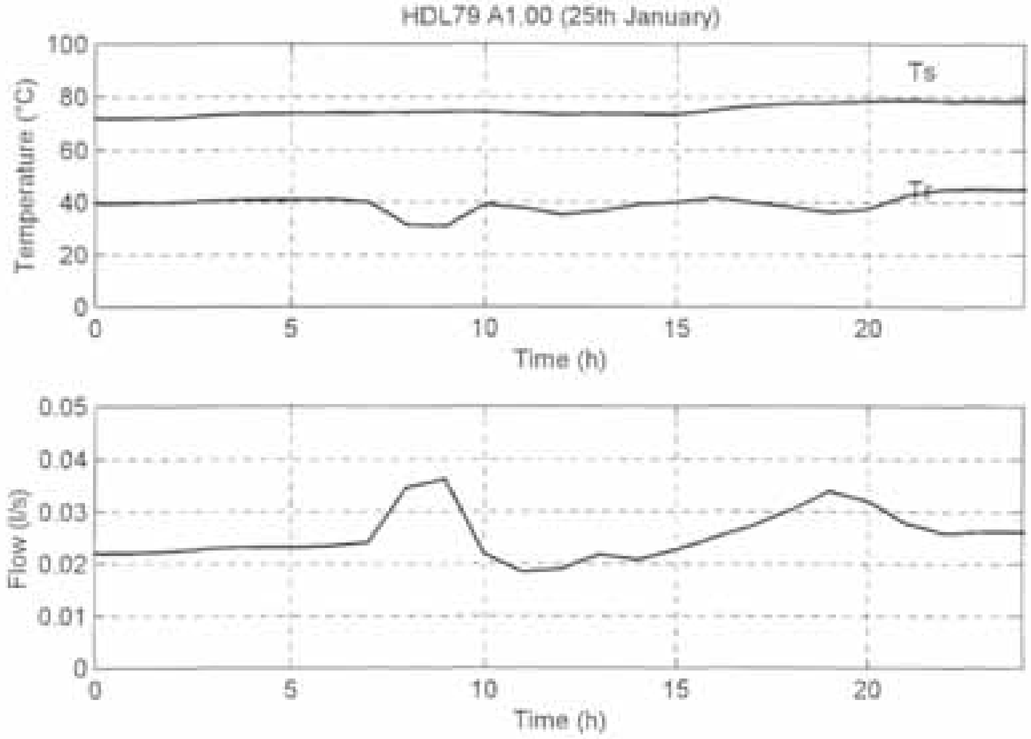

Figure 4.17 - Results for row houses in London - winter - direct connection

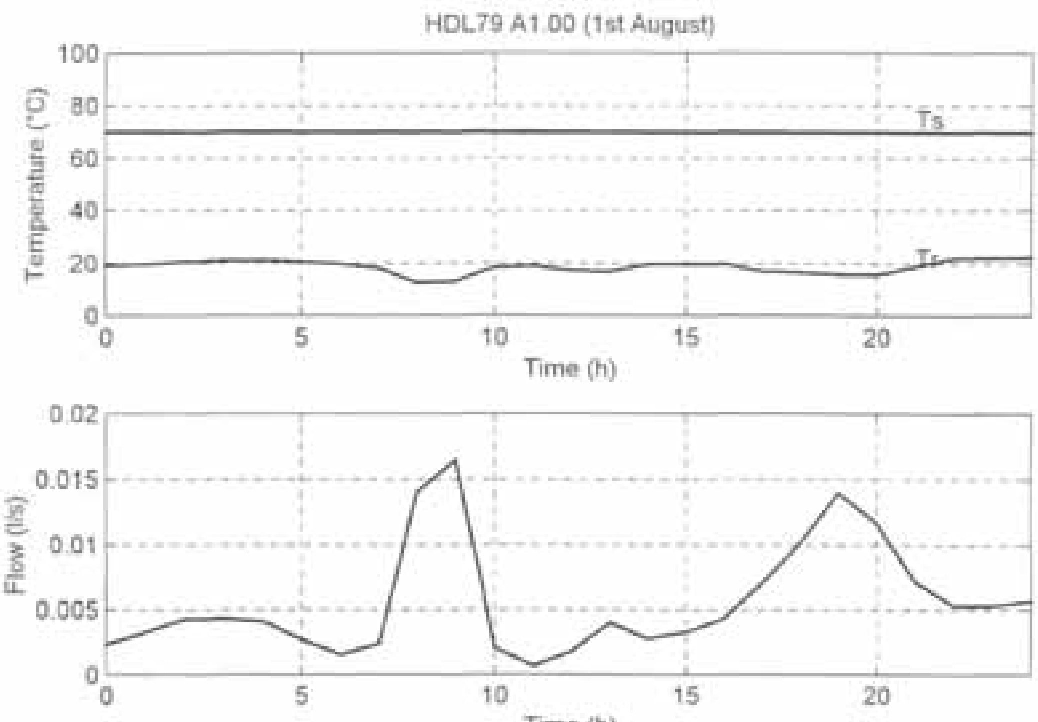

Figure 4.18 - Results for row houses in London - summer - direct connection

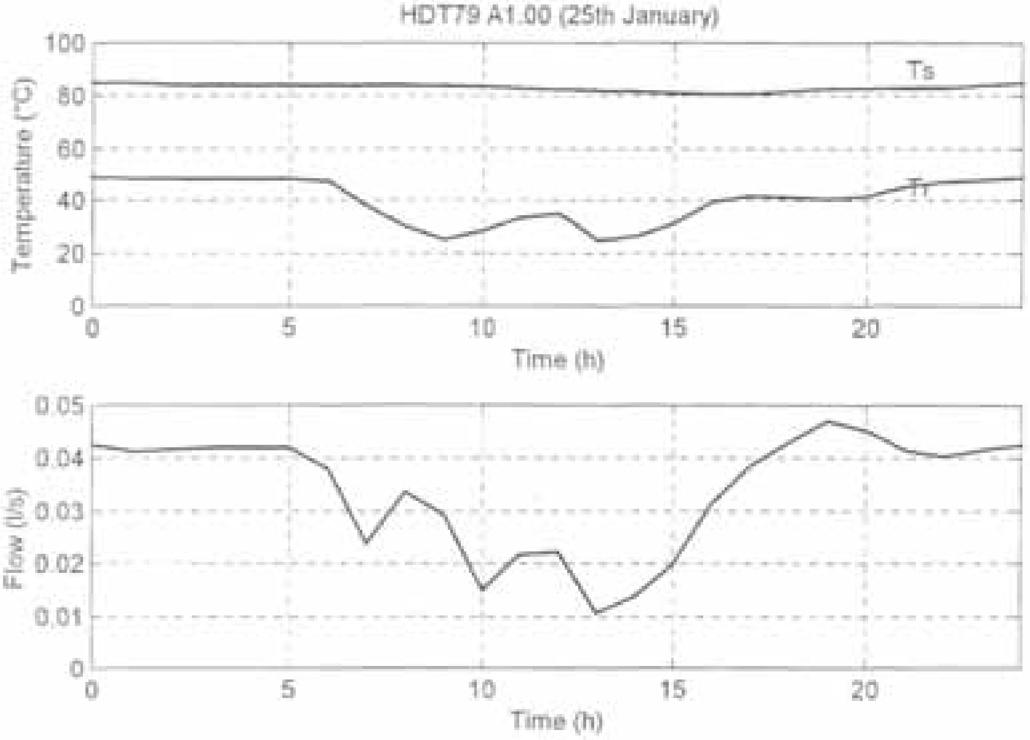

Figure 4.19 - Results for row houses in Toronto - winter - direct connection

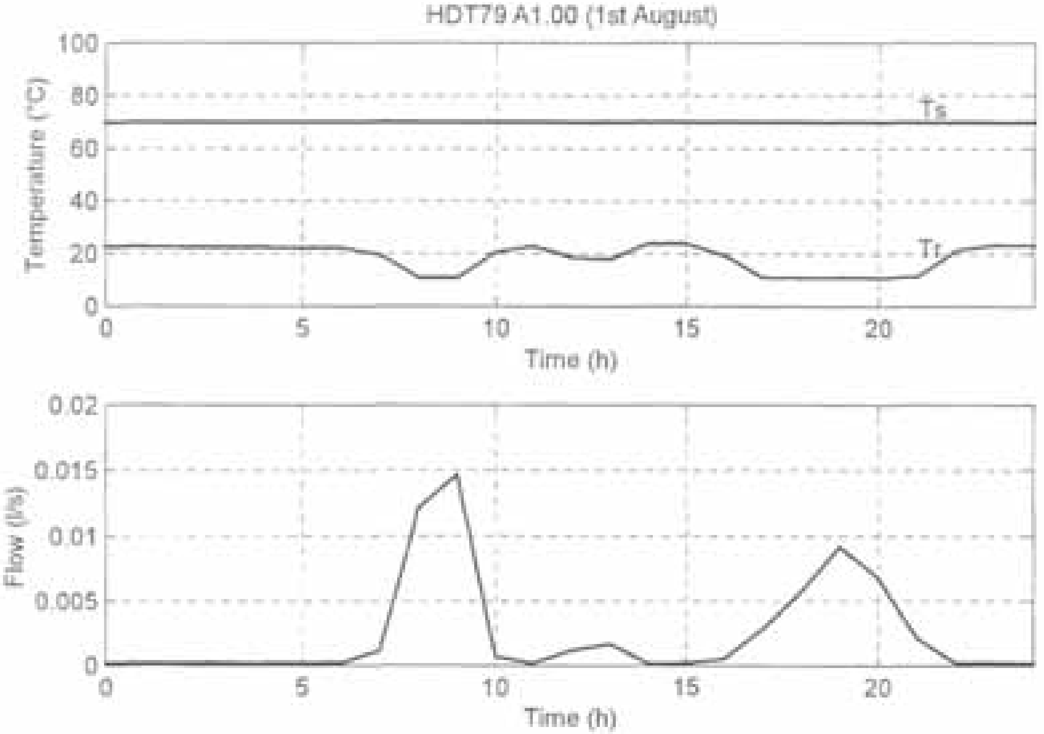

Figure 4.20 - Results for row houses in Toronto - summer - direct connection

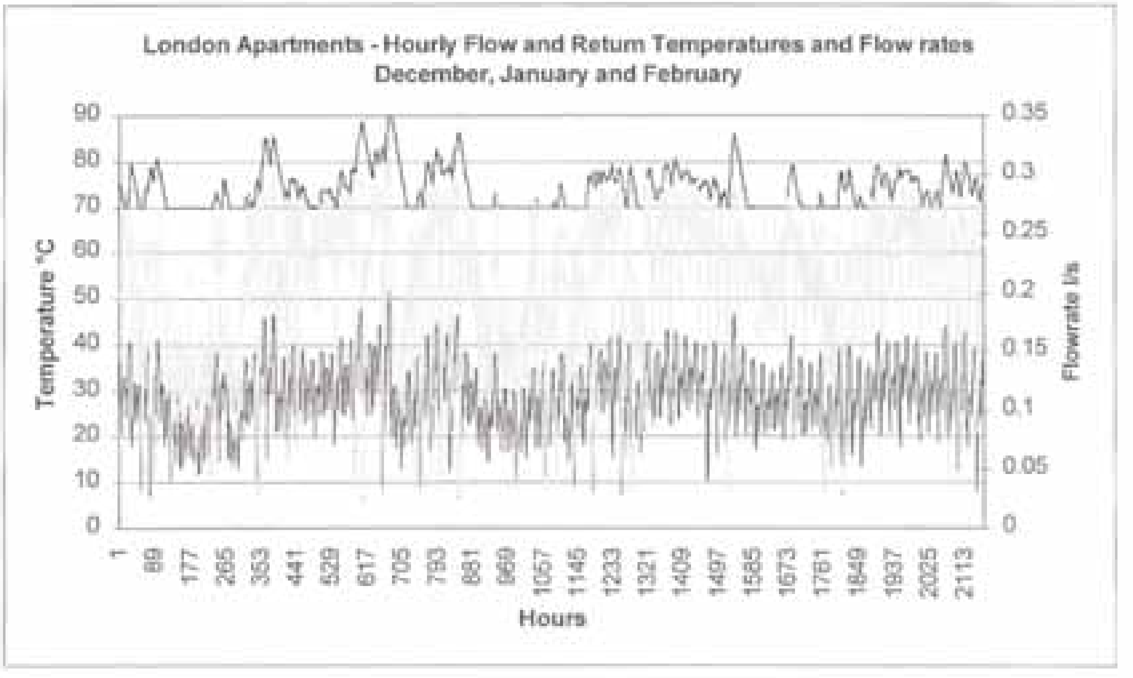

Figure 4.21 - Results for the winter 3 months for apartment buildings in London

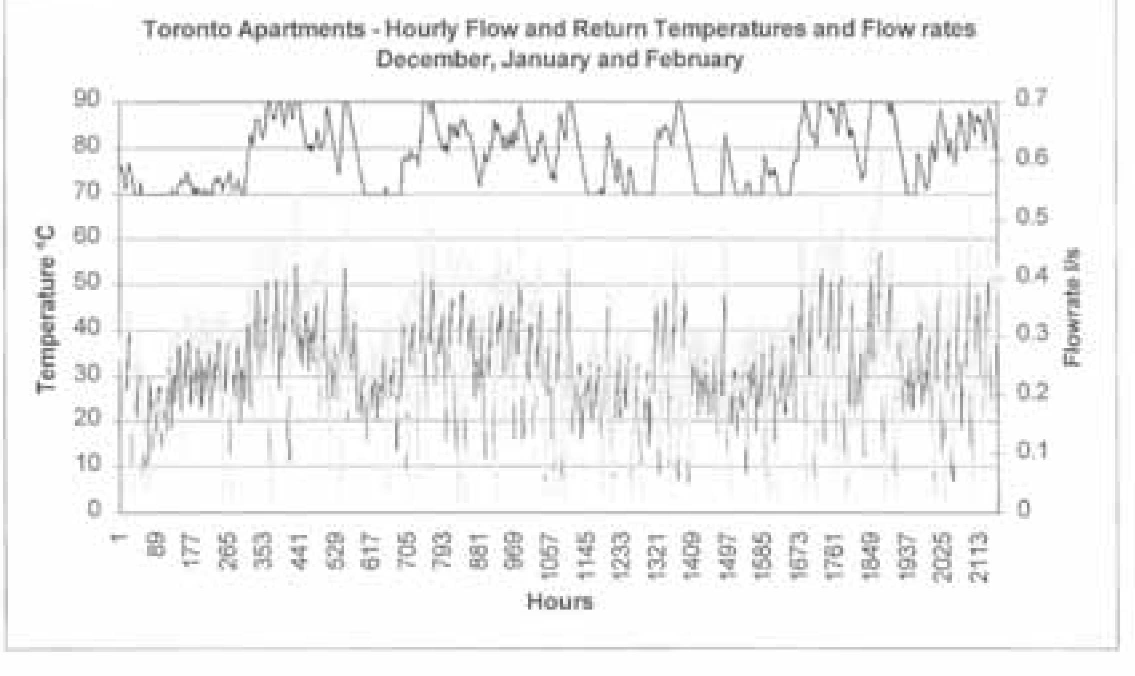

Figure 4.22 - Results for the winter three months for apartment buildings in Toronto

4.4 Capital cost of building heating system

4.4.1 Cost Elements

The capital cost of a building heating system comprises the following principal elements:

- radiators and their control valves
- air heating coils
- primary/secondary heat exchanger if indirect connection
- hot water heat exchanger
- circulating pumps and pressurisation system
- air supply and extract fans
- heating distribution pipework within the building
- air distribution ductwork within the building
- hot water distribution pipework within the building
- controls and metering

Whilst the capital costs of all of these elements are to some extent dependent on operating temperatures, the most significant variable costs are the radiators, air heating coils and heat exchangers where the size of equipment is dependent on the temperature differences available to produce the heat transfer. These elements are discussed in turn below.

4.4.2 Radiators

The cost of a radiator system will consist of a fixed element (for valves and pipework) and a variable element depending on the surface area of the radiator.

Radiator prices obtained from suppliers in the UK have been analysed and it was found that the costs are linearly related to the standardised heat output and the surface area to within +/- 3%. The capital cost of the radiators has therefore been calculated using the area ratios for each case as defined in section 4.2.7.

Table 4.5 - Cost of installed radiator capacity (US$/kW)

	Flow temperatures °C			
Return temps °C	**Area Ratio**	**90**	**80**	**70**
55	1	81.3	92.4	107.0
48	1.15	93.5	106.3	123.0
45	1.25		115.5	
44	1.25	101.6		133.8
42	1.35			144.5
41	1.35	109.8	124.7	
38	1.5	122.0	138.6	160.5
34	1.75		161.7	187.3
33	1.75	142.3		

It can be seen that the costs double for say a 70/38 system when compared to a 90/55 system. This results in a penalty of approximately 10% of a typical heat selling price which will need to be offset by the benefits obtained from lower operating temperatures at the CHP plant if these lower temperatures are to be economic.

The above analysis assumes that the number of radiators is constant. If the size of the radiators for the lower temperatures becomes such that a second radiator is needed in a room then the costs will be higher as additional radiator control valves will be needed. The space occupied by larger radiators may also be a disadvantage if the building insulation levels are poor.

4.4.3 Air-coils

The cost of an air-coil heating system will consist of a fixed element (for fans, ductwork, control valves) and a variable element depending on the design of the heating coil. The heating coil design is determined mainly by the number of rows and the number of fins.

The cost of finned heating coils for airhandling plant have been obtained from a major UK supplier (AAF, 1998) for a range of DH temperature cases and, as expected, the lower the operating temperatures the more expensive the air heating coil (see Table 4.6). The cost of an air heating coil is very much less than that of a radiator as the heat transfer to the air is forced convection and the heat transfer is very efficient using finned tubes. As a result although the air heating coil cost doubles from 90/70 to 70/40 this increase is relatively unimportant in the total cost of a heating project.

Table 4.6 - Cost of air heating coils (US$/kW) based on a 150kW coil

Return	Flow temperatures °C		
temps °C	90	80	70
70	3.7	n/a	n/a
60	4.3	6.2	n/a
50	6.1	6.4	6.9
40	6.4	6.9	7.4

4.4.4 Capital cost of domestic water heating systems

We can assume that the cost consists of a fixed element and a cost dependent on the size of the heat exchanger. Costs have been obtained from heat exchanger manufacturers in Finland for a range of flow and return temperatures to define the relationship, assuming a 5°C to 55°C rise on the hot water service side and a 15°C return temperature from the DHW 150kW heat exchanger:

90°C flow US$19.2/kW
70°C flow US$21.8/kW

4.4.5 Capital cost of building connections

The main cost factor is the differential cost between indirect or mixing connection and direct connection. Where indirect connection is used the connection costs will have some dependence on the temperature difference across the heat exchanger.

Table 4.7 - Cost of indirect connection substations US$/kW (heating and hot water)

Return	Flow temperatures		
temps	90	80	70
60	22.4	24	27.2
50	20	22.4	24
40	16	17.6	18.4

4.5 Operating costs of building heating systems

Operating costs of the heating system within the building such as electricity for pumps and fans will vary slightly with the temperatures selected but this cost variable has been ignored as it will be small compared to the district heating pumping energy cost.

5. The Network Models

5.1 District Heating Network Costs

The total cost of a heat distribution system comprises three elements: capital, pumping energy and heat losses. The designer of the network seeks to optimise the pipe sizes, once flow rates have been determined, so that the total cost taking into account these three elements is minimised. For example a system with larger diameters will be more costly to construct and will have higher heat losses but will use less energy in pumping as the pressure drops will be less. This pipe sizing optimisation process is illustrated in Figure 5.1 for the apartment block network.

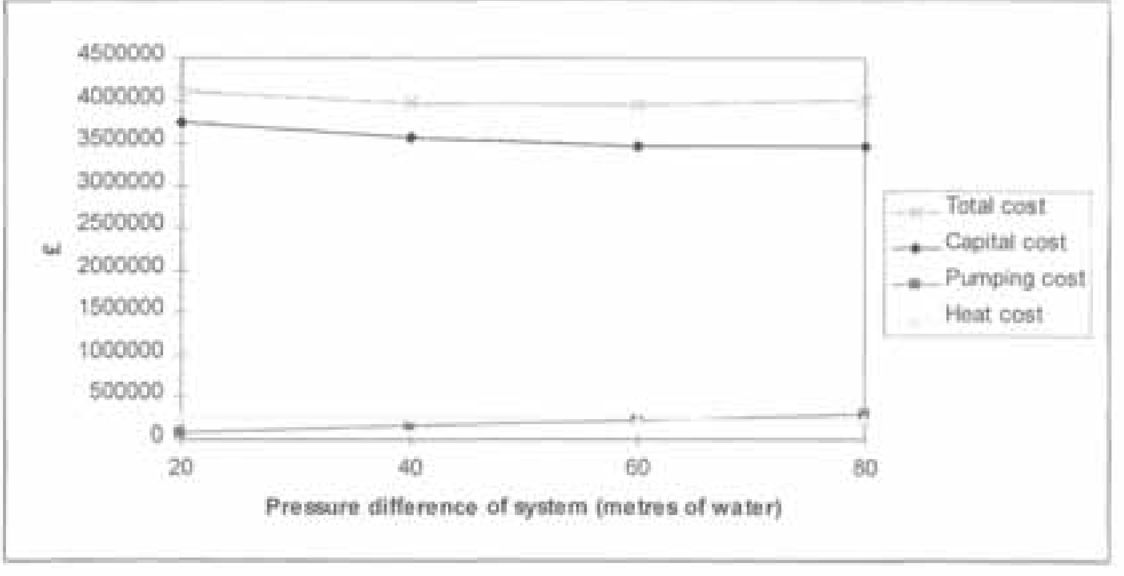

Figure 5.1- Optimisation of Pipe Sizes in the Apartment Block Network (London)

For a single pipeline it is straightforward to carry out an optimisation but for a complex network a computer programme is normally used. The System Romet programme has been developed by Ramboll, consulting engineers in Copenhagen, to carry out these cost minimisation calculations and was used for each of the three notional networks serving the different building types. The programme automatically selects pipe sizes to satisfy given pressure constraints and to minimise total lifetime cost. Pipes located near to the pumps are reduced in size as the pressure difference is available until a maximum water velocity is reached. Assumptions on pumping electricity costs and load factors are made based on typical figures (see 5.5 below). Once the network has been sized in this way and the capital cost established, the actual electrical energy needed for the pumps and the additional heat to take account of the heat losses from the network, is calculated in more detail, on an hour by hour basis, as part of the Heat Production Model (see section 6). This two-stage approach avoids a more complex iterative process between the two models with no significant loss of accuracy.

Capital cost estimates are based on an average of costs per metre of trench which were obtained with the assistance of the Expert Group members. Typical costs from Germany were taken from (AGFW, 1997). The costs obtained are plotted in Figure 5.2 against internal diameter from which a relationship has been derived with the following formula:

$$\text{Capital cost} = A+B*d^n$$

where typically for an urban installation (but not a city centre):

A=£150
B=£1,800
n=1.3

and d is the internal pipe diameter in m.

The data from Sweden, Canada, Germany and the UK agree with this formula to within 15% however, the costs from Denmark were higher than this average and figures from Finland were generally lower.

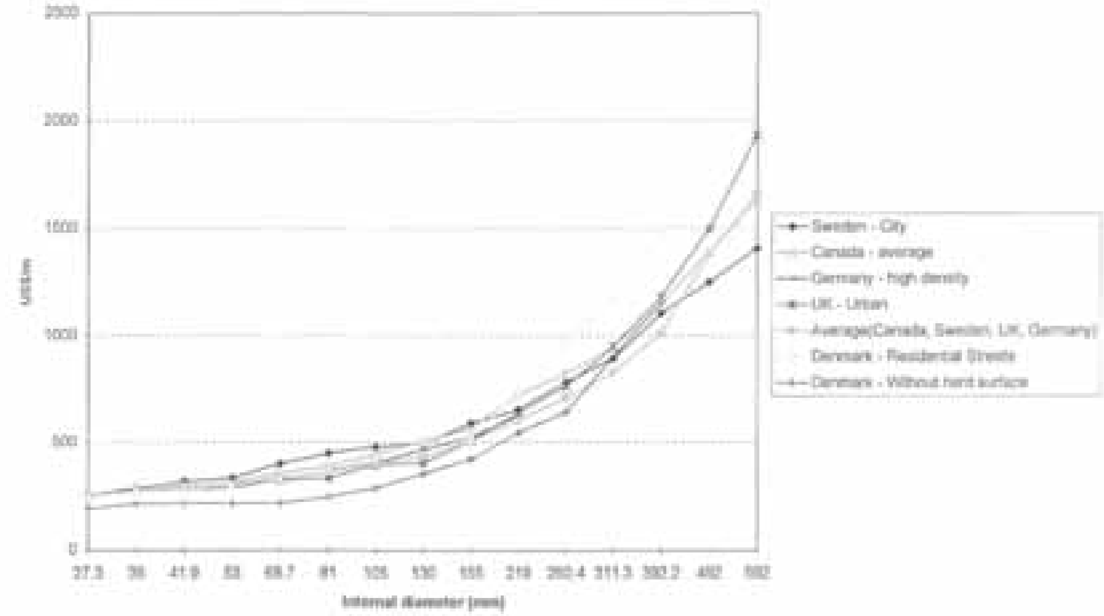

Figure 5.2- Installed Costs of District Heating Pipes from some IEA member countries

For each network the heat loss rate per °C temperature difference (between DH water and ambient) is calculated from the schedule of pipe sizes and lengths forming the output of the hydraulic optimisation for use in the Heat Production Models (see section 6).

5.2 The Apartment Blocks Model

A network model has been developed as shown on Figure 5.3 for apartment blocks spaced to give a heat density of 3.5 kW/m (in London). The characteristics of the network are given in Table 5.1.

Table 5.1- Characteristics of apartment block network

No. of blocks connected	80	
Length of network	11555	m
Total peak demand (London)	40000	kW
Linear heat demand density (London)	3.5	kW/m
Total peak demand (Toronto)	53000	kW
Linear heat demand density (Toronto)	4.6	kW/m

The results of the hydraulic model calculations for this network are shown in Figure 5.4. For each temperature difference the capital cost is determined for the pipe sizes and pressure difference where the total cost is minimised.

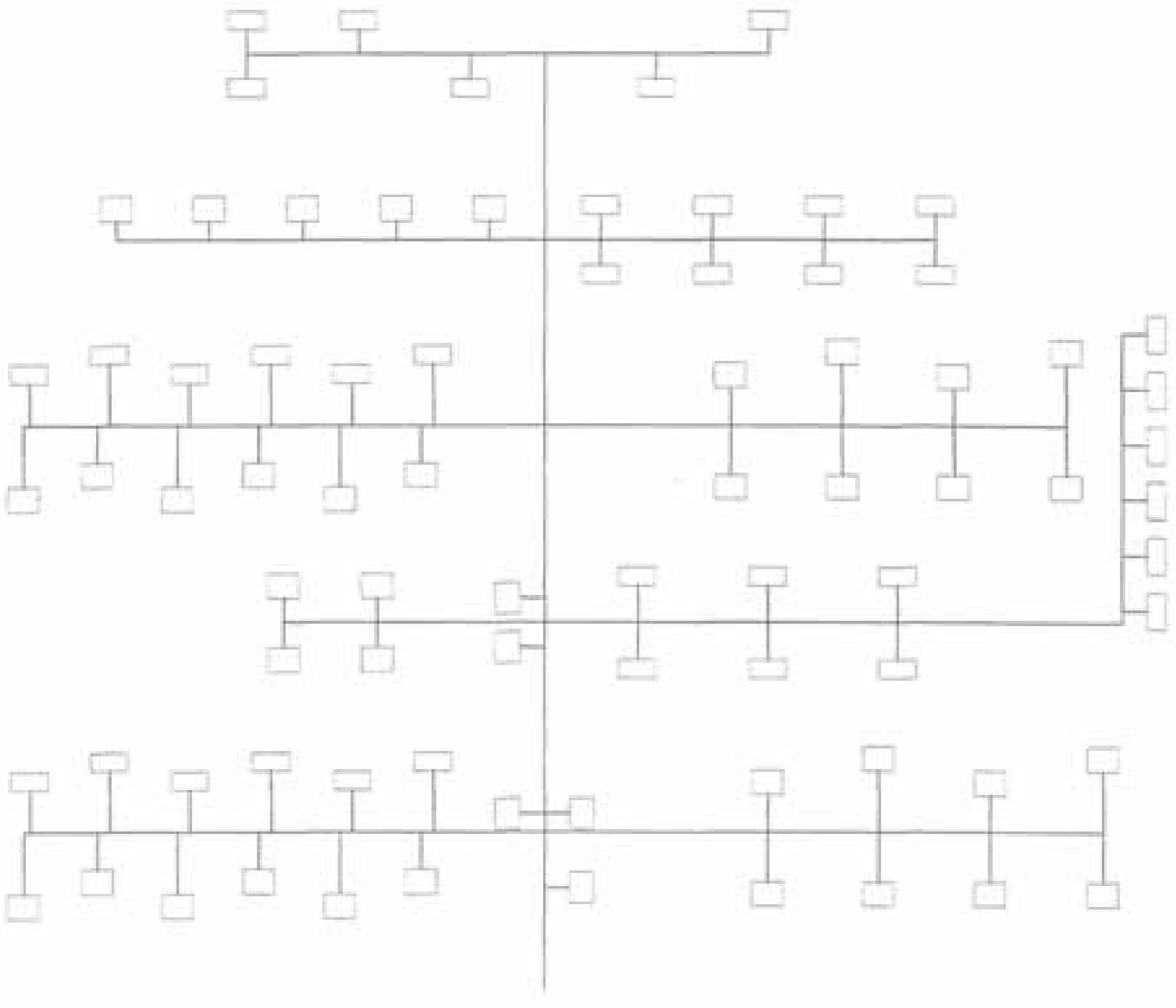

Figure 5.3- The apartment block network

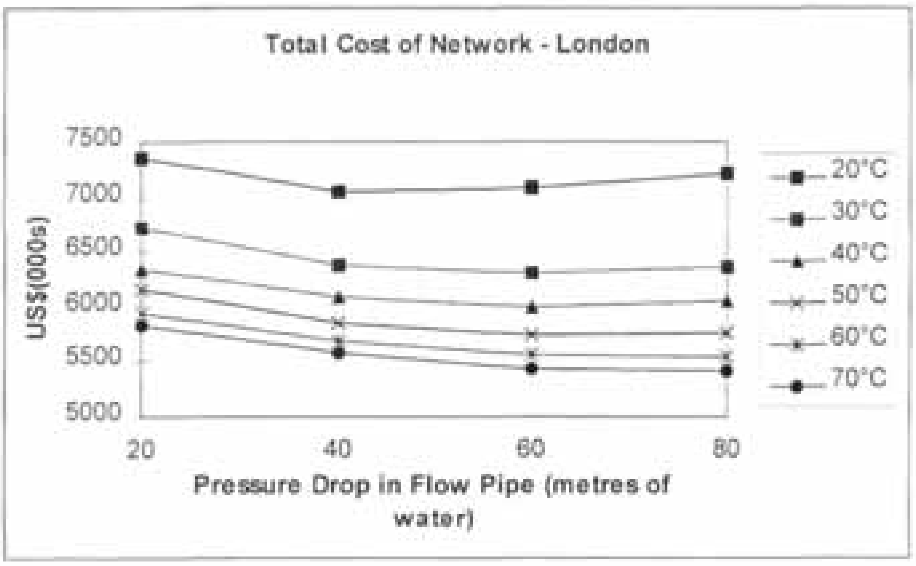

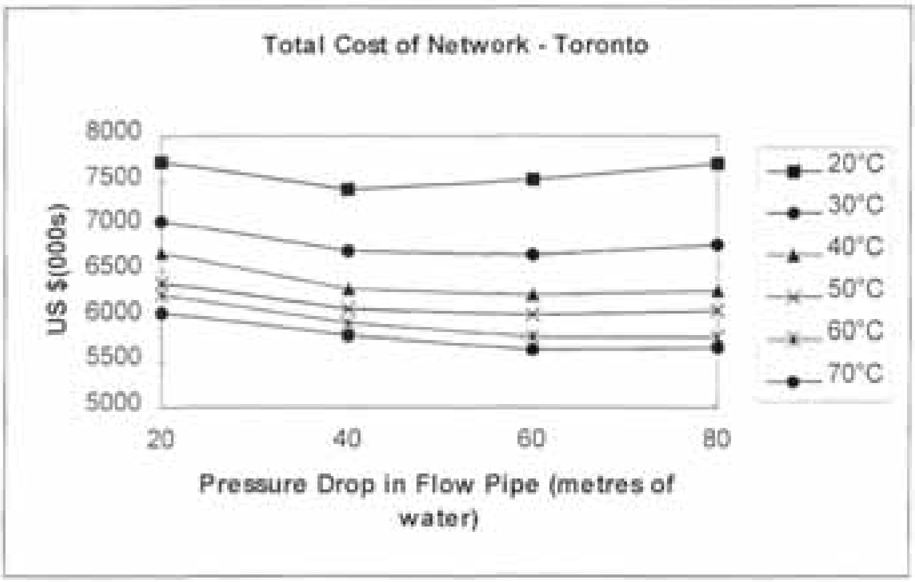

Figure 5.4 - Cost of District Heating Networks - Apartments

5.3 The Row Houses Model

A network model has been developed as shown on Figure 5.5 for rowhouses with a linear heat density of between 1.35 and 2.0 kW/m. The characteristics of the network are given in Table 5.2.

Table 5.2- Characteristics of rowhouses network

No. of houses connected	7,300	
Length of network (including house connections)	26,000	m
Total peak demand (London)	35,040	kW
Linear heat demand density (London)	1.35	kW/m
Total peak demand (Toronto)	53,290	kW
Linear heat demand density (Toronto)	2.0	kW/m

The results of the hydraulic model calculations for this network are shown in Figure 5.6. As for the apartment blocks, for each temperature difference the capital cost is determined for the pipe sizes and pressure difference where the total cost is minimised.

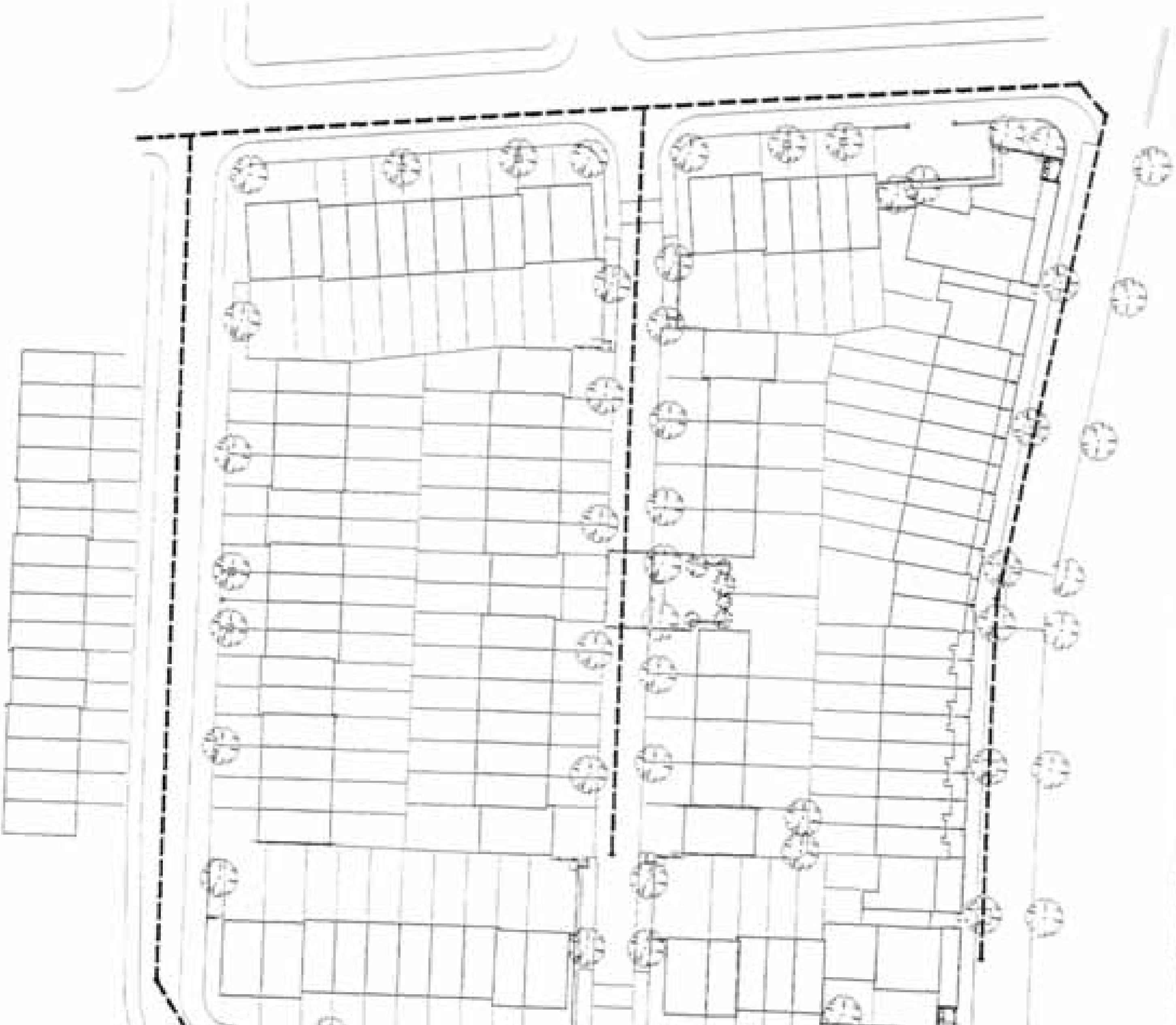

Figure 5.5- An example of the rowhouses network

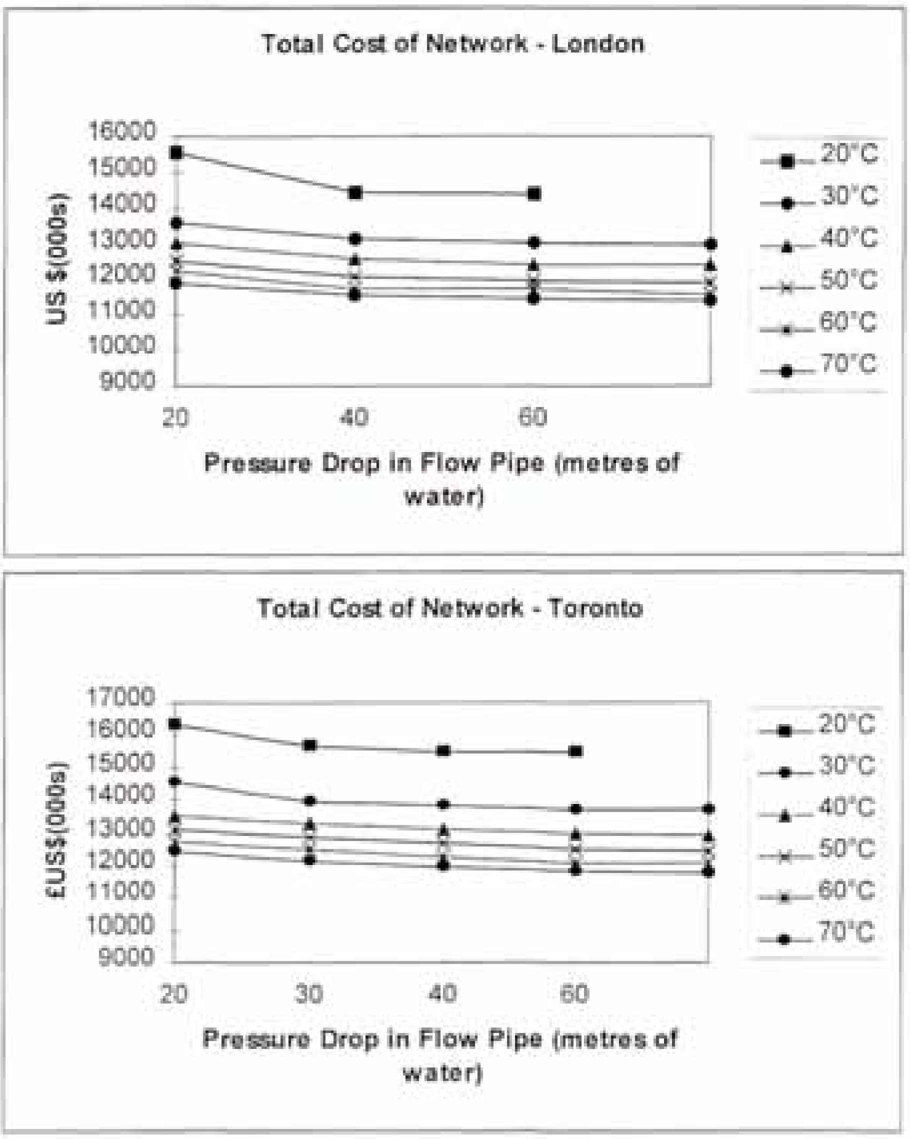

Figure 5.6: Cost of District Heating Networks - Rowhouses

5.4 The Commercial Building Model

A network model has been developed as shown on Figure 5.7 for commercial buildings spaced to give a relatively high linear heat density of 5-8 kW/m. The characteristics of the network are given in Table 5.3.

Table 5.3- Characteristics of commercial building network

No. of commercial buildings connected	62	
Length of network	8,200	m
Total peak demand (London)	43,000	kW
Linear heat demand density (London)	5.3	kW/m
Total peak demand (Toronto)	66,000	kW
Linear heat demand density (Toronto)	8	kW/m

The results of the hydraulic model calculations for this network are shown in Figure 5.8. As for the apartment blocks, for each temperature difference the capital cost is determined for the pipe sizes and pressure difference where the total cost is minimised.

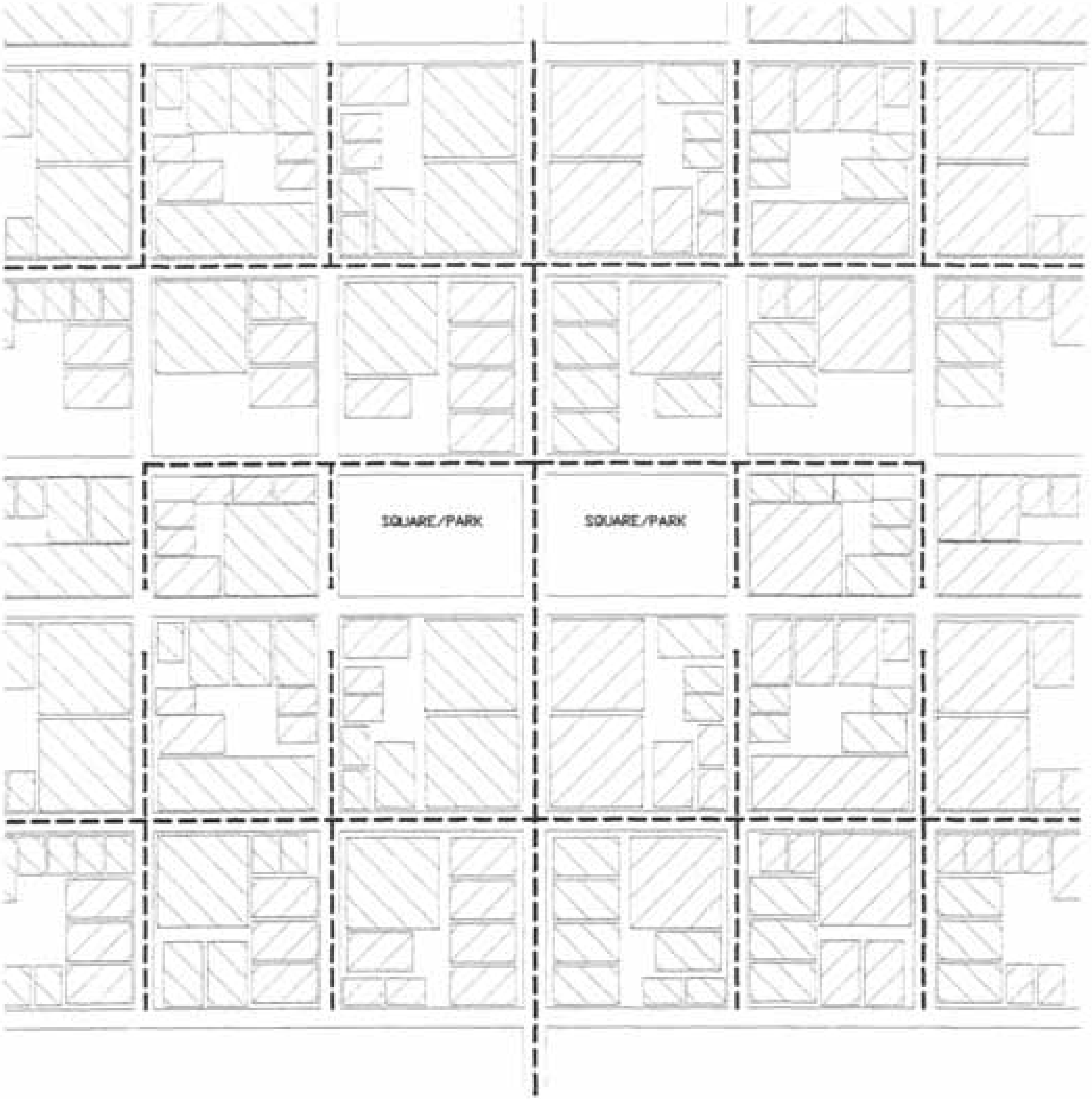

Figure 5.7- The commercial building network

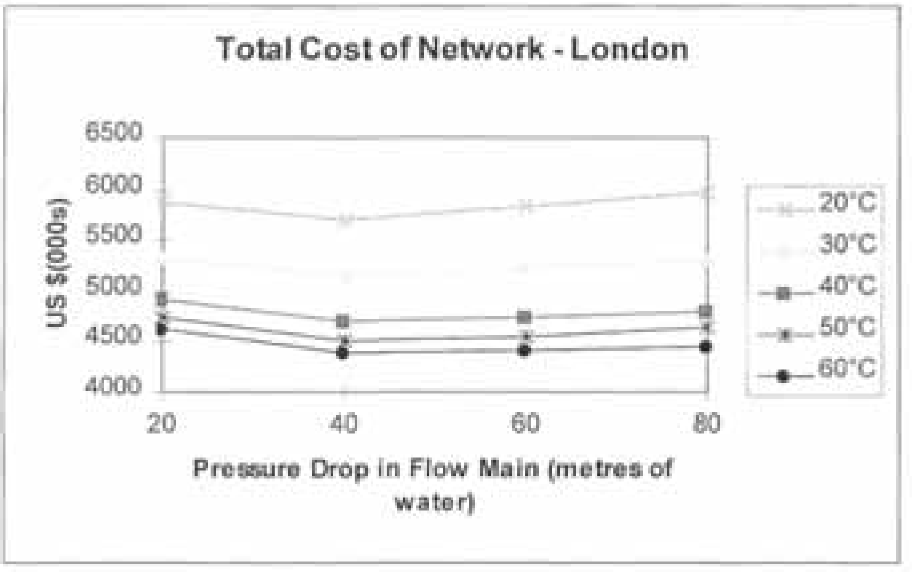

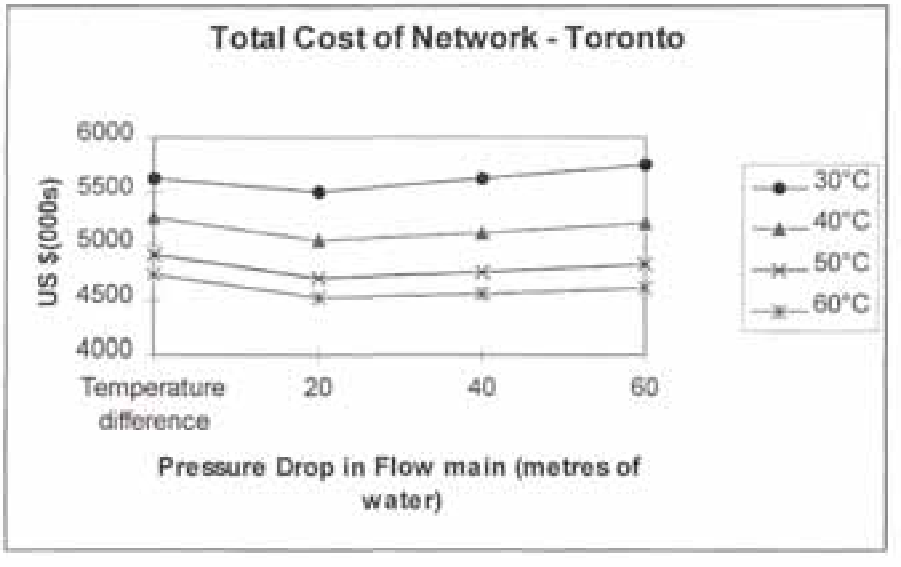

Figure 5.8- Cost of District Heating Networks – Commercial

5.5 Direct and Indirect Connections

A direct connection where the district heating water is used as the heat transfer medium of the building's heating systems is only possible if the maximum design temperatures and pressures of the district heating system are equal to or lower than the design parameters of the building's heating system. If that is the case then there is generally an economic benefit as the cost of the intermediate heat exchanger and associated controls and the secondary circuit pump and pressurisation equipment is avoided. In addition as there is no heat transfer between a primary and secondary circuit the district heating supply temperature can be lower than with an indirect connection for the same size of heat emitters. This lower supply temperature will bring other economic benefits in lower costs of heat production. As the analysis in this report is limited to temperatures below 90°C, which is considered to be acceptable for direct connection, we have assessed both direct and indirect connection cases to establish the potential economic benefit of direct connection.

It is normally the pressures in the district heating network that govern whether a direct connection is possible. In the optimisation of network pipe diameters discussed above the optimum was found to occur with relatively high maximum system pressures, typically about 8 -12 bar (see Figures 5.4, 5.6

and 5.8). However, the optimum is relatively flat and a lower pressure of around 7 bar would involve only marginally higher lifetime costs. For a direct connection of typical steel panel radiators a maximum pressure of 7 bar is normally required. To achieve this either a sub-optimum pressure field is needed (i.e. larger pipes) or the pumping arrangement must be changed from the single central pumping station assumed in the network analysis described above. If additional pumps are located within the network this allows maximum pressures to be reduced without having to oversize the pipes. We have therefore concluded that there is a negligible cost penalty for the network if a direct connection approach is assumed.

6. The Heat Production Models

6.1 General Description

6.1.1 Typical Operating Days

The outputs of the building simulation models are the district heating flow rates and flow and return temperatures for each hour of the year from which the heat demand in kW in each hour can also be calculated. The heat demand and flow and return temperatures have been used in the Heat Production Model to calculate the operation of the CHP plant, the energy used by the district heating pumps and the heat losses from the heat mains network on an hour by hour basis.

Heat demand profiles are often described by a load-duration diagram, which plots the heat demand against the number of hours that the level of demand occurs. If the value of electricity was constant then the load duration curve would be all that is required to analyse the operation of a CHP plant. On most electricity systems however the value of electricity varies between night and day and with the seasons depending on the plant mix on the system. Consequently it is also necessary to know how the demand varies over say a day in winter or a day in summer and a load duration curve does not provide this information. The ideal situation would be to model an average year on an hour by hour basis using heat demand and electricity price information. Although the hourly information was available from the Canmet modelling work using this information directly in a CHP/Boiler computer spreadsheet model was not practical even with a fast PC. The additional accuracy was not considered necessary or justified for the comparative analysis work of this project. The CHP/Boiler model therefore uses an Excel spreadsheet comprising 16 typical days in the year with each day divided into 24 hourly periods. The demand pattern is defined by 384 numbers, 4.4% of the 8,760 needed if hourly data was used.

The basis of the Heat Production Model is therefore an hour by hour simulation for 16 typical days of the year using standard spreadsheet software (Microsoft Excel Version 7.0) to calculate the energy flow in each hour. The days were selected to enable the variations of both heat demand and electricity prices that are likely to occur to be characterised (see Table 6.1).

Table 6.1 - Definition of Typical Days

Day No.	No. of days for London	No. of days for Toronto	Description
1	50	68	Summer Weekday
2	20	27	Summer Weekend
3	43	57	Spring/Autumn Weekday
4	17	22	Spring/Autumn Weekend
5	44	35	Shoulder (1) Weekday
6	18	14	Shoulder (1) Weekend
7	43	30	Shoulder (2) Weekday
8	17	11	Shoulder (2) Weekend
9	36	22	Winter (1) Weekday
10	14	8	Winter (1) Weekend
11	25	23	Winter (2) Weekday
12	10	9	Winter (2) Weekend
13	13	17	Winter (3) Weekday
14	5	7	Winter (3) Weekend
15	8	12	Peak/design Weekday
16	2	3	Peak/design Weekend

6.1.2 Inputs to the Model

The inputs to the Heat Production Model are:

- For each hour of the day and for each typical day: the flow and return temperatures at the buildings connected and the corresponding flow rates at the buildings connected (obtained from the Building Models)
- CHP and boiler plant efficiencies and other performance data including availability
- Heat loss rate for the network in W/mK for flow and return pipes using the pipe sizes derived in the Network Models
- Electricity prices for each hour of the typical days derived from UK Pool Prices for 1996 (see Figure 6.2)
- Gas price assumed to be equivalent to 0.8p/kWh (HHV) throughout
- CHP maintenance cost
- CHP capital cost
- Maximum pressure difference required by DH pumps at maximum flow

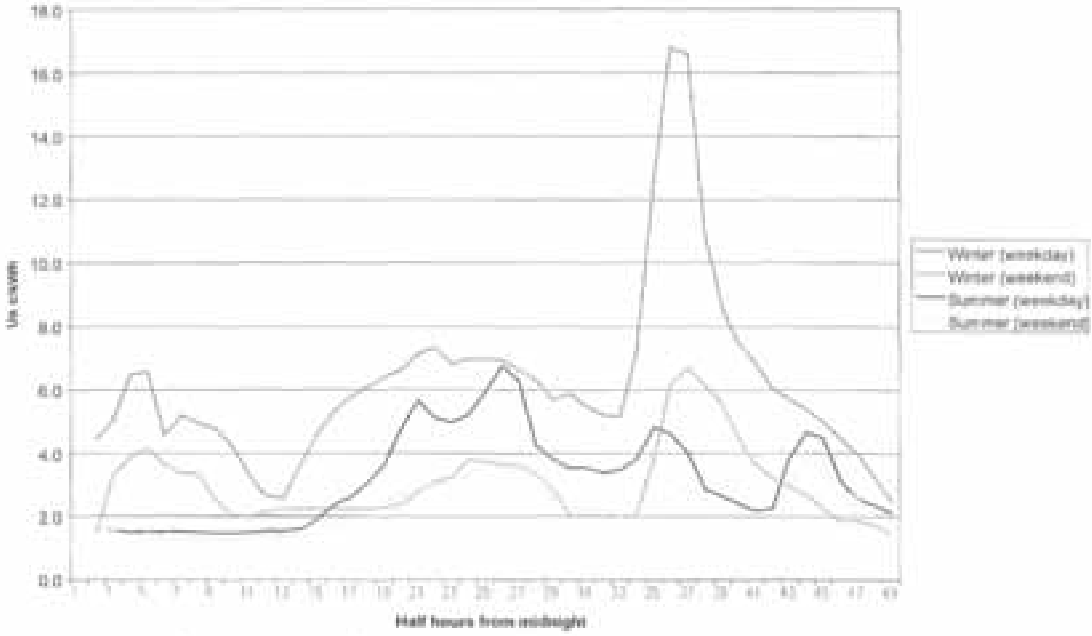

Figure 6.2 - Typical variation in electricity prices from UK Pool Prices

6.1.3 Other assumptions

The size of the CHP plant has been selected so that approximately 80% of the total heat provided is obtained from the CHP plant and 20% from boilers. This proportion is typical of CHP/DH systems but ideally a separate economic analysis should be carried out to determine the optimum size of CHP plant. The thermal efficiency of the boilers is assumed to be a constant 80% in all cases although lower operating temperatures could lead to higher efficiencies if condensing boilers are used (see section 12.2).

The spark-ignition engine and back-pressure CCGT plant are assumed to operate during the day period only (17 hours out of 24). This is a typical situation for an electricity system with some nuclear or hydro-electric stations where the night-time electricity price is significantly lower than the day price.

Where the CHP plant does not operate at night a thermal store has been included in the model to enable surplus heat during the day to supply the DH network at night thereby avoiding the unnecessary use of boiler fuel. The size of the thermal store is again ideally determined by a cost optimisation study and will be very dependent on the electricity tariff structure. A further complexity is that the amount of energy stored for a given volume is determined by the temperature difference in the network. It was therefore assumed that the storage volume would be set at a level which eliminated most but not all of the night-time boiler use with a temperature difference of 35 °C and that this volume would be kept constant giving a small advantage in overall costs to cases with temperature differences greater than 35 °C and a small disadvantage to cases with smaller temperature differences. The thermal store was assumed to of the atmospheric pressure type.

In the gas engine and CCGT cases it has been assumed that the CHP plant is operated to follow the heat demand, i.e. heat dumping is not included.

CHP availability is modelled by assuming that the CHP plant operates for 95% of the time with outages spread uniformly across the year.

5.1.1 Outputs from the model

From the time-varying district heating temperatures the heat mains losses are calculated and added to the building heat demands to give a total heat demand at the CHP plant. For each type of CHP plant formulas have been derived to calculate the energy flows as the heat demand varies.

The outputs from the model are:

- Heat mains losses
- Heat demand at the CHP/Boiler plant
- Heat supplied from CHP
- Heat supplied by boilers (peak and standby)
- CHP fuel use
- Boiler fuel use
- Electricity generated
- Electricity for DH pumps and other auxiliaries
- Net electricity generated
- Income from electricity generated (or lost income in the case of steam turbine plant)
- Cost of heat production taking account of capital, fuel, net electricity income and CHP maintenance

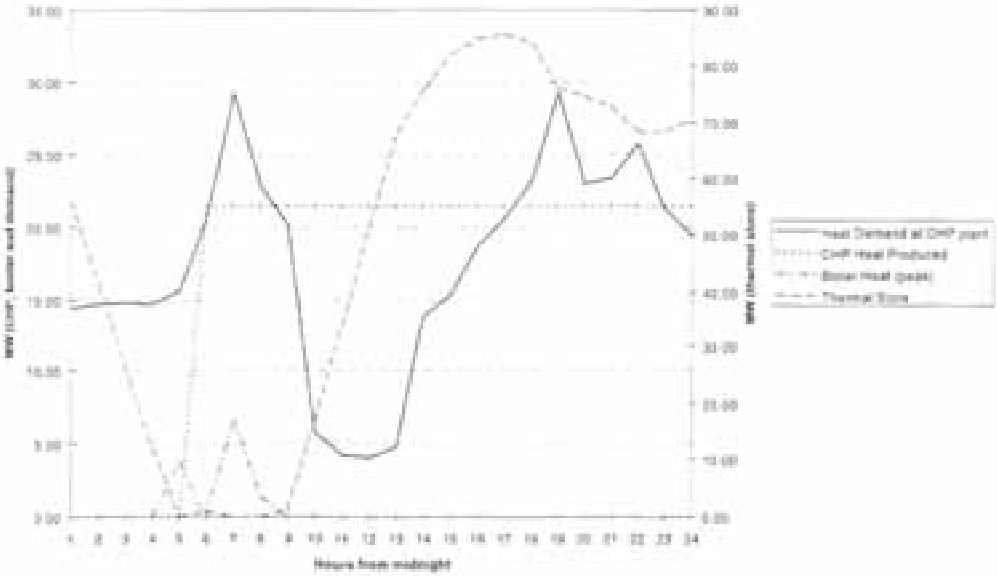

Figure 6.1 – Example of heat production model output for an autumn day for a spark-ignition gas-engine CHP plant and a thermal store

6.2 Heat Production Model with Spark-Ignition Gas-Engine CHP

6.2.1 Capital Cost

As a first approximation the capital cost of the plant is not considered to be significantly affected by the district heating operating temperatures at least not in comparison with the effect of temperatures on the cost of the network or building heating systems. In the UK a typical spark-ignition gas-engine station of around 10 MWe would have a capital cost of £500/kWe installed (US$ 800/kWe, Euro 720/kWe).

6.2.2 CHP Performance

The performance of the plant will vary with the flow and return temperatures. The electrical output of the engine is effectively fixed but the amount of heat which can be usefully recovered is very dependent on the district heating temperatures. The information obtained from Wartsila (Wartsila, 1997) for a 3.1MWe gas-engine CHP plant is given in Table 6.2. Provided temperatures are low enough to capture the engine jacket water heat, further reductions in flow and return temperatures increase the heat recovery from two sources:

- heat from the aftercooler can be recovered for return temperatures below about 50 °C (depending on the actual engine characteristics).
- heat recovered from the exhaust gases can be increased with lower return temperatures as the gases can be cooled more

For flow temperatures below 90°C and return temperatures below 50°C the additional heat output from using lower temperatures is small, for example a 4% increase is obtained when using a 70°C/40°C system compared to a 90°C/50°C system.

Table 6.2 Heat output in kW from Wartsila W16V25SG

Return	**Flow temperatures °C**					
temps °C	**120**	**110**	**100**	**90**	**80**	**70**
100	1723	n/a	n/a	n/a	n/a	n/a
90	1768	1768	n/a	n/a	n/a	n/a
80	2762	2872	2907	n/a	n/a	n/a
70	3358	3391	3424	3457	n/a	n/a
60	3446	3480	3513	3546	3578	n/a
50	3533	3567	3601	**3634**	3667	3699
40	3621	3655	3689	3722	3755	3788

Table 6.3 - Heat output expressed as a ratio to the heat output at 90°C flow, 50°C return

Return	**Flow temperatures °C**					
temps °C	**120**	**110**	**100**	**90**	**80**	**70**
100	0.47	n/a	n/a	n/a	n/a	n/a
90	0.49	0.49	n/a	n/a	n/a	n/a
80	0.76	0.79	0.80	n/a	n/a	n/a
70	0.92	0.93	0.94	0.95	n/a	n/a
60	0.95	0.96	0.97	0.98	0.98	n/a
50	0.97	0.98	0.99	**1.00**	1.01	1.02
40	1.00	1.01	1.02	1.02	1.03	1.04

This data is used in the operating model and effectively determines the amount of fuel needed to meet the demand. For the same size engine, more boiler fuel is needed for the higher operating temperatures where the amount of useful heat recovery is less.

This study has concentrated on temperatures below 90°C and although most spark-ignition engines are used to supply small-scale low temperature systems it is interesting to note that if the *return* temperature is low enough (less than 70°C) the heat recovery rate for a flow temperature of 120°C is only 3% lower than that at 90°C flow.

The other assumptions on CHP performance are given in Table 6.4.

Table 6.4 Heat Production Model - Spark-Ignition Engine CHP - Assumptions

Item	Units	Assumed Value
Electrical efficiency	%	36.0
Overall efficiency at 90° C/50 ° C	%	80.0
Boiler efficiency	%	80.0
CHP Availability	%	95.0
Maintenance cost	p/kWh e	0.4

6.3 Extraction-Condensing Steam Turbine CHP Plant

6.3.1 Capital Cost

The steam turbine is assumed to be an extraction-condensing type which might typically be used with a waste-to-energy plant or a larger central power station. The capital cost of the plant is again assumed to vary only marginally with district heating operating temperatures. In some electricity markets where there are separate payments for providing plant capacity the capacity credit for the plant will also be reduced unless a thermal store permits full electrical output to be produced at times of peak electricity demand.

For the purposes of this project we have assumed that the additional capital cost associated with the district heating supply is small and independent of operating temperatures and can be neglected. The capital cost of the whole generating plant is assumed to be financed by electricity sales and waste disposal income.

6.3.2 CHP Performance

There is a cost in producing heat from an extraction-condensing turbine because the electrical output of the plant reduces when heat is extracted from the turbine. This 'lost electricity' has a value which determines the cost of heat.

The amount of lost electricity is defined by the formula:

electricity lost = z * heat produced

To determine the z-factor a formula in (Winkens, 1986) has been used:

$$z = 0.00148 * T_f + 0.000784 * T_r - 0.04365$$

As a comparison, an analysis of a typical two-stage heating arrangement from an extraction-condensing turbine has been carried out using the STPRO plant modelling software. Table 6.5 shows the z-factor calculated from both the Winkens formula and the STPRO model for the range of temperatures under consideration. As the results are close it was decided to use the Winkens formula directly in the Heat Production model to calculate the reduction in electricity output in each hour using the hourly variation in temperatures and hence calculate the cost of heat production in any hour.

Table 6.5 - z-factor calculated for a range of operating temperatures

Return Temps (°C)	Derivation of 'z'	Flow Temperatures (°C)		
		90	80	70
80	Winkens STPRO	0.152 0.136	n/a	n/a
70	Winkens STPRO	0.144 0.133	0.130 0.120	n/a
60	Winkens STPRO	0.137 0.129	0.122 0.117	0.107 0.104
50	Winkens STPRO	0.129 0.126	0.114 0.114	0.099 0.102
40	Winkens STPRO	0.121 0.123	0.106 0.112	0.091 0.101

Table 6.6 - Lost electricity expressed as a ratio to the electricity lost at 90°C flow, 50°C return (Winkens formula)

Return	Flow Temperatures		
Temps	**90**	**80**	**70**
80	1.18	n/a	n/a
70	1.12	1.01	n/a
60	1.06	0.95	0.83
50	**1.00**	0.88	0.77
40	0.94	0.82	0.71

From Table 6.6 it can be seen that 30% less electricity is lost at temperatures of 70°C/40°C compared to 90°C/50°C. It can also be seen that reductions in return temperature have less effect than reductions in flow temperature; a drop of approximately 20°C in return temperature is required to achieve the same benefit as a 10°C drop in flow temperature.

6.4 Combined Cycle Gas Turbine Plant

6.4.1 Capital Cost

The capital cost of a combined cycle gas turbine plant is very dependent on size. Published prices (GTW, 1997) indicate a basic cost of US$800/kWe as typical for a turnkey CCGT in the range 50-100 MWe output. The cost reduces to around $400/kW for 200-500MWe power stations. For this study the smaller size and higher price has been assumed.

In recent years, a number of small combined cycle plants have been built specifically to supply district heating schemes. Discussions were held with one supplier, ABB-Stal, who advised that the capital cost of the plant would not vary significantly with the district heating operating temperatures. As discussed in section 2.3.4 we have only considered a Combined Cycle CHP plant using a backpressure turbine with the addition of a district heating economiser. There will be a small saving in the capital cost of this economiser as the district heating temperatures are reduced but this will be offset by an increase in cost for the larger diameter low pressure steam pipework supplying the steam/DH heaters. These small changes in capital cost have been ignored.

6.4.2 CHP Performance

As the fuel input is fixed by the gas turbine the performance of the plant can be defined by the amount of power and heat that can be produced for a range of DH operating temperatures. This in turn is determined by the performance of the low pressure stages of the steam turbine. The electrical output is determined by the extract pressures which in turn are determined by the steam temperature which is taken to be 5°C above the district heating leaving temperatures circuit. There are a wide range of CCGT configurations using gas turbines from 20MW to 200MW and we have assumed typical performance for a relatively small-scale plant of around 50-100 MW.

The district heating economiser is sized to give an exhaust gas outlet temperature of 75°C which is typical for return temperatures below 60°C. As the return temperature is reduced further more heat could be extracted but the 75°C is normally an economic limit for gas exit temperature. Lower design return temperatures could lead to a slightly smaller economiser and a corresponding saving in capital cost but this is considered negligible.

In operating the plant the amount of power produced will be dependent on the ambient air temperature and the amount of cooling available to the steam turbine from the DH system. As the heat demand falls it would be normal practice for the heat extracted from the economiser to be reduced first so that the maximum steam condensing rate can be maintained and the steam turbine electricity production maximised.

Table 6.7 Heat Production Model - Combined Cycle CHP (<100MW) - Assumptions

Item	Units	Assumed Value
Electrical efficiency at 15 °C air temp (higher calorific value basis) at maximum heat and power production	%	41.5
Overall energy efficiency at 90° C/50 ° C DH temps (higher calorific value basis)	%	81.0
Boiler efficiency (higher calorific value basis)	%	80.0
CHP Availability	%	95.0
Maintenance cost	p/kWhe	0.4

6.5 Summary of the influence of DH operating temperatures on heat production costs

Within certain bounds (return temperatures less than 70°C), the heat production costs from a spark-ignition engine are largely independent of DH operating temperatures.

In contrast, the steam turbine plant is heavily influenced by operating temperatures which leads to the common operating strategies of:

- reducing the DH flow temperature as external temperatures rise and the heat demand falls
- using peak boilers to increase the flow temperature to meet a rise in demand rather than to maintain a constant flow temperature and increase the DH flow rates

The combined cycle plant can be considered as an intermediate type as although the plant is still dominated by the steam cycle the additional heat recovery from the exhaust gases by the district heating economiser is nearly independent of operating temperatures.

7 Apartment Block Case Studies Results

7.1 Presentation of the results

The total cost of heat has been plotted against the design temperature difference Tf-Tr used for the network design with a separate curve for each selected flow temperature.

The cost of heat is expressed in both US dollars and Euros per kWh of heat delivered and includes both capital and operating costs. There are three elements:

- the building internal cost (radiators and substation)
- the operation cost which is the cost of heat production at the CHP and boiler plant including the pumping cost
- the network cost (capital element)

The heat losses from the netwrok result in an additional heat production requirement and are therefore reflected in the operation cost.

The importance of the results is not so much in the absolute cost values but in the *differences* between the costs for the various temperatures assumed. In order to assess how important these cost differences are in relation to the development of a CHP/DH scheme it was decided to express all costs as an annualised cost per unit of heat delivered to the buildings. In economic terms this is equivalent to calculating a heat selling price that will provide the necessary return on capital employed and cover all annual operating costs. The cost differences that are shown on the graphs can then be related to the typical energy selling prices for DH or other fuels and an assessment made as to whether these differences are important enough to influence the general economic viability of the scheme.

In the key, Tf = 90-70 and Tf = 80-70 represents the cases where the flow temperature is reduced from 90°C and 80°C respectively to 70°C in the summer.

7.2 Spark-Ignition Gas-Engine CHP Cases

The results for these cases are presented in Figures 7.1, 7.2, 7.3 and 7.4.

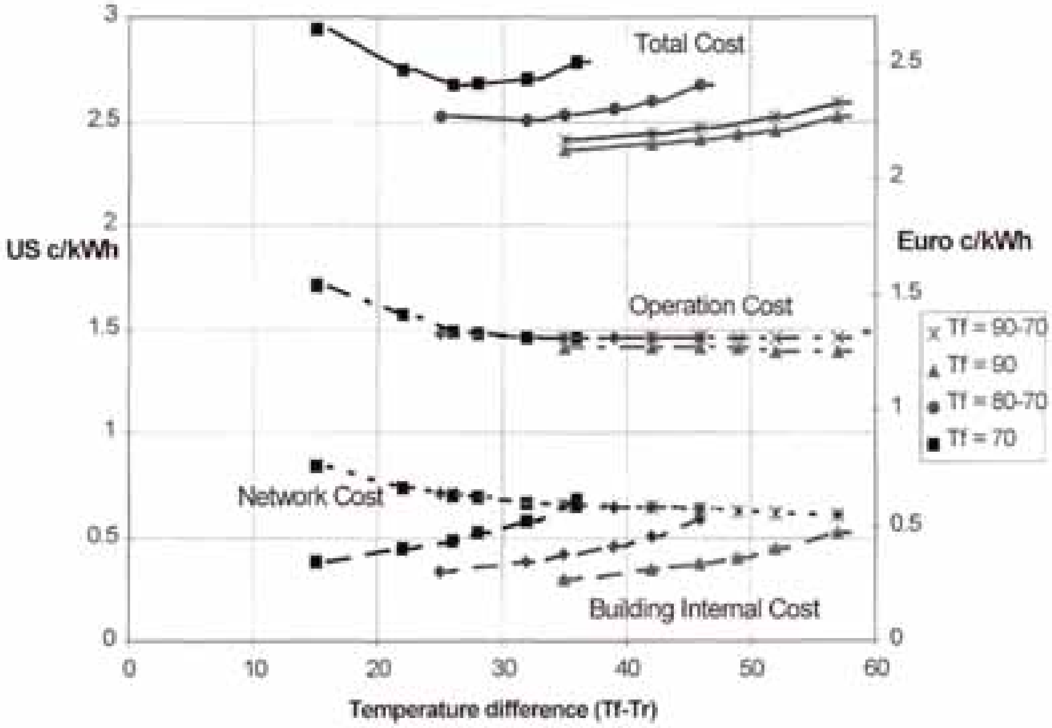

Figure 7.1- Spark-Ignition Gas-Engine CHP - Apartment Blocks in London - Direct Connection

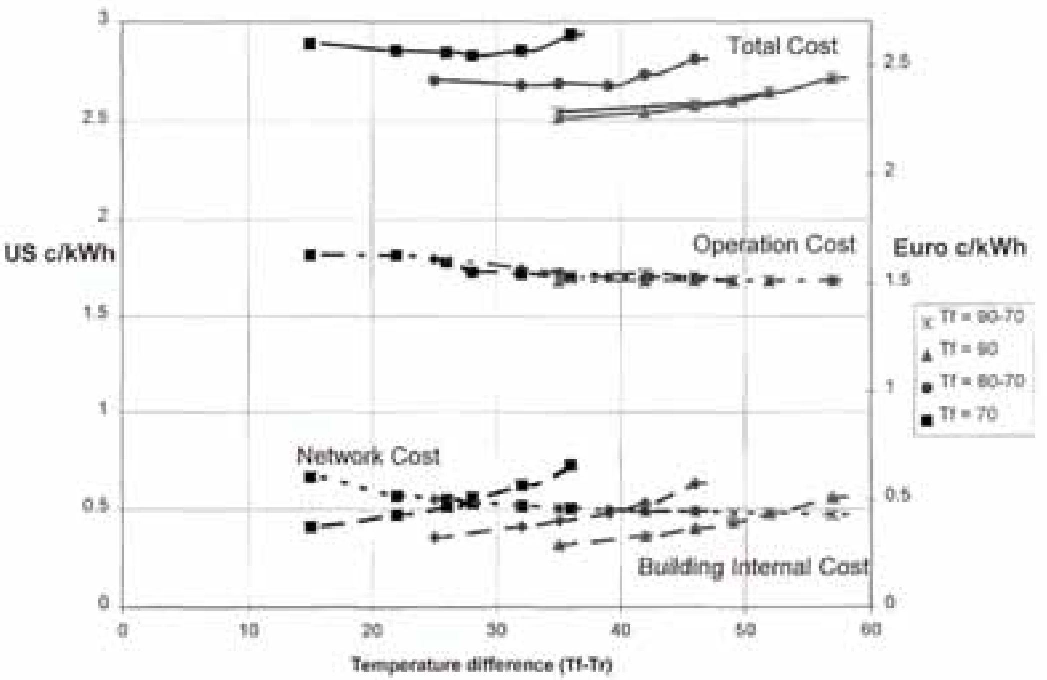

Figure 7.2- Spark-Ignition Gas-Engine CHP - Apartment Blocks in Toronto - Direct Connection

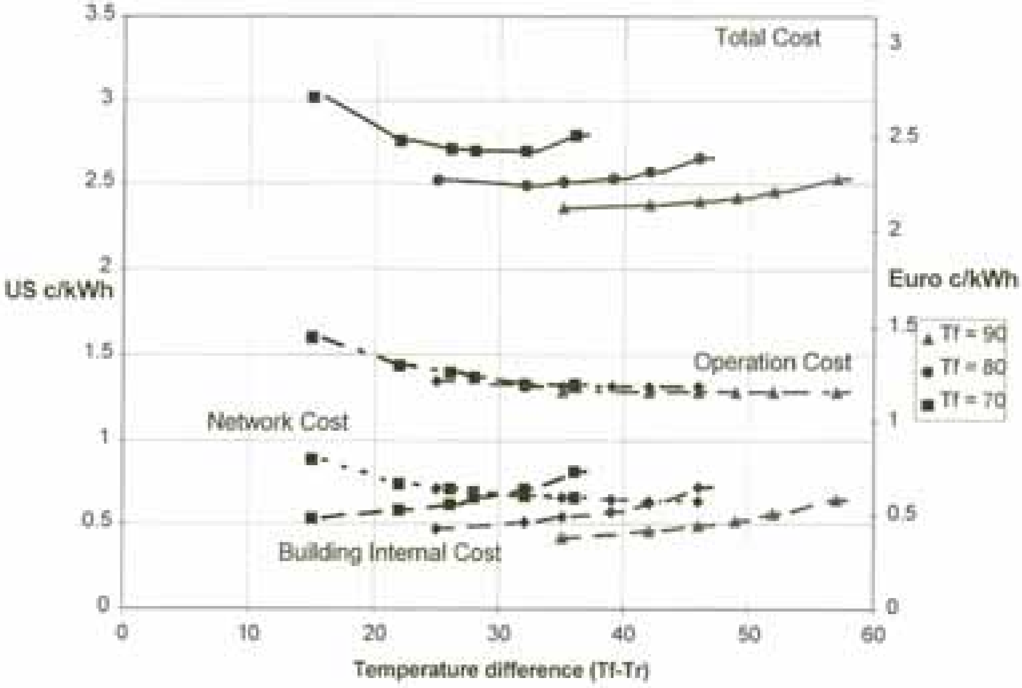

Figure 7.3- Spark-Ignition Gas-Engine CHP - Apartment Blocks in London - Indirect Connection

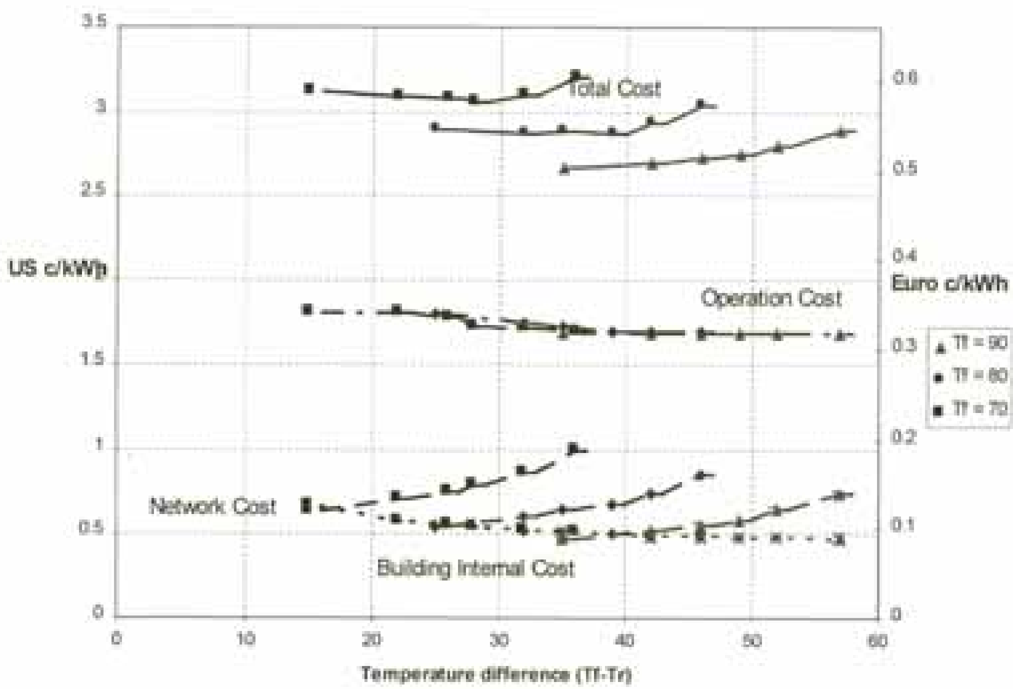

Figure 7.4- Spark-Ignition Gas-Engine CHP - Apartment Blocks in Toronto - Indirect Connection

7.3 Steam Turbine CHP Cases

The results for these cases are presented in Figure 7.5, 7.6, 7.7 and 7.8.

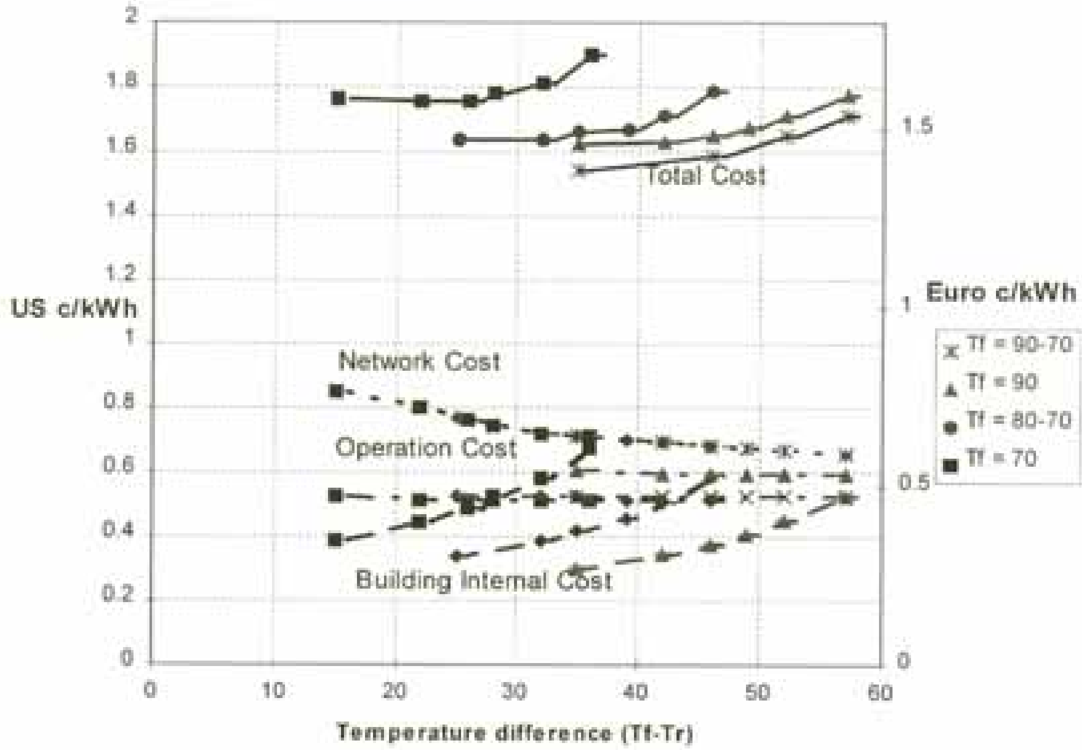

Figure 7.5- Steam Turbine CHP - Apartment Blocks in London - Direct Connection

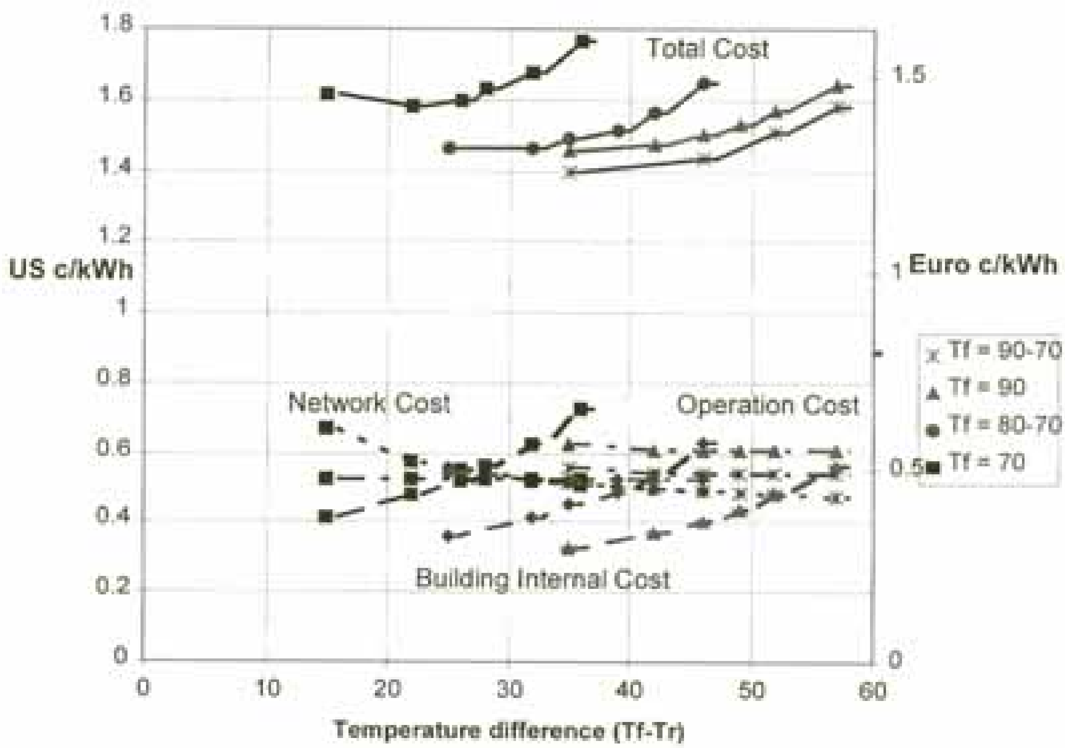

Figure 7.6 Steam Turbine CHP - Apartment Blocks in Toronto - Direct Connection

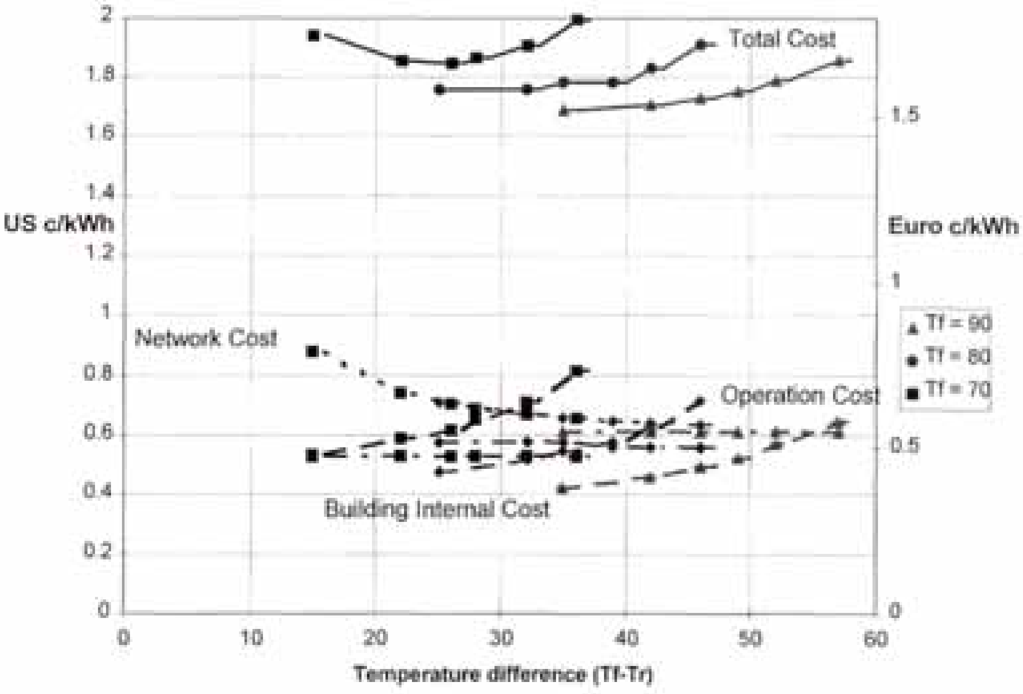

Figure 7.7 Steam Turbine CHP - Apartment Blocks in London -Indirect Connection

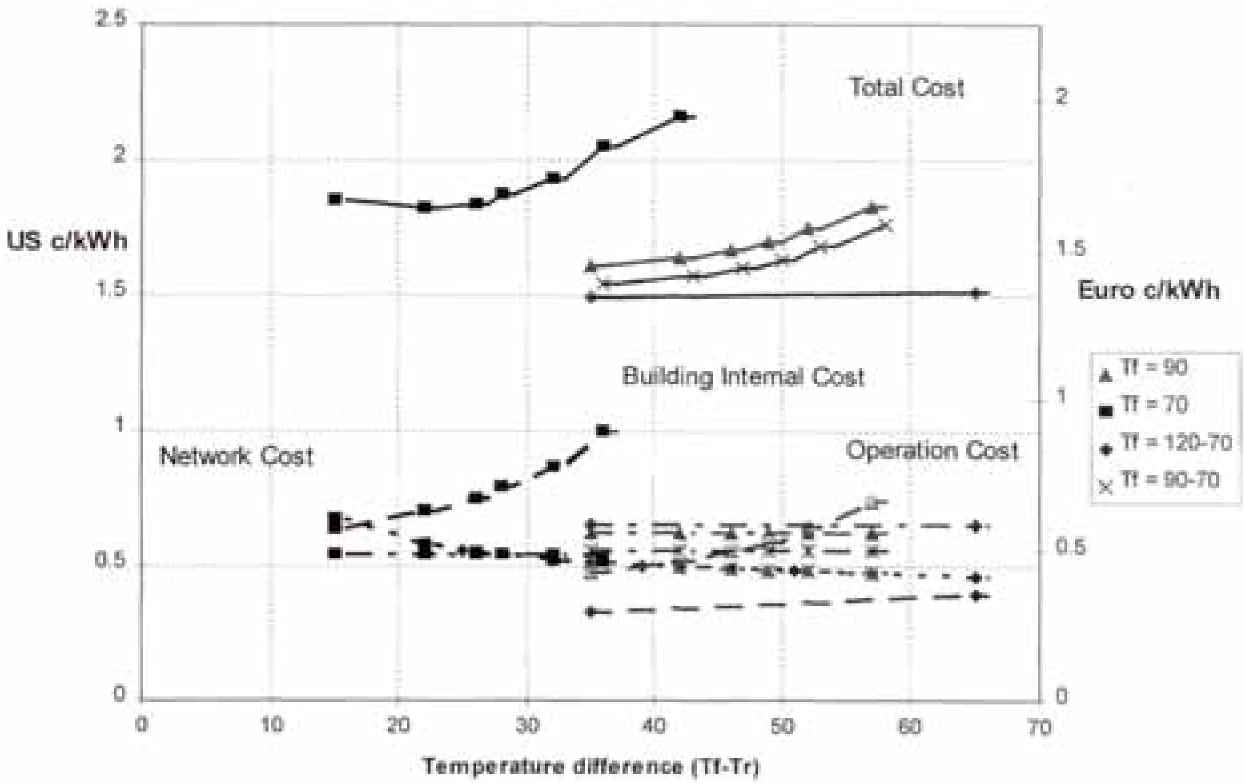

Figure 7.8 Steam Turbine CHP - Apartment Blocks in Toronto - Indirect Connection

7.4 Combined Cycle CHP Cases

The results for these cases are presented in Figures 7.9, 7.10, 7.11 and 7.12.

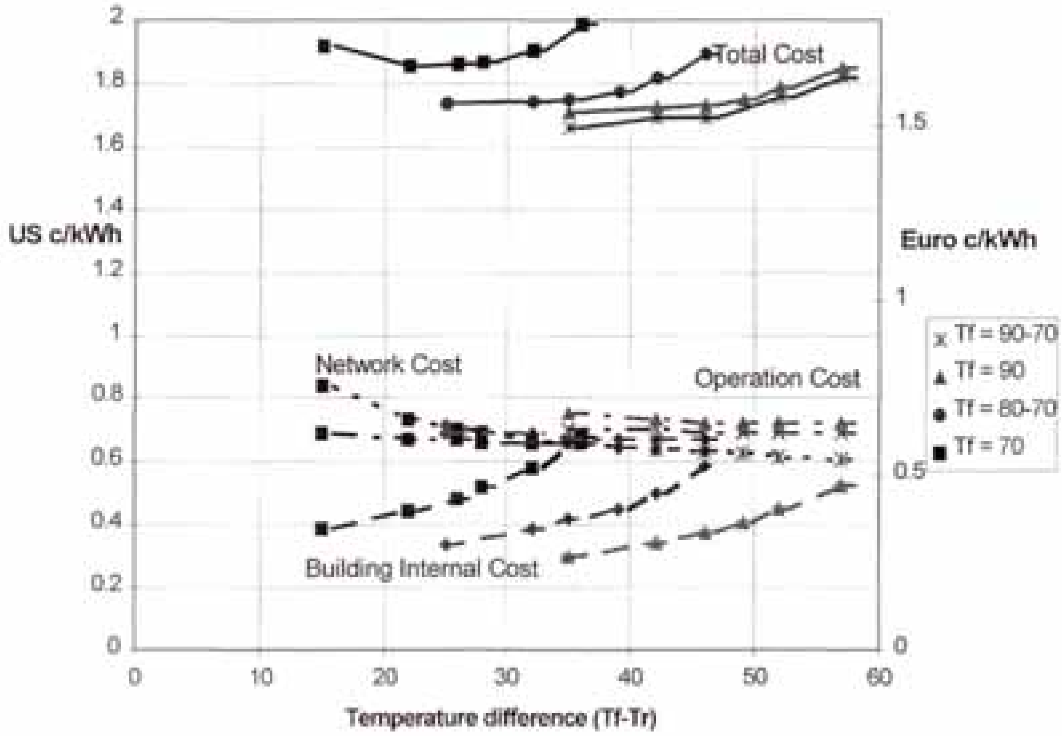

Figure 7.9- Combined Cycle CHP - Apartment Blocks in London - Direct Connection

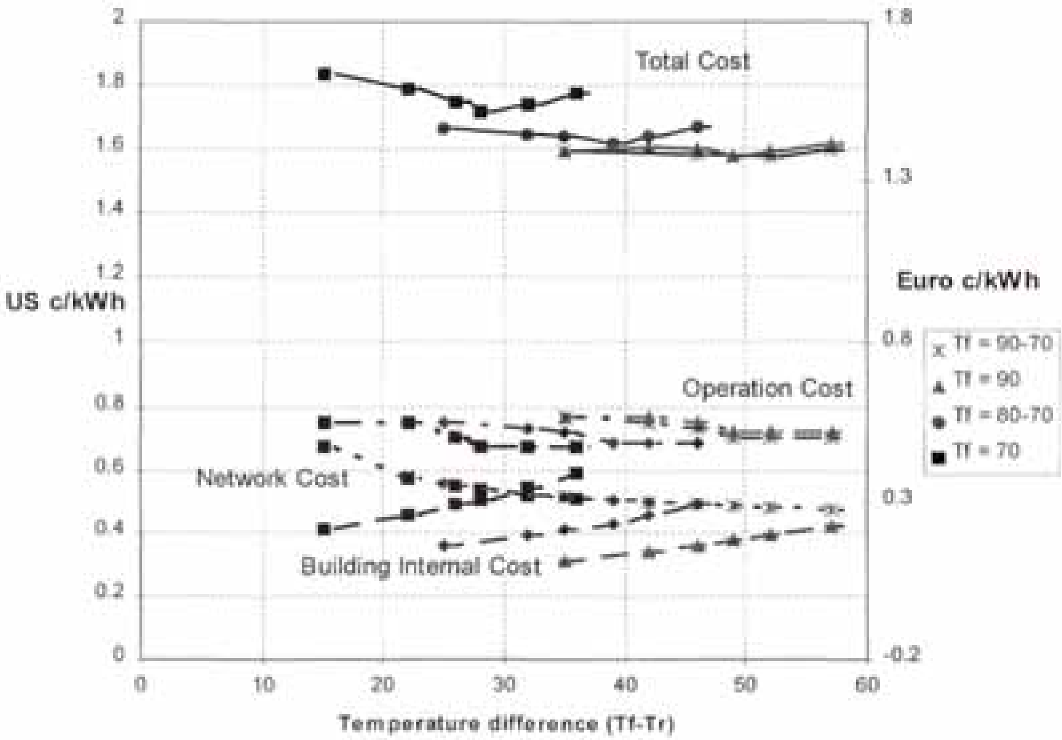

Figure 7.10- Combined Cycle CHP - Apartment Blocks in Toronto - Direct Connection

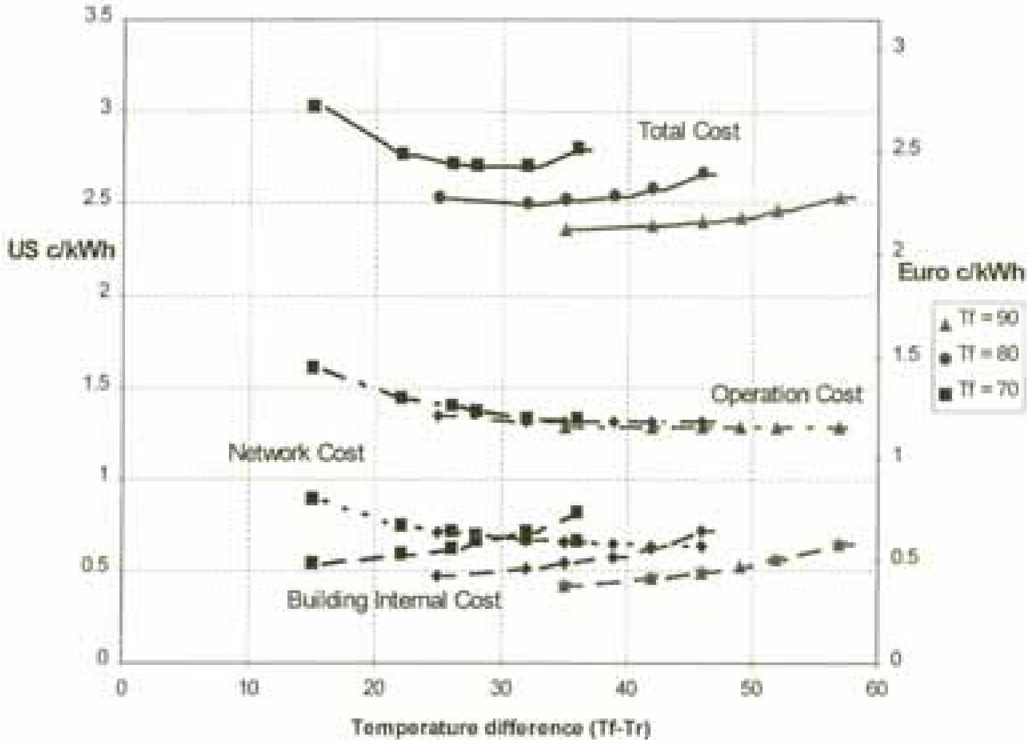

Figure 7.11- Combined Cycle CHP - Apartment Blocks in London - Indirect Connection

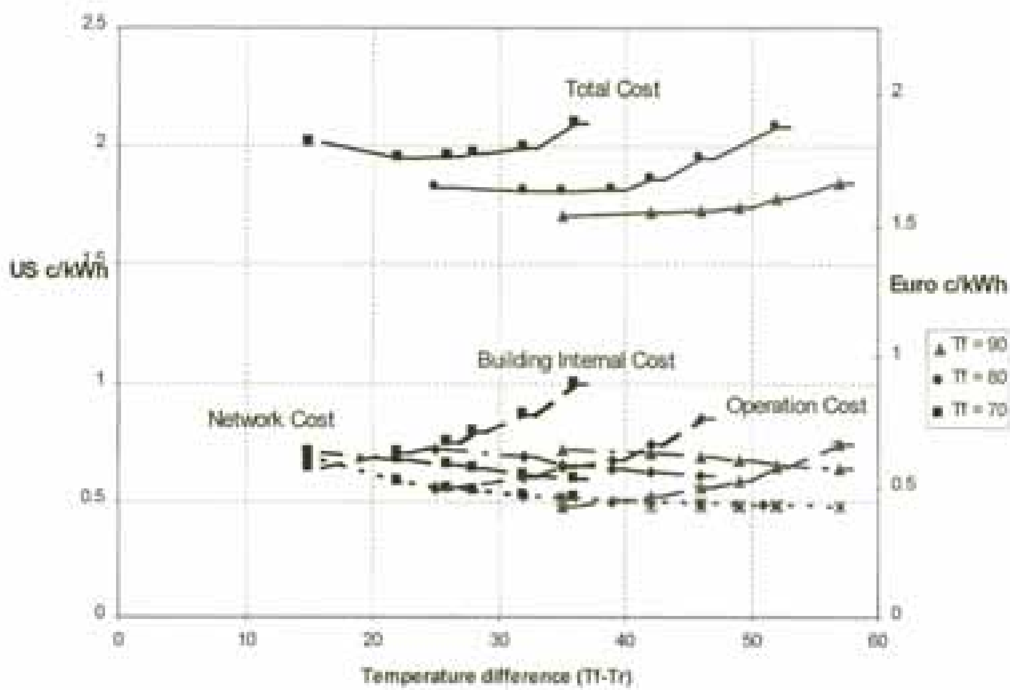

Figure 7.12- Combined Cycle CHP - Apartment Blocks in Toronto - Indirect Connection

8 Row-house Case Studies Results

8.1 Spark-Ignition Gas-Engine CHP Cases

The results for these cases are presented in Figures 8.1 and 8.2.

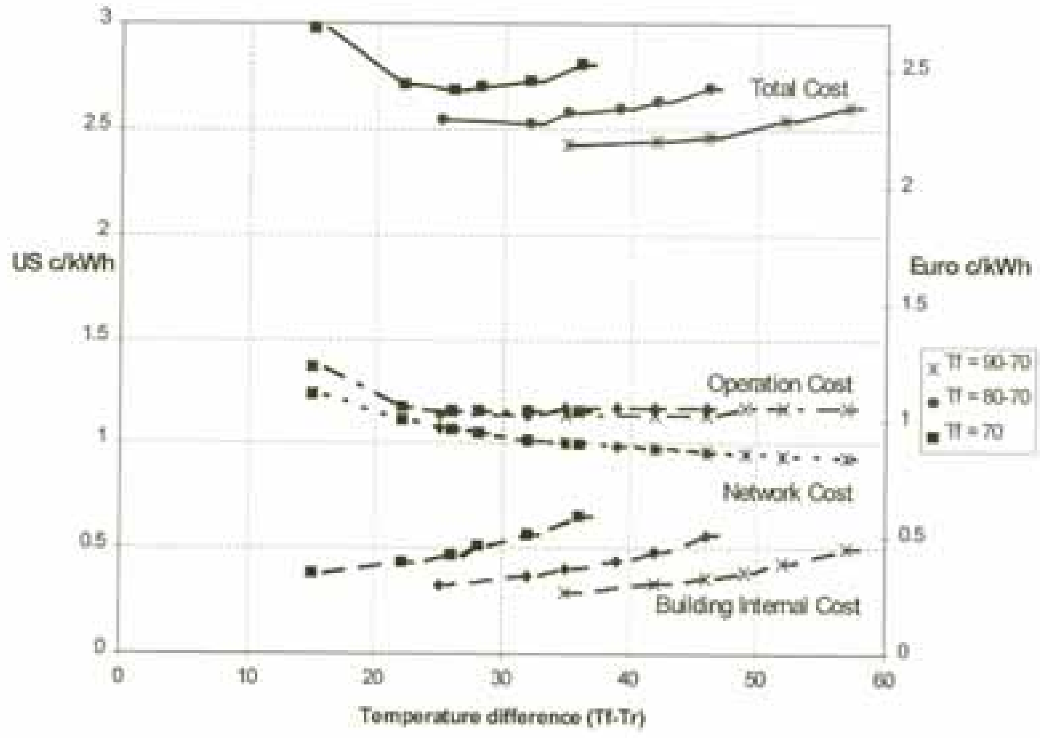

Figure 8.1: Spark Ignition Gas-engine CHP - Row houses in London

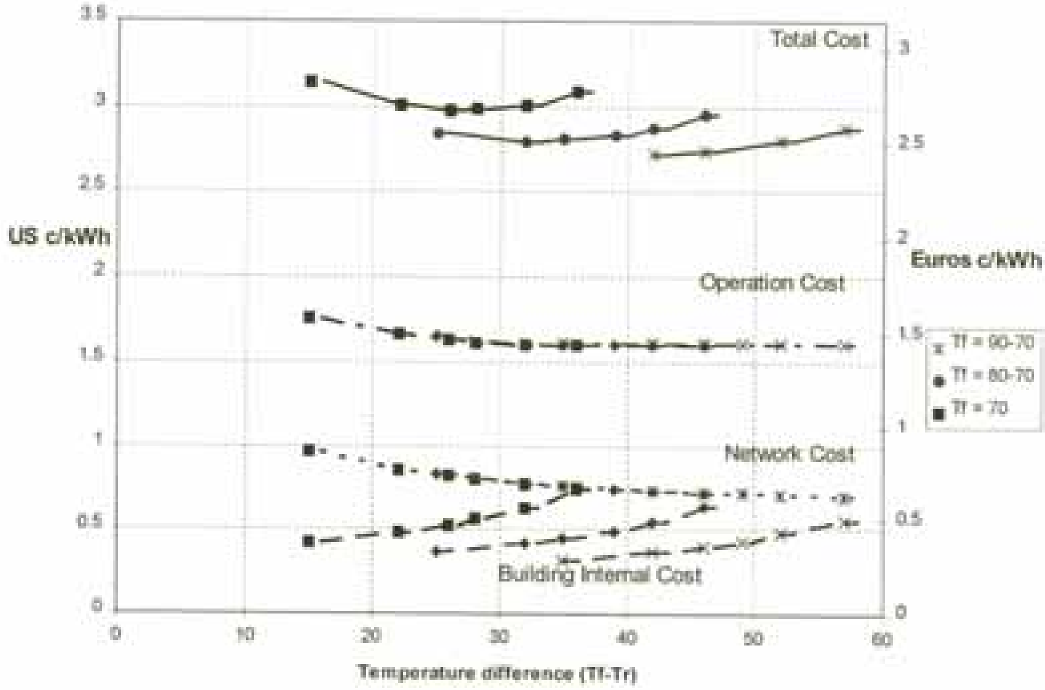

Figure 8.2: Spark Ignition Gas-engine CHP - Row houses in Toronto

8.2 Steam Turbine CHP Cases

The results for these cases are presented in Figures 8.3 and 8.4.

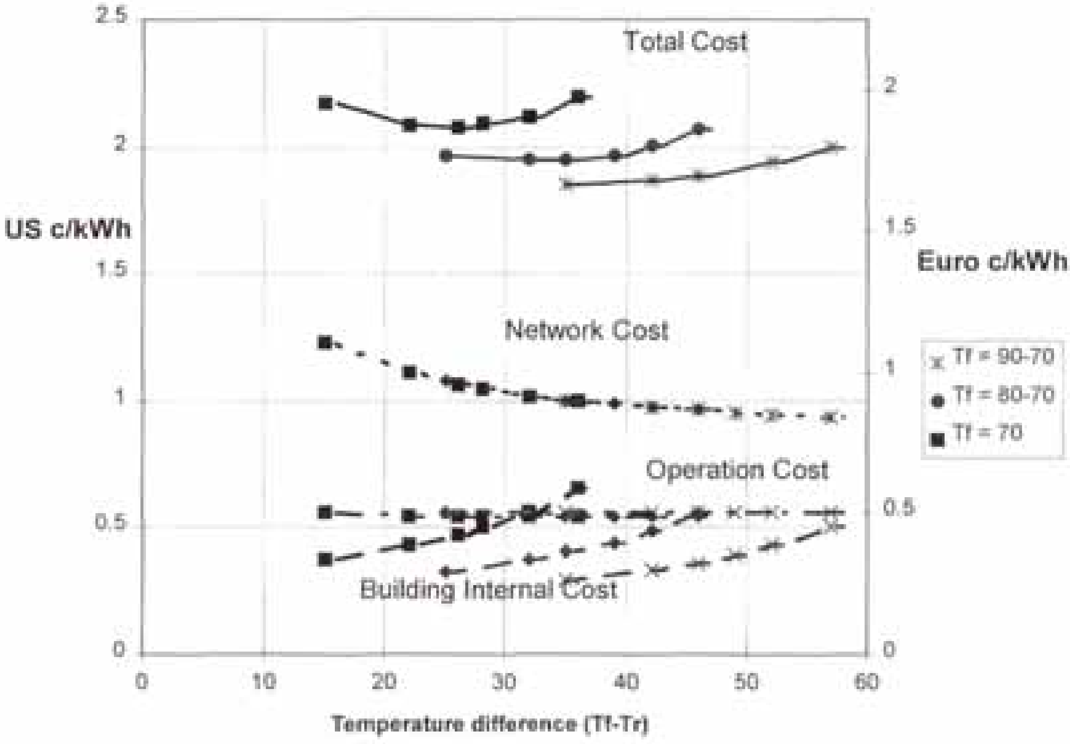

Figure 8.3: Steam Turbine CHP - Row houses in London

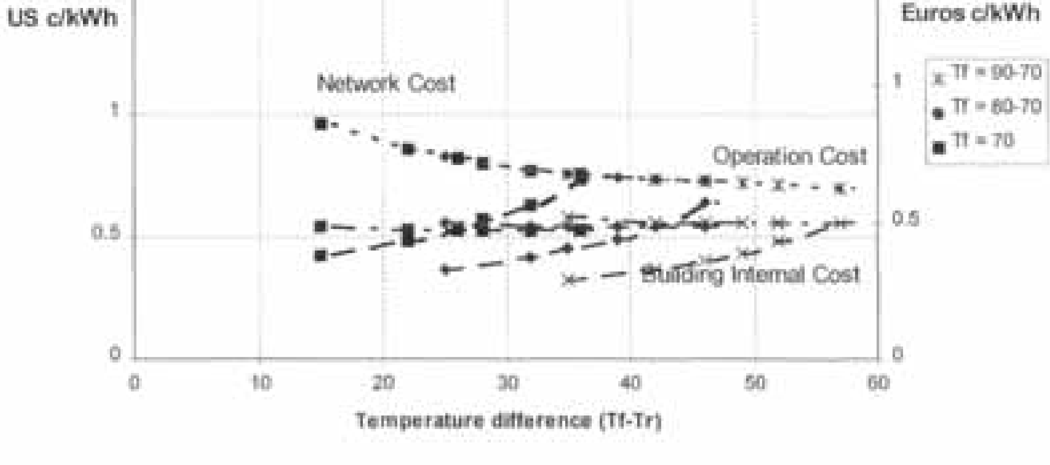

Figure 8.4: Steam Turbine CHP - Row houses in Toronto

8.3 Combined Cycle CHP Cases

The results for these cases are presented in Figures 8.5 and 8.6.

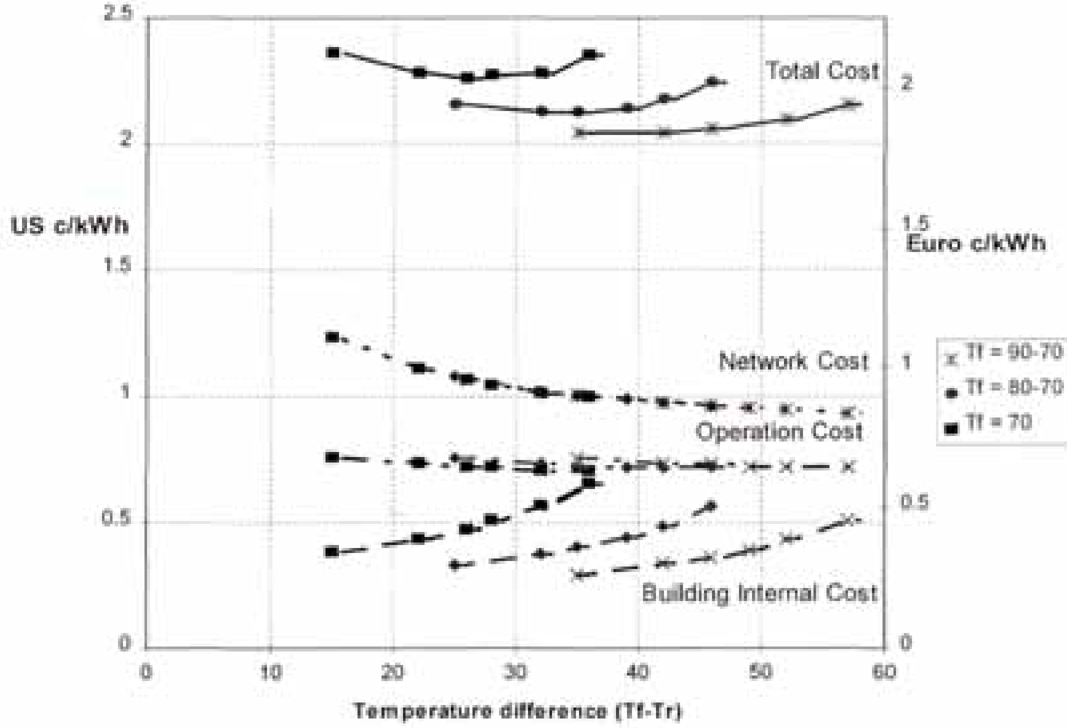

Figure 8.5- Combined Cycle CHP - Row houses in London

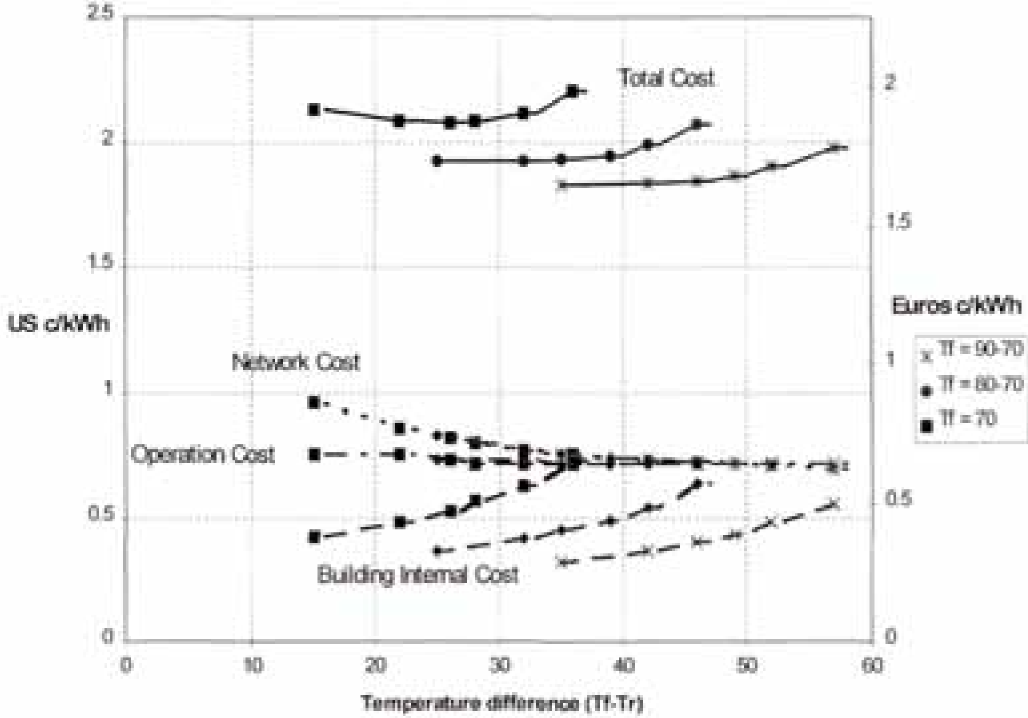

Figure 8.6: Combined Cycle CHP - Row houses in Toronto

9 Downtown Area Case Studies Results

9.1 Spark-Ignition Gas-Engine CHP Cases

The results for these cases are presented in Figures 9.1 and 9.2.

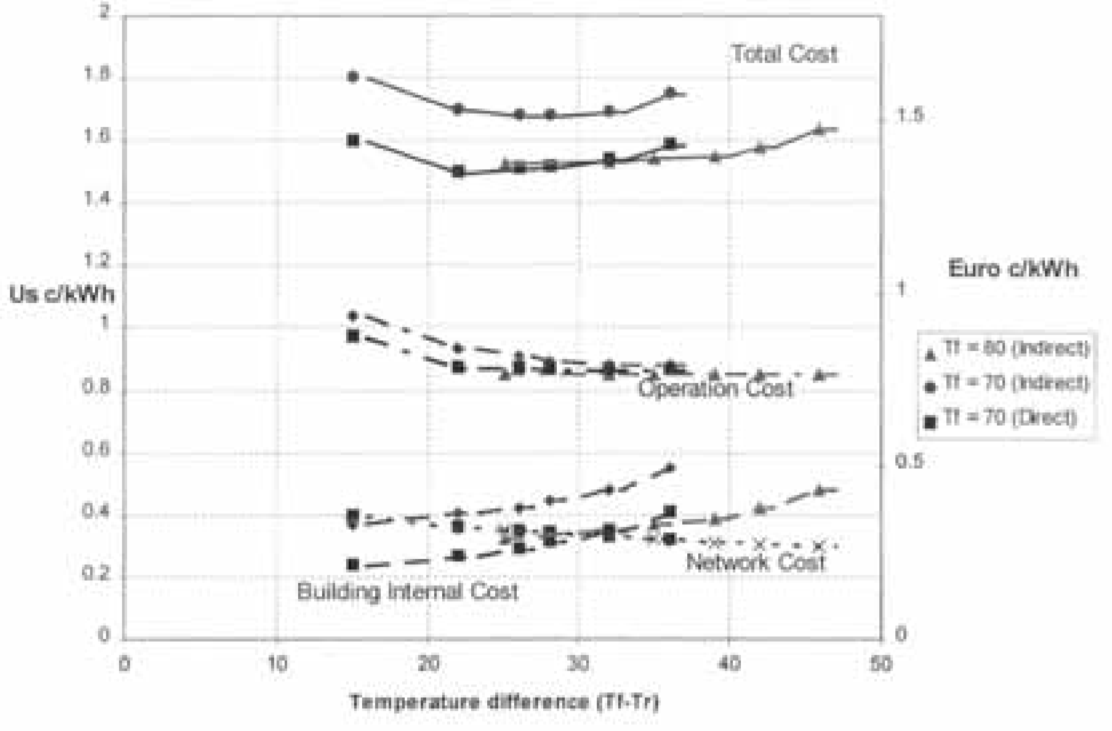

Figure 9.1- Spark-Ignition Gas-Engine CHP - Commercial Buildings in London

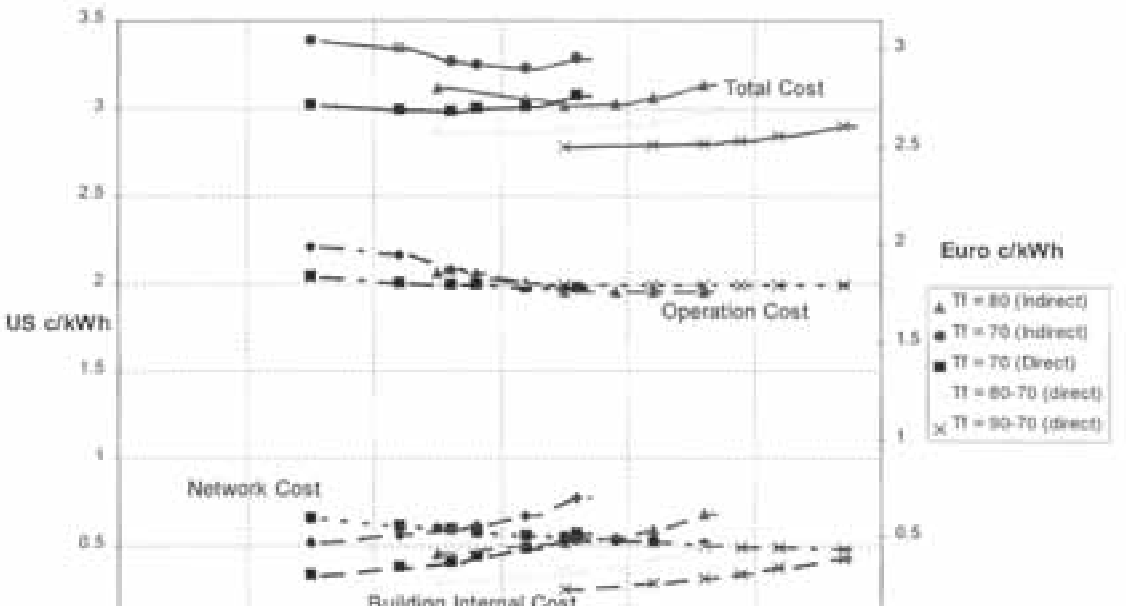

Figure 9.2- Spark-Ignition Gas-Engine CHP - Commercial Buildings in Toronto

9.2 Steam Turbine CHP Cases

The results for these cases are presented in Figures 9.3 and 9.4.

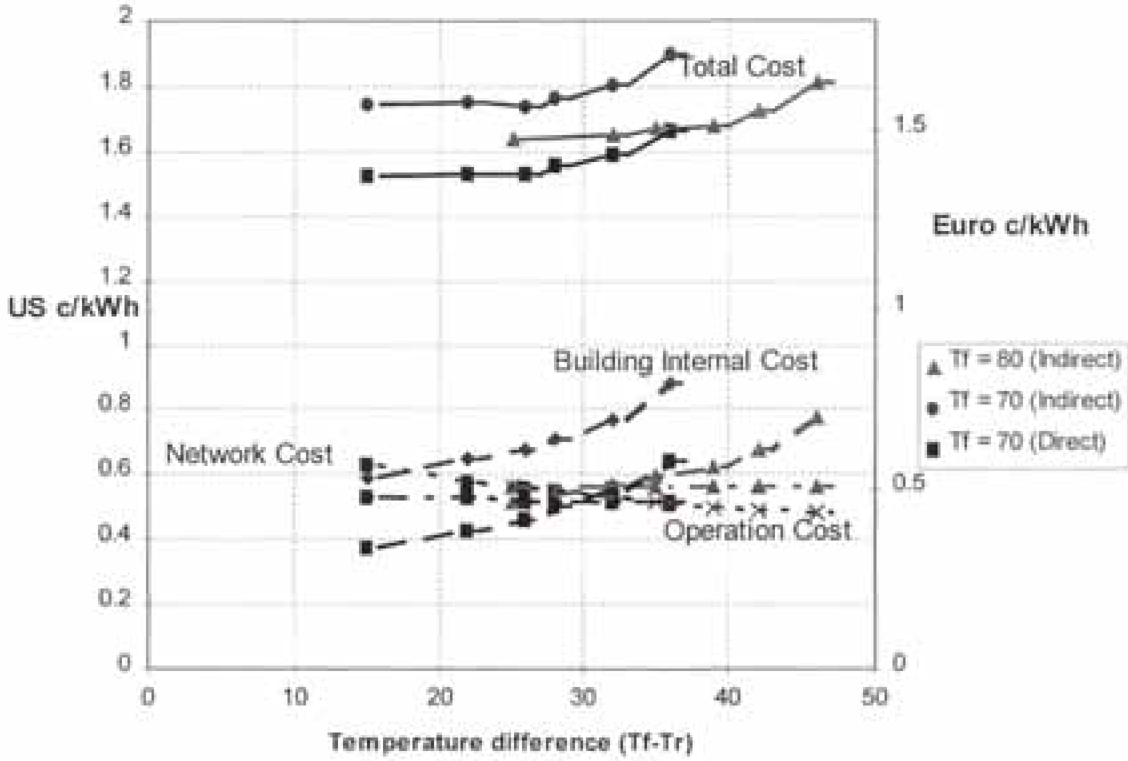

Figure 9.3- Steam Turbine CHP - Commercial Buildings in London

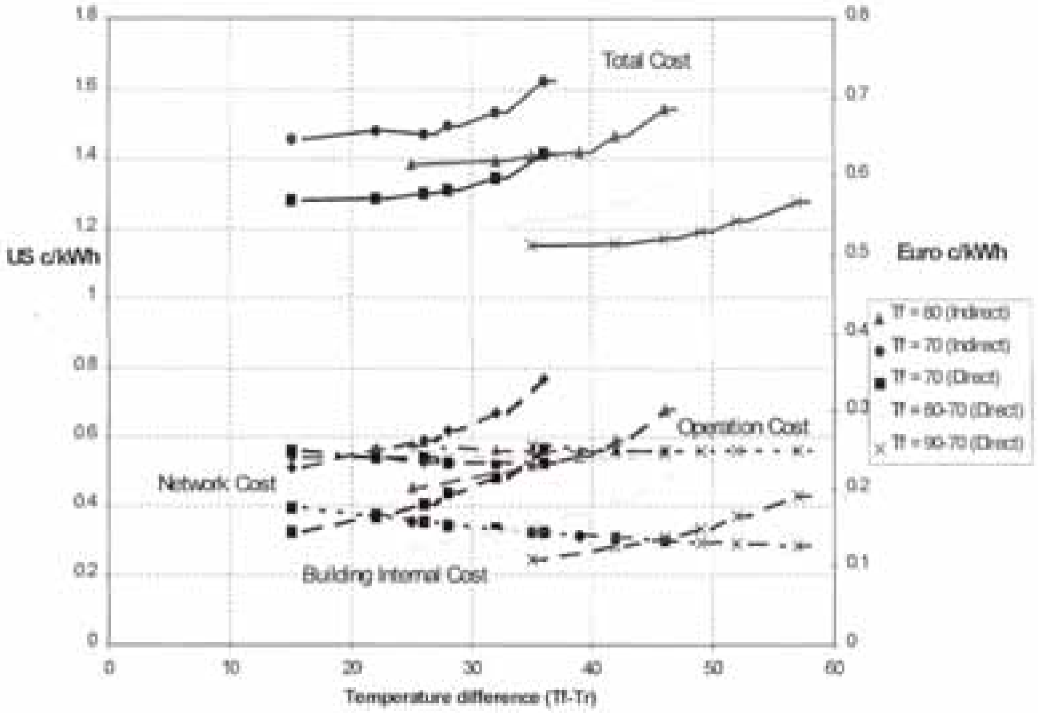

Figure 9.4- Steam Turbine CHP - Commercial Buildings in Toronto

9.3 Combined Cycle CHP Cases

The results for these cases are presented in Figures 9.5 and 9.6.

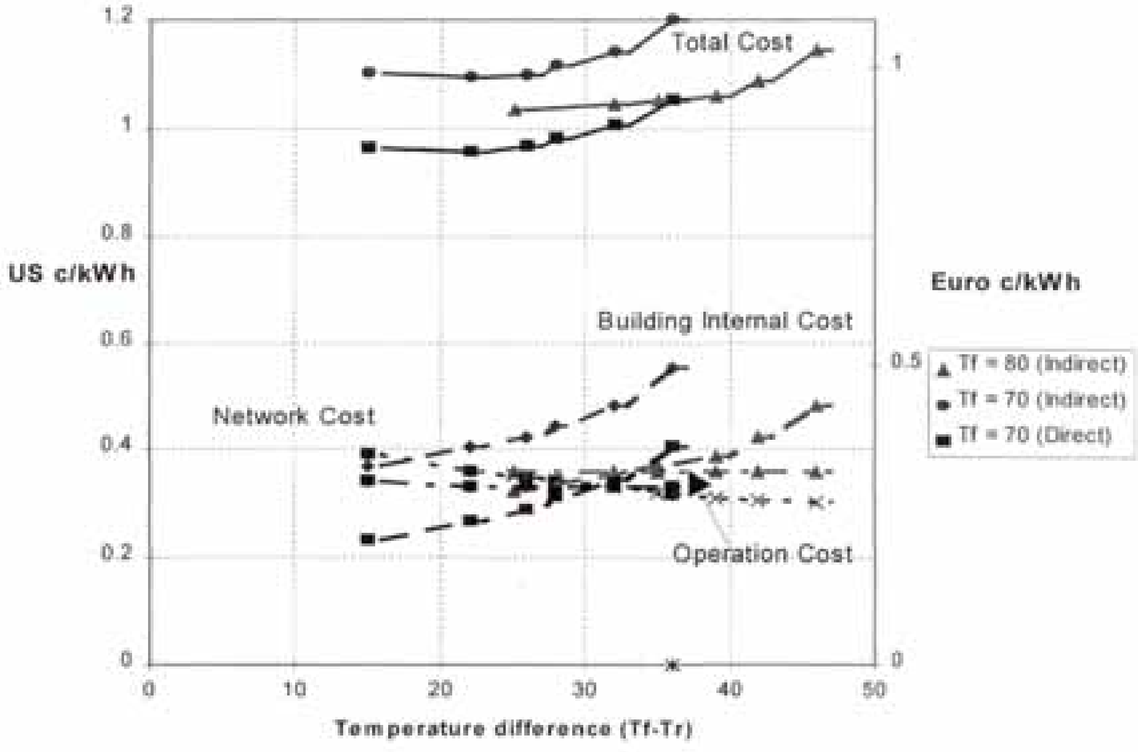

Figure 9.5- Combined Cycle CHP - Commercial Buildings in London

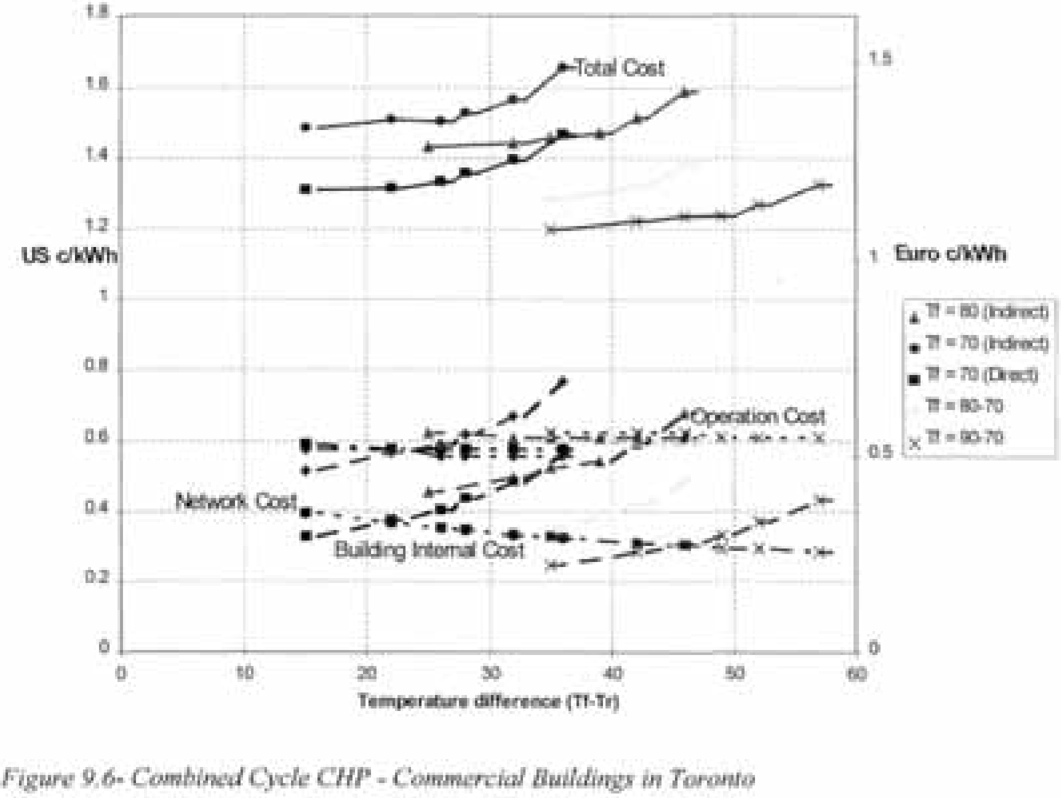

Figure 9.6- Combined Cycle CHP - Commercial Buildings in Toronto

10 Interpretation of Results

10.1 General

Although there are a large number of assumptions involved in the modelling of the case studies, and in any given actual situation alternative assumptions will be needed, the results of this analysis are considered to be valid in indicating a general trend for the optimisation of CHP/DH designs.

10.2 The Apartment Blocks Model

The various cost elements calculated for the apartment blocks models are presented in Figures 7.1 to 7.11. In this section we discuss the results for the London climate and direct connection. The impact of the climate and the type of connection is discussed in sections 10.5 and 10.8 below.

Heat production costs

Figure 7.1 provides comparative results for a London climate using spark-ignition gas engine CHP plant as the main heat supply source. As might be expected there is only a small variation in heat production cost with temperature provided the temperature difference is more than 30°C. The higher costs associated with the smaller temperature differences are due to the higher flow rates and hence pumping energy. The constant 90 °C flow case gives a lower cost of heat production than the variable 90°C case because the flow rates over the year are lower and the pumping energy is less.

Figure 7.5 shows the case for heat supply from a steam turbine CHP plant. The cost of heat production varies significantly with temperature with the lowest cost for the constant 70°C case. The difference in cost of heat production between the constant 70 °C case and the variable temperature case of 90°C reducing to 70°C in summer is relatively small because the higher temperatures are only required for a small part of the year.

The Combined Cycle Gas Turbine results in Figure 7.9 are very similar to the spark-ignition gas engine case although the total cost is lower.

Network costs

The network costs reduce as the temperature difference increases as expected but there is gradually less benefit above about 40°C temperature difference as the diameters are then smaller and the cost variation with diameter is less marked for smaller sizes (see Figure 5.2).

Building Internal Costs

These costs show a significant dependency on temperatures as a result of the cost of radiators with a variation for example of about 0.25 USc/kWh between a 90°C/55°C case (35°C temperature difference) and a 70°C/40°C case.

Total costs

The spark-ignition engine case (Figure 7.1) shows that the lowest total costs are found with a constant flow temperature of 90°C. The 90°C curve is very flat so the selection of an optimum return temperature is not too critical within the range 45°C < Tr < 65°C. There is a cost penalty in using sub-optimum temperatures such as 70°C flow, 40°C return; this selection would increase costs by 0.3 USc/kWh which in the UK would represent about 6% of the final heat selling price.

For the steam turbine case (Figure 7.5) the benefit of lower heat production costs for the 70°C flow temperature case is more than offset by the higher radiator cost, so that the constant 90°C case has a lower total cost than the 70°C case. However, the lowest total cost is for the variable temperature case (90°C reducing to 70°C in summer) which combines the benefits of being able to design the radiators and the network with peak temperatures of 90°C with the ability to extract heat at the lower temperatures for most of the year. The variation in total cost with return temperatures is very small within the range 45°C < Tr < 60°C.

For the CCGT cases (Figures 7.9 & 7.10) the variable temperature is again preferred because the majority of the heat is provided from the steam turbine although as some heat is taken from the district heating economiser the difference between the variable temperature and the fixed temperature is reduced.

10.3 Row Houses Model

The main difference with the row houses model is that the lower heat density means that network costs are relatively greater and the influence of this cost element is more significant. The total cost in Figures 8.1 to 8.6 is at a minimum in all cases for a maximum flow temperature of 90°C and a return temperature of about 55°C. Again the return temperature is not critical within the range 45°C < Tr < 60°C. The cost penalty from using a constant 70°C temperature is about 0.3 USc/kWh which in the UK would represent about 6% of the final heat selling price.

10.4 Commercial Buildings Model

This model has the highest heat density and the impact of the network costs is therefore reduced. Also, part of the heating system uses air coils which are relatively inexpensive and the variation in cost with temperatures is negligible. Hence the benefit of using a 90°C peak flow temperature is reduced although in all cases it is still the preferred option. If all of the heating system used air coils then the difference between the 90°C case and the 70°C would be negligible for a temperature difference of about 35°C (see Figure 9.4).

10.5 The influence of climate on the optimum operating temperatures

The more extreme continental climate would be expected to show that meeting of peak demands by varying the flow temperature would have a greater advantage.

Apartment Blocks cases

By comparing Figures 7.5 and 7.6 it can be seen that the total heat cost is lower in Toronto than in London principally because the cost of the network per unit of heat sold is lower. The comparison of load factors given in Table 4.4 shows that the load factor for London is slightly higher than for Toronto. Although a higher load factor improves the economics of CHP/DH the capital investment in the network per unit of heat supplied is higher so the overall total cost of heat in London is higher than in Toronto.

In both cases the optimum temperatures are very similar with the variable 90°C-70°C case preferred with a return temperature of 55°C. The results for the other cases are also very similar and we can conclude that the influence of climate on optimum operating temperatures is very small.

10.6 The influence of the heat density of the buildings supplied on the optimum operating temperatures.

It could be predicted that a low density scheme will mean that network costs dominate and increasing Tf-Tr will be the most important factor at the expense of higher heat production costs. Comparison of the three built form cases indicates very little difference between the results provided the temperature difference is above 30°C

10.7 The benefits of reducing operating temperatures in relation to external air temperature

For the steam turbine plant reducing operating temperatures in summer is often considered worthwhile because the increase in pumping energy is more than offset by the increase in electricity generation. The simulation models confirm that this practice is economic as shown in Figures 7.5 and 7.6. In each case the variable flow temperature case results in lower overall heat prices although the benefit is relatively small.

For the spark-ignition CHP the variable temperature operation results in slightly higher prices as a result of the higher pumping costs and no significant benefit is obtained from the lower heat losses in the network, or lower heat production costs, see Figures 7.1 and 7.2.

10.8 The differences between indirect and direct connection

Figures 7.3 and 7.4 show the results for indirect connection supplied from spark-ignition engines. Although the total cost is slightly higher for the indirect case the optimum temperatures are unchanged.

Indirect connection of the apartment blocks supplied from steam turbine CHP has also been modelled for constant flow temperatures of 70 °C, 80 °C and 90 °C. The results given in Figures 7.7 and 7.8 show that the 90°C flow temperature is preferred with the total costs being about 5% higher than for direct connection.

11 Discussion

11.1 Practical Cases and Existing Schemes

The analysis in this project assumes that a new CHP/DH scheme is being planned and that the buildings in each scheme are all of one type. In practice most CHP/DH schemes will involve a mix of existing and new heating systems and both commercial buildings and residential buildings will be supplied. As the results of the various cases are all very similar and the differences in total cost are relatively small, provided mid-range temperatures are assumed these will be equally applicable regardless of the mix of building type.

The various case studies have all been based on the premise that all of the buildings require new heating systems. This is useful to establish the long term optimum strategy for a scheme, as in the lifetime of the central plant and district heating mains, existing heating systems are likely to need replacement. Two other questions remain however:

1. .If the existing buildings have a heating system designed for higher temperatures than the optimum but otherwise suitable for connection to district heating, is it worthwhile replacing the existing systems or accepting the cost penalty imposed by the current design temperatures?

   From inspection of the results, we can conclude that the cost penalty of operating an existing building heating system with say a 90°C flow and a 60°C return temperature will be much less than the cost of replacing the radiators to permit operation at the optimum temperatures. However, if to match the existing mean radiator temperatures the temperature difference has to be reduced to less than 20°C (e.g. 90°C flow, 75°C return) then replacing the existing heating systems may be preferable.

2. If the existing radiators have been generously sized using a low temperature standard such as that used in Sweden (60°C/40°C), and there is therefore no need to consider the costs of installing new radiators in the economic analysis, then what are the optimum operating temperatures?

   From inspection of the Figures above we can conclude that in all cases the advantage of a large temperature difference in reducing network costs still outweighs any benefits in heat production costs, i.e. a 90°C peak flow temperature and 35°C return will still be preferable to a 70°C flow 35 °C return even if the radiators can be retained for either option.

11.2 General Observations

There has been an identifiable trend in recent years for lower temperatures to be used even with established networks (IEA, 1996 N5). The results presented here indicate that the optimum design temperatures would be 90°C flow and 55°C return for most systems supplying residential areas.

The main reason for this result is that for most heat densities the network cost is the most important cost element and increasing the temperature *difference* as far as possible leads to significant cost savings. If the peak temperature is limited to 70°C then the maximum temperature difference that can be used without increasing radiator costs is reduced. Also, when a variable flow temperature system is used, the peak temperature of 90°C only occurs for a relatively short period of time and the additional costs of heat production, even from steam turbine CHP plant, are relatively small and do not outweigh the benefits of lower network and radiator costs.

In general, for a given flow temperature there is very little difference in the total heat cost in increasing the temperature difference in the system by reducing return temperatures. A +/-10°C variation in return temperature results in less than 3% variation in total heat costs. The benefits of lower heat production costs, heat losses, pumping costs and network costs from lower return temperatures are all offset by the increased cost of radiator surface. In addition, achieving temperature drops of more than 40°C can lead to very low flow rates in radiators which are difficult to control and with air-coils additional costs for thicker tubes to accommodate stresses from differential expansion.

If, however, lower return temperatures can be obtained from existing installations without major capital investment (eg. improved controls) then this can be cost effective and will increase the spare capacity in the network.

From the case studies for housing presented above a reduction in peak flow temperature from the optimum of 90°C to 70°C results in a cost increase of about 0.15 to 0.25 USc/kWh which, in the UK, would represent about 4% to 6% of the final heat selling price (about 4 USc/kWh in the residential market). Whether this cost difference is an acceptable price to pay for the improvements in energy efficiency which would be achieved by using lower temperatures will need to be evaluated on a case by case basis. In some contexts this small penalty in the heat selling price may be considered worthwhile. However if the heat price rises too far and heat customers switch to alternative boiler only heating then the more major environmental benefits of using CHP/DH will be lost.

11.3 Implications of alternative sources of heat

In the longer term there are a number of reasons why the lowest possible operating temperatures could be adopted. Once a temperature norm has been established it is difficult and expensive to reduce temperature levels as the building heating systems would need to be replaced to maintain the design heat output. The potential for a district heating scheme to distribute heat from a number of alternative or renewable heat sources is a major potential long term advantage of the technology. Such sources are:

- industrial waste heat
- solar heat
- heat pumps
- geothermal

All of these sources are more easily and economically utilised at low temperatures. Establishing a district heating network with the potential for future flexibility of heat source i.e. with a maximum flow temperature of 70°C will in most cases carry a cost penalty however the results of this research shows that the penalty is relatively small and may be worthwhile. In many cases the amount of heat available from the above sources will be limited and the heat will be used to pre-heat the return water before the majority of the heating is provided from the CHP or boiler plant. In these circumstances it is the *return* temperature that is the main factor determining whether such heat sources can be utilised and as the graphs show there is a much smaller penalty in designing for lower return temperatures.

11.4 Environmental benefits of lower operating temperatures

The main aim of this research has been to establish the economic optimum with respect to operating temperatures. Many countries are seeking to reduce their CO_2 emissions to comply with the Kyoto agreement and given that the cost penalty in operating with lower temperatures is relatively small it is useful to assess how much CO_2 reduction benefit can be achieved from lower DH operating temperatures. The approach is necessarily simplistic but a general indication may be helpful.

It has been established above that the operation of steam turbine CHP plant is the most sensitive to operating temperatures and it is in these applications that the greatest CO_2 benefit will be found.

For the apartment block model in London supplied from steam turbine CHP, at a temperature of 70°C constant the amount of lost electricity is about 23% less than for the constant 90°C case (see table 6.6). This saving in lost electricity is effectively a fuel saving at other power plants which, depending on the marginal power plant on the system, will result in a reduction in CO_2 emissions.

For a single apartment block with an annual heat demand of 1370 MWh the annual electricity demand is estimated at 396 MWh. If 80% of the heat is supplied from a steam turbine CHP plant the amount of 'lost electricity' can be calculated for two temperature levels 90°C/50°C and 70°C/40°C according to the z-factors in Table 6.5.

The difference in lost electricity between these two cases is (0.129-0.091) x 1096 = 41 MWh. This is about 10% of the estimated electricity demand for the apartment block. Hence the reduction in flow temperature from a constant 90°C to constant 70°C would reduce the primary energy and CO_2 emissions associated with the electricity demand of the apartment block by about 10%.

11.5 The use of 120°C flow temperatures

On the advice of the Experts Group the thrust of this research project was to establish the benefits of using lower temperatures for district heating with the maximum temperature of 90°C. As the results showed that the network cost is an important factor it is logical to consider whether higher flow temperatures than 90°C would lead to lower costs as the temperature difference can be increased further. There are a number of areas where costs will increase however as a result of :

- additional costs on the network to accommodate expansion
- the use of plastic pipes would not be possible
- additional heat losses
- the need to have indirect connections to buildings
- higher heat production costs from steam turbine CHP

To evaluate the various costs the model for apartment blocks in Toronto was used with heat supplied from steam turbine CHP. The results are given in Figure 7.8 for a temperature difference of 65°C i.e. 120°C flow, 55°C return. The flow temperature is assumed to be reduced to 70°C in summer. The network cost is lower than the 90°C case due to the larger temperature difference (we have ignored any cost penalties from expansion provision). The radiators are assumed to be designed for 90°C / 50°C. The total cost of heat is almost identical to the 90°C case but would be higher if the additional costs for thermal expansion provision were taken into account.

The second case evaluated is for a temperature difference in the network of 35°C which has the benefit of reducing the radiator cost by using higher secondary temperatures (90°C/70°C has been assumed). The total cost for this case is slightly lower than the 90°C case however this difference would be eroded if the network cost was 10% higher which is to be expected if the additional costs for thermal expansion provision were taken into account.

By comparing Figure 7.8 to Figure 7.6 it can be seen that the benefit of direct connection is much more significant than the differences between the temperature cases. A cost of heat of 1.4 US c/kWh for direct connection at 90°C is predicted compared to 1.5 US c/kWh for indirect connection and 120°C. We can therefore conclude that if direct connection is technically feasible (no pressure incompatibility) then a 90°C temperature will be preferable to 120°C. If indirect connection has to be used then there is a negligible difference between 90°C and 120°C and the 90°C flow temperature should be used because of the potential environmental advantages.

12 Sensitivity Analysis

12.1 Sensitivity to Economic Parameters

To calculate a total cost of heat, the capital costs are annualised by using a discount (interest) rate and a lifetime for the project. As the optimisation is balancing the benefits of lower operating costs with higher capital costs the choice of these factors may well determine the optimum condition.

The calculations in the report have been based on a 20 year evaluation period and a discount rate of 10% which is typical for a private sector financed scheme. As a sensitivity we have re-evaluated the case of apartment blocks supplied from a steam turbine plant for a 30 year evaluation period and a 5% discount rate. The results are shown in Figure 11.1 which shows that the influence of the network capital cost and the radiator costs is much reduced due to the lower discount rate but that the optimum temperatures remain at 90°C flow, 55°C return.

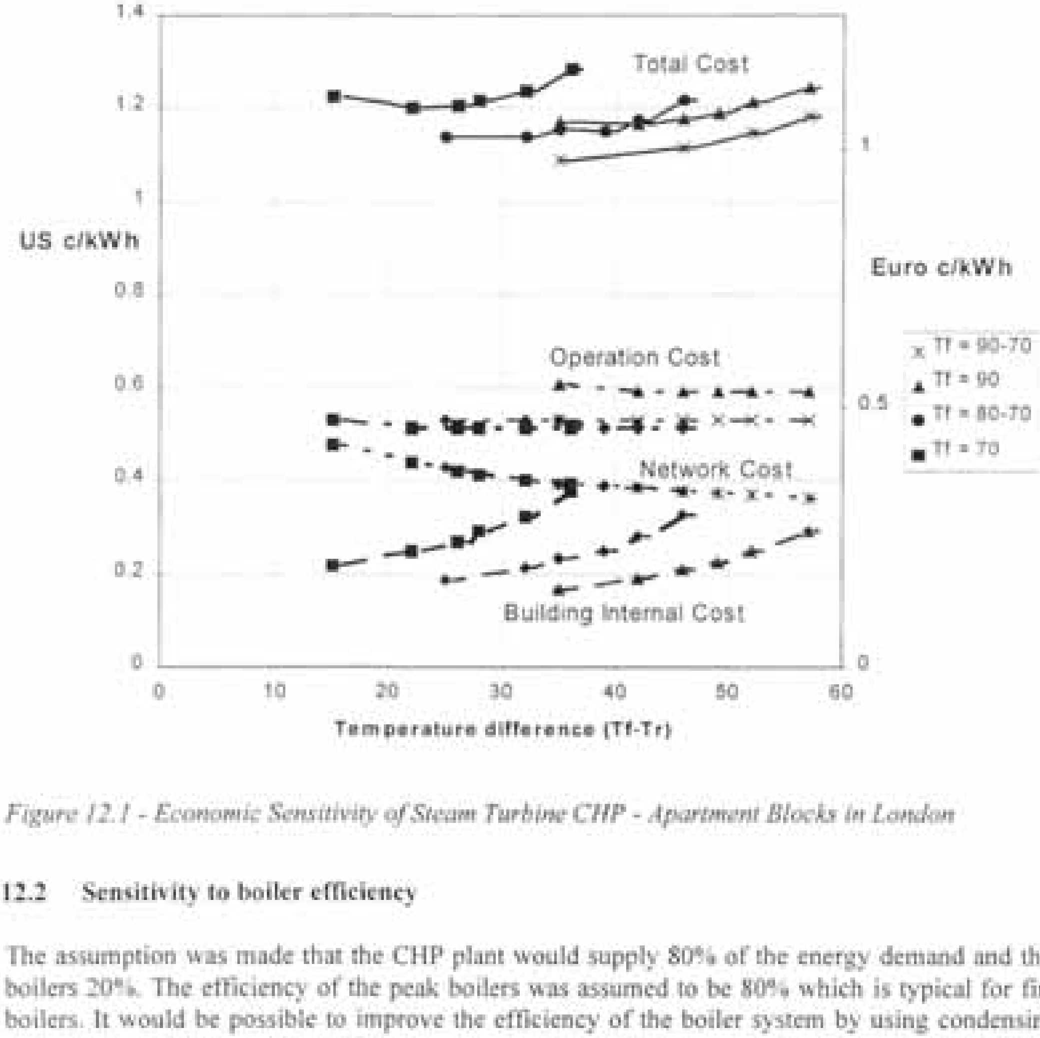

Figure 12.1 - Economic Sensitivity of Steam Turbine CHP - Apartment Blocks in London

12.2 Sensitivity to boiler efficiency

The assumption was made that the CHP plant would supply 80% of the energy demand and the peak boilers 20%. The efficiency of the peak boilers was assumed to be 80% which is typical for fire-tube boilers. It would be possible to improve the efficiency of the boiler system by using condensing heat exchangers which would be particularly effective as the return temperature is reduced. Whilst this is a feasible proposal it is unlikely to be economic given the relatively short running hours of the boilers. The effect of this has been analysed for the case of the London apartment blocks supplied from a steam turbine using the variation of boiler efficiency with return temperature given in Table 12.1.

Table 12.1 Variation in boiler efficiency with DH return temperatures

return temperature (°C)	30	40	50	60
boiler efficiency (HHV) (%)	91	88	83	80

The results are shown in Figure 11.2 which indicates that there is a 4% reduction in the operation cost compared to the base case results and a negligible effect on the total cost pattern.

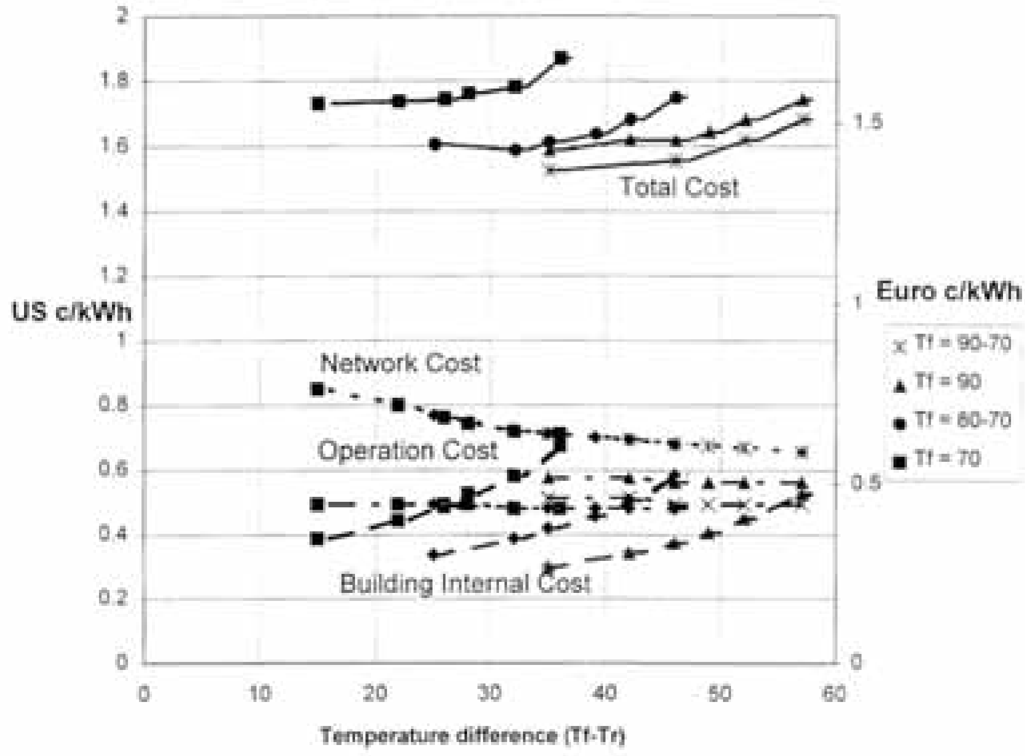

Figure 12.2 - Boiler efficiency sensitivity on Steam Turbine CHP - London Apartment Blocks

12.3 Sensitivity to electricity prices

If electricity prices are relatively high, then the benefit of using lower temperatures with the steam turbine CHP will be increased. By inspection of Figure 7.6 (Toronto Apartment Blocks) it can be seen that the difference in operating cost between the constant 90°C flow case and the 70°C flow case would need to be about three times larger to make the 70°C total cost the same as the 90°C case. This is clearly an unrealistic prospect in the foreseeable future and we can conclude that the results are relatively insensitive to electricity prices.

12.4 Sensitivity to Heat Density

The selection of the cases already provides a method of illustrating how the optimum varies with heat density, by comparing the row houses with the commercial network where the linear heat density varies from about 1.5kW/m to 8 kW/m. However as there are also differences in heat demands a sensitivity calculation has been carried out on the London apartment blocks case by doubling the heat demand at each block (e.g. assuming the blocks are twice as long) so that the heat density also doubles.

The results are shown in Figure 12.3 which can be compared to Figure 7.5. The doubling of the heat density reduces the influence of the network costs but the total cost pattern remains the same.

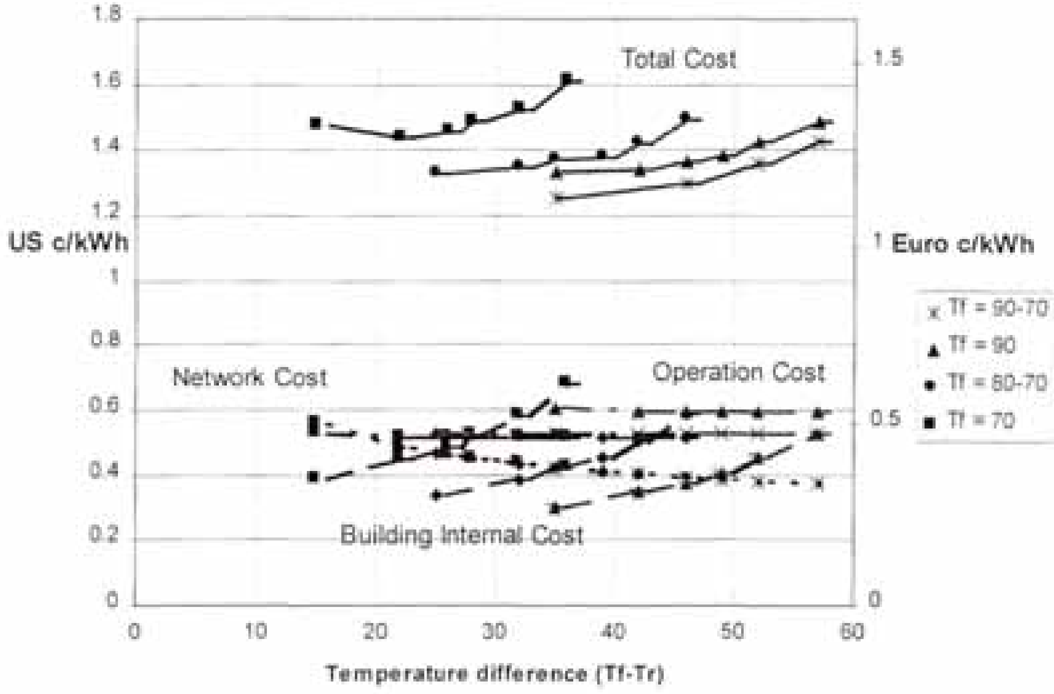

Figure 12.3 - Heat Density sensitivity on Steam Turbine CHP – London Apartment Blocks

13 Conclusions

Simulink Models

1. The Simulink software has been shown to be a viable tool to simulate a building and its heating system to predict, for each hour of a typical year, the flow rates and return temperatures that will occur in a district heating system supplying the building.

2. The results from the Simulink models were compared with field measurements and good agreement has been demonstrated with a relative error of +/- 6.2% for a radiator system and +/- 4.3% for a fan-coil system. The maximum deviation in overall heat transfer for a plate heat exchanger was 5.5%.

Optimisation of district heating operating temperatures

3. The economic optimum design temperatures for a district heating scheme using CHP heat and supplying apartment blocks or row houses have been found to be 90°C flow and 55°C return. This conclusion assumes a 20 year economic evaluation period and a 10% discount rate

4. The differences in climate between London and Toronto are not significant enough to affect the optimum temperature selection.

5. The cost penalty in using sub-optimum operating temperatures is relatively small, typically 4% to 6% of the heat selling price if for example the flow temperature is reduced from 90°C to 70°C.

6. CHP/DH systems supplied from steam turbine plant will benefit from the operating practice of reducing the flow temperature as the ambient air temperature rises and the heat demand falls, i.e. from a 90°C flow temperature at peak demand to 70°C in summer.

7. CHP/DH systems supplied from gas-engines will not benefit from lower flow temperatures in summer as the reduction in network heat losses do not compensate for the higher cost of pumping energy as a result of the higher flow rates.

8. For a given flow temperature and for temperature differences more than 30°C, the variation in total heating supply cost for changes in return temperature is very small, less than 3%, so for the 90°C flow temperature, return temperatures in the range 45°C to 60°C can still be considered optimal. This is because the benefit of a lower network cost as a result of the larger temperature difference is offset by the additional cost of larger radiators.

9. For CHP/DH schemes using steam turbine plant and supplying commercial buildings at a high heat density there may be an advantage in designing for peak flow temperatures less than 90°C, provided a high proportion of the heating demand is met from air heating coils rather than radiators where the cost penalty of additional heating surface is much less.

10. Where existing heating systems are to be connected to a new district heating system it will generally be worthwhile retaining the radiators and operating at a sub-optimum condition rather than replacing the radiators. This conclusion is at least valid for a mean temperature in the existing radiators of 75°C and below.

11. Where existing heating systems have already been designed for low temperature operation (i.e. a mean temperature of less than 55°C) it may still be worthwhile designing the CHP/DH system with higher flow temperatures and a large temperature difference to minimise the network costs.

12. If heat is available from renewable energy or other low grade waste heat sources then there may be additional benefits in designing with lower *return* temperatures to enable pre-heating of the return water to be achieved at low cost and maximise the contribution from these energy sources.

13. The total costs for indirectly connected systems were slightly higher than for direct connection but the same conclusions regarding temperature optimisation are valid.

14. If the flow temperature is increased to 120°C then indirect connection will be necessary and the total cost was found to be higher than the directly connected 90°C system. If an indirectly connected 90°C system is compared with a 120°C indirectly connected system the costs are very similar and the 90°C system would be preferred because of the potential for improved environmental performance, the use of plastic carrier pipes and lower maintenance costs.

15. For the apartment DH system supplied from an extraction-condensing steam turbine CHP plant a reduction in operating temperature from a constant 90°C to a constant 70°C would reduce the CO_2 emissions associated with the electricity supplied to the customers on the scheme by about 10%.

14 References

AAF, 1998, *Private communication from AAF Ltd*, London UK dated 5th June 1998

AGFW 1997 - *Neuartige Warmeverteilung*, Franz-Georg W. Witterhold, AGFW

BRE/AERE, 1981, *District Heating Combined with Electricity Generation: A study of some of the factors which influence cost-effectiveness*, Building Research Establishment and Atomic Energy Research Establishment, UK, 1981

GTW, 1997, Gas Turbine World - 1997 Handbook

IEA, 1995 N3: IEA Annex IV Report 1996:N3.1 – Guideline to Planning and Building of District Heating Networks, GEF Ingenieurgesellschaft für Energietechnik und Fernwärme mbH

IEA, 1995: *IEA Annex IV Report 1996: N5 - Efficient Substations and Installations*, SINTEF, Lund Institute of Technology, En Eff Technologies Inc, The University of Sasketchawan

Lawaetz, H. 1985: "*Varmtvandsforbrug i Boliger. Målinger af Vand-og Energiforbrugets Størrelse og Fordeling*", Teknologisk Institut, Denmark, 1985, (in Danish). ISBN 87-7511-544-1

Ramboll, 1998, *Private communication from Ramboll, Consulting Engineers*, Copenhagen August 1998

Snoek, 1997 *Cost-performance optimisation of low-temperature heating systems by statistical analysis of full-year simulation*, 6th International Symposium District Heating and Simulation, Reykjavik August 28th-30th 1997, C.W.Snoek, L.Yang, T.Onno

Volla, R. et al. 1996: "*Efficient Substations and Installations*", SINTEF, the Norwegian Institute of Technology, , IEA District Heating and Cooling Project Report published by NOVEM, Sittard, The Netherlands, 1996. ISBN 90-72130-88-X.

Wartsila, 1997 *Private communication from Wartsila NSD UK Ltd to Merz Orchard*, 8th August 1997

Winkens, 1986: *'Economic Outgoing Temperatures in DH Supply'*, Fernwarme International yearbook 1988

Yang, L. 1994: "*District Heating House Stations with Hot Water Storage-Simulation and Evaluation of Dynamic Performance*", Ph.D. dissertation, Centre for District Heating Technology, Laboratory of Heating and Air Conditioning, Technical University of Denmark, Lyngby, Denmark, 1994. ISBN 87-88038-30-0.

Appendix A - The Use of Simulink for Building Heating Simulations

Appendix A SIMULINK Model Detail

A.1 SIMULINK Block Diagrams for Building Heating Systems

SIMULINK (The Math Works Inc.) software was applied to build simulation models for the six different types of building heating systems described in Chapter 4.

SIMULINK is built on the MATLAB numeric computation system (MATLAB, also by the Math Works Inc., is an interactive environment for numeric computation that specialises in working with matrices.) It is a software package for simulation of continuous and discrete dynamic processes. The models created in SIMULINK are graphical in natural. Therefore, it is possible to model a complex system rapidly, cleanly, intuitively, and without having to write so much as a single line of code.

In the present study, dynamic models for plate heat exchangers, radiators, fan coils, controllers, control valves, buildings and row houses were pre-built in SIMULINK as subsystems in icon form. To create a SIMULINK model (block diagram) for a building heating system, the component icons can be dragged to the SIMULINK model worksheet and be connected as required.

SIMULINK block diagrams for these building heating systems are presented in this section, and the inputs and outputs of the models are described. Detailed model descriptions for the components in the building heating systems will be described in the next section, Appendix A.2.

A.1.1 SIMULINK Block Diagrams for Directly and Indirectly Connected 2-stage Heating Systems for the Apartment Building

Figure A.1.1 shows the SIMULINK block diagram for a directly-connected, 2-stage heating system for the apartment building (c.f. Fig. 4.5 for the diagram). The indirectly-connected, 2-stage heating system is shown in Fig. A.1.2 (c.f. Fig.4.6 for the diagram.) The inputs of these two models are the same, i.e.:

- DH supply temperature, °C
- DHW consumption (flow rate), m^3/s
- Cold water temperature, °C
- DHW circulation inlet temperature, °C
- DHW circulation water flow, m^3/s
- Outside temperature, °C
- Internal gain, kW. The only internal gain applied to the model was due to the DHW circulation line. Internal gain from lighting, occupants, etc. was neglected in this model.
- Solar radiation, kW/m^2, used to calculate the solar gain.

These inputs can be constant or variable. If the inputs are variable, they can be computed and stored in a MAT file in binary file mode. This was done in our modelling work. The sample time interval can be arbitrary. If an output value is needed at a time that falls between two values in the file, the value is automatically linearly interpolated between the appropriate values during the simulation.

Information about:

- sizes of the heat exchangers used in the DHW and space heating systems, radiators, controllers and control valves
- characteristics of the building (heat loss factor, south facing window area, thermal capacities of fast response mass and slow response mass, and area/thermal mass ratio)
- set-point for the DHW temperature, room temperature, secondary side supply temperature to the radiators, etc.

was provided to SIMULINK by executing several short MATLAB programs before the actual simulation was executed.

SIMULINK allows retrieval of signals at any required point in time by connecting this point to a virtual scope, to workspace, or to output files. In the present study, simulation results were output to MAT files. The amount of data collected and the time steps at which the data was collected were determined by block parameters. The Sample Time parameter (in To File block) allowed the specification of a sampling interval at which to collect points. This parameter was useful when using a variable-step solver where the interval between time steps may not be the same.

For the block diagram shown in Fig. A.1.1, the outputs are:

- DH return temperature, °C
- DH return temperature after the post-heater for the DHW system, °C
- Total district heating flow rate to the heating system, m^3/s
- DH flow rate to the space heating (radiator) system, m^3/s
- DH return temperature from the space heating system, °C
- Total heat loss from the building, kW

For the block diagram shown in Fig. A.1.2, the outputs are:

- DH return temperature, °C
- DH return temperature after the post-heater for the DHW system, °C
- DH return temperature from the heat exchanger for the space heating system, °C
- Total district heating flow rate to the heating system, m^3/s
- DH flow rate to the heat exchanger for the space heating system, m^3/s
- Secondary side flow rate to the radiators, m^3/s
- Secondary side return temperature from the radiators, °C

In the current study, the output data files were collected at 10-minute intervals. These data were then averaged to generate hourly data files that could be loaded to spreadsheets for an analysis of system economics.

It should be noted that the effect of pipes connecting the heat exchangers and radiators were not considered in the model. The influence of the pipes on the temperature drop and time delay is insignificant due to relatively short pipe length. This assumption was also applied to the other building heating system models described in this section.

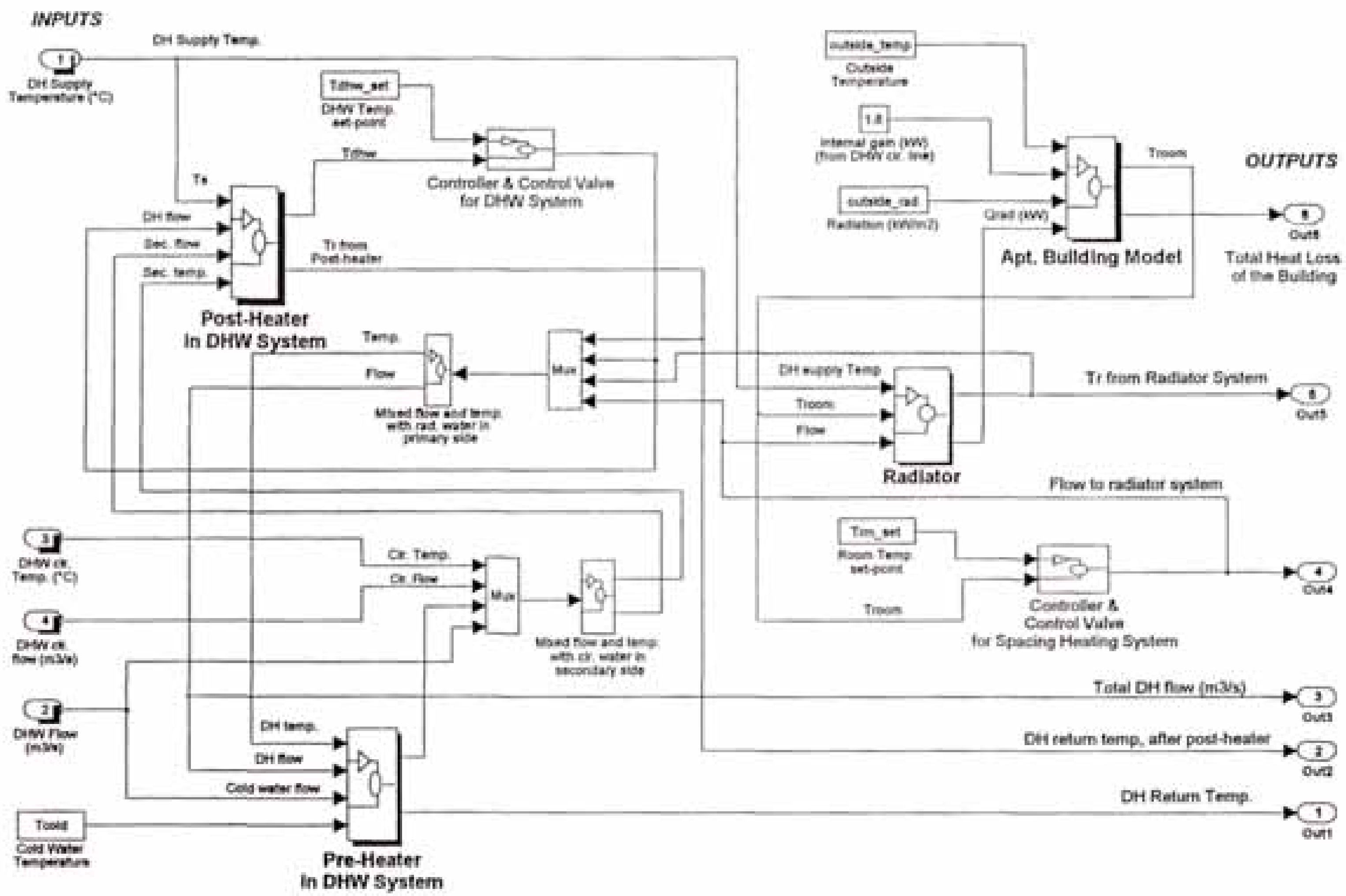

Fig. A.1.1 SIMULINK Block Diagram for a Directly-Connected, 2-Stage Heating System for the Apartment Building.

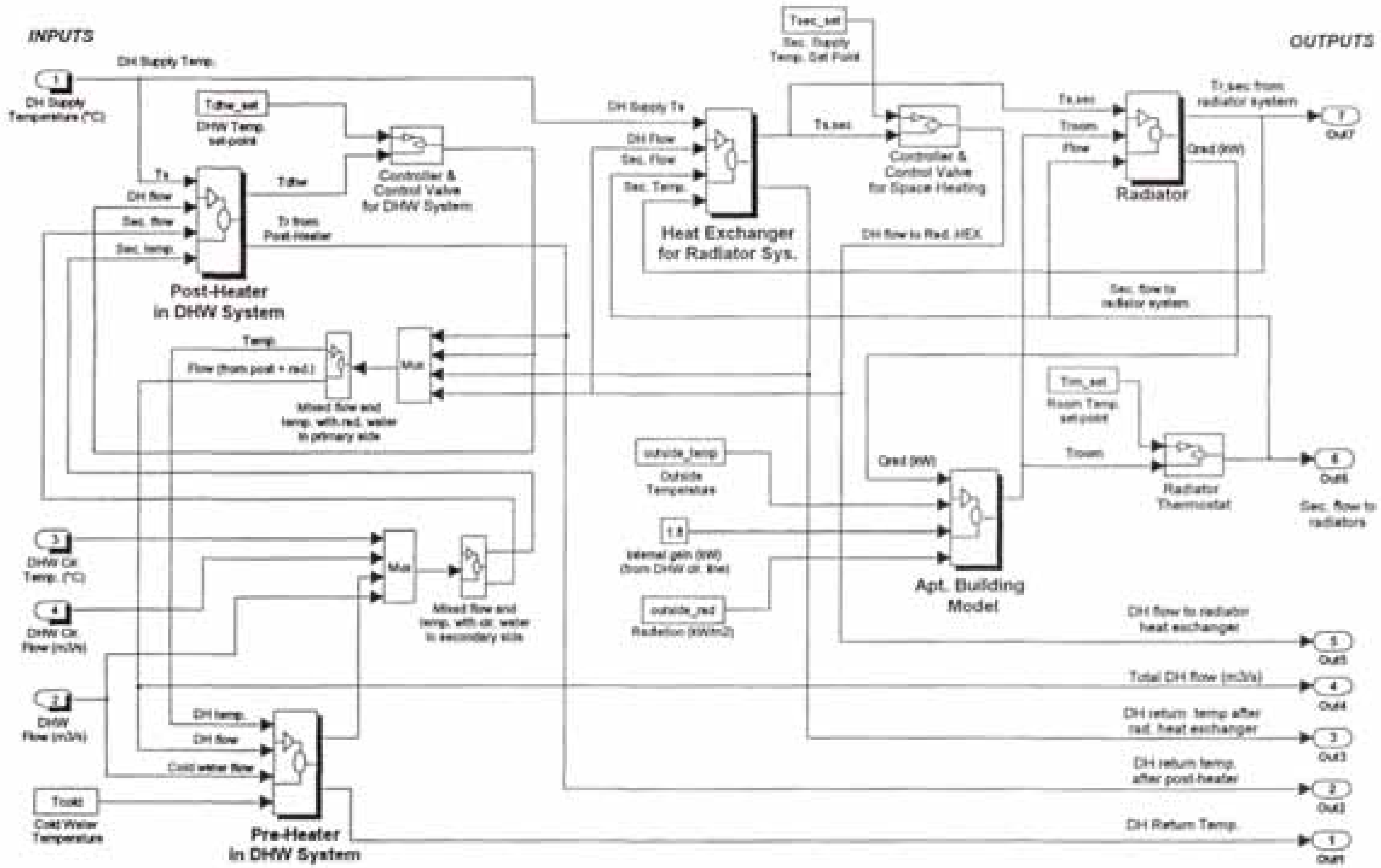

Fig. A.1.2 *SIMULINK Block Diagram for an Indirectly-Connected, 2-Stage Heating System for the Apartment Building.*

A.1.2 SIMULINK Block Diagrams for Directly and Indirectly Connected Parallel Heating Systems for the Row House

Figure A.1.3 shows the SIMULINK block diagram for a directly-connected, parallel heating system for the row house (c.f. Fig. 4.7 for the diagram.) The SIMULINK block diagram for an indirectly-connected, parallel heating system is shown in Fig. A.1.4 (c.f. Fig. 4.8 for the diagram.) The inputs of the two models are:

- DH supply temperature, °C
- DHW consumption (flow rate), m^3/s
- Cold water temperature, °C
- Outside temperature, °C
- Solar radiation, kW/m^2, used to calculate the solar gain.

Information about:

- sizes of the heat exchanger for the DHW and the space heating systems, radiators, controllers and control valves
- characteristics of the house (heat loss factor, south facing window area, thermal capacities of fast response mass and slow response mass, and area/thermal mass ratio)
- set-point for the DHW temperature, room temperature, secondary side supply temperature to the radiators, etc.

was provided to SIMULINK by executing several short MATLAB programs before the actual simulation was executed.

For the block diagram shown in Fig. A.1.3, the outputs are:

- DH return temperature, °C
- DH return temperature from the DHW system, °C
- DH return temperature from the space heating (radiator) system, °C
- Total district heating flow rate to the heating system, m^3/s
- DH flow rate to the space heating (radiator) system, m^3/s

For the block diagram shown in Fig. A.1.4, the outputs are:

- DH return temperature, °C
- DH return temperature from the DHW system, °C
- DH return temperature from the heat exchanger for the space heating system, °C
- Total district heating flow rate to the heating system, m^3/s
- DH flow rate to the heat exchanger for the space heating system, m^3/s
- Secondary side flow to the radiators, m^3/s
- Secondary side return temperature from the radiators, °C

The output data files were collected at 10-minute intervals. These data were then averaged to generate hourly data files that could be loaded to spreadsheets for an analysis of system economics.

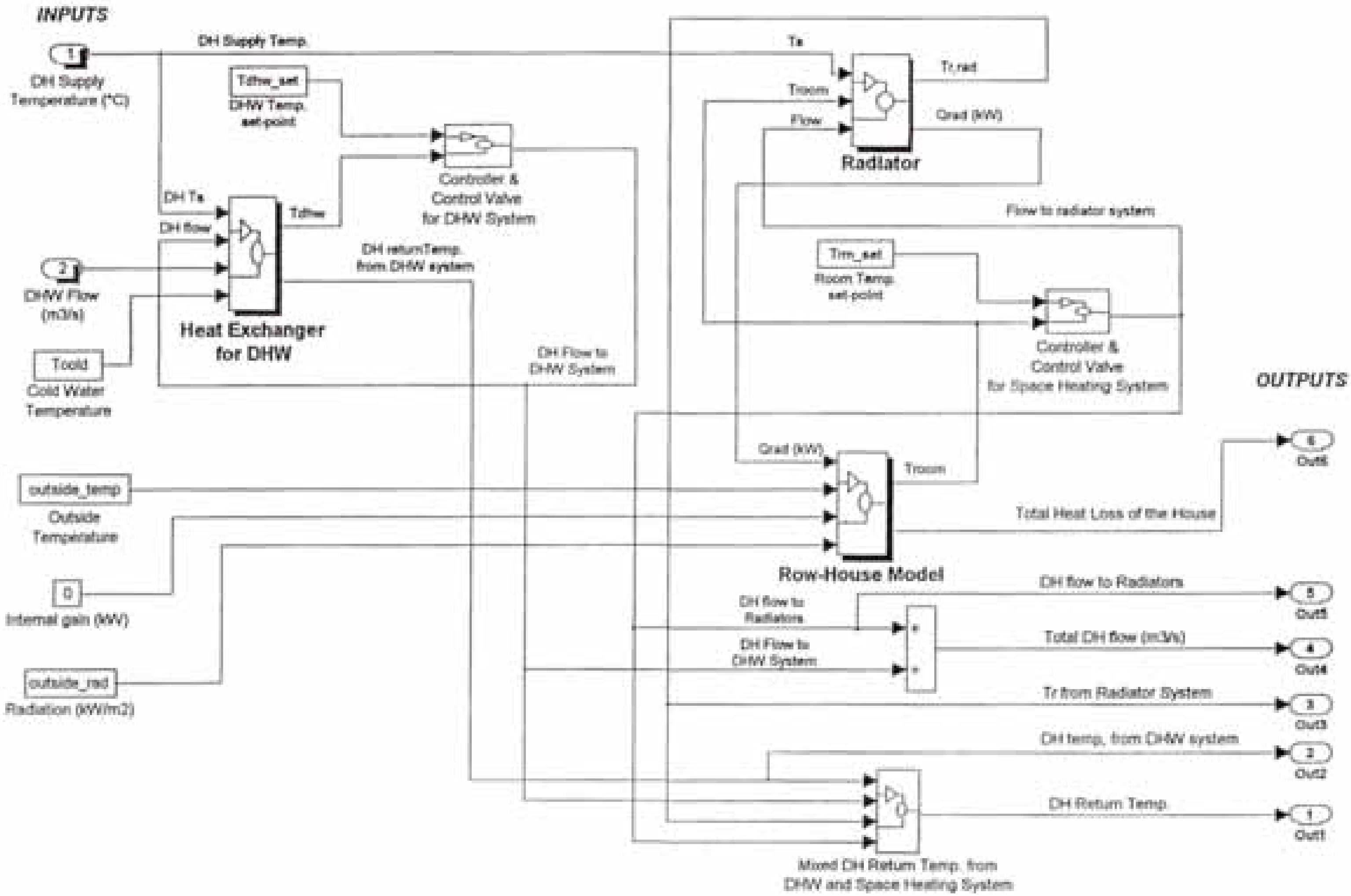

Fig. A.1.3 SIMULINK Block Diagram for a Directly-Connected, Parallel Heating System for the Row House.

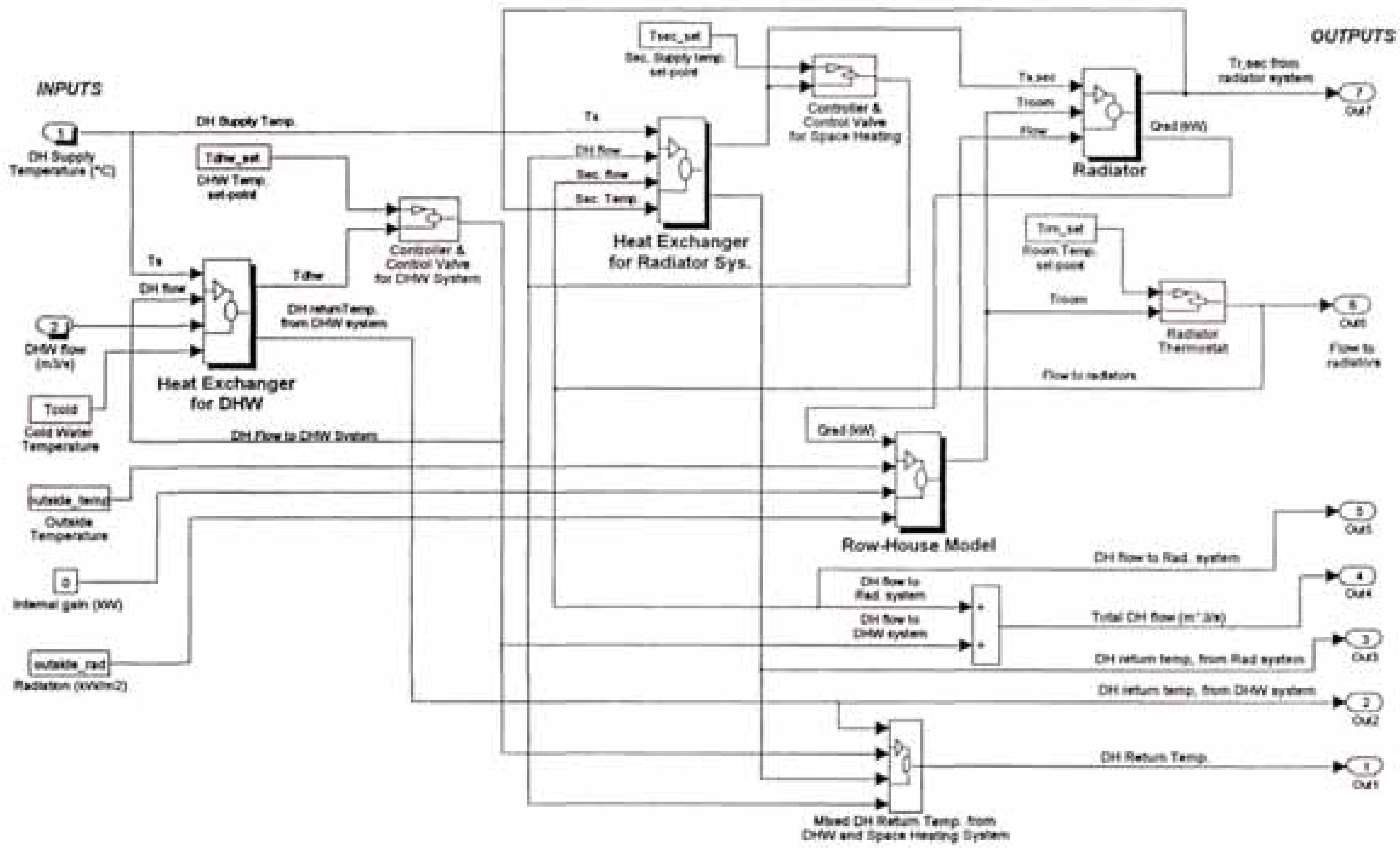

Fig. A.1.4 *SIMULINK Block Diagram for an Indirectly-Connected, Parallel Heating System for the Row House.*

A.1.3 SIMULINK Block Diagrams for Directly and Indirectly Connected Heating Systems for the Commercial Building

Figure A.1.5 shows the SIMULINK block diagram for a directly-connected heating system for the commercial building (c.f. Fig. A.4.9 for the diagram.) The indirectly-connected system is shown in Fig. A.1.6 (c.f. Fig. 4.10 for the diagram.) The inputs of these two models are the same:

- DH supply temperature, °C
- Outside temperature, °C
- Internal gain, kW
- Air flow rate to the fan coil, m^3/s

Information about:

- sizes of the heat exchangers, the radiators, fan coils, controllers, 2-way and 3-way control valves
- characteristics of the building (heat loss factor, south facing window area, thermal capacities of fast response mass and slow response mass, and area/thermal mass ratio)
- set-point for the room temperature, outlet air temperature from the fan coil, secondary side supply temperature to the radiators, etc.

was provided to SIMULINK by executing several short MATLAB programs before the actual simulation was executed.

For the block diagram shown in Fig. A.1.5, the outputs are:

- DH return temperature from the heating system, °C
- Total DH flow rate to the heating system, m^3/s
- Flow rate to the fan coil system, m^3/s
- DH flow rate to the radiator system, m^3/s
- DH return temperature from the radiator system, °C
- Total heat losses of the building, kW

For the block diagram shown in Fig. A.1.6, the outputs are:

- DH return temperature from the heating system, °C
- Total DH flow rate to the heating system, m^3/s
- DH return temperature from the radiator system, °C
- Flow rate to fan coil system, m^3/s
- DH flow rate to the radiator system, m^3/s
- Secondary side flow rate in the radiator system, m^3/s
- Secondary side return temperature from the radiator system, °C

The output data files were collected at 10-minute intervals. These data were then averaged to generate hourly data files that could be loaded to spreadsheets for an analysis of system economics.

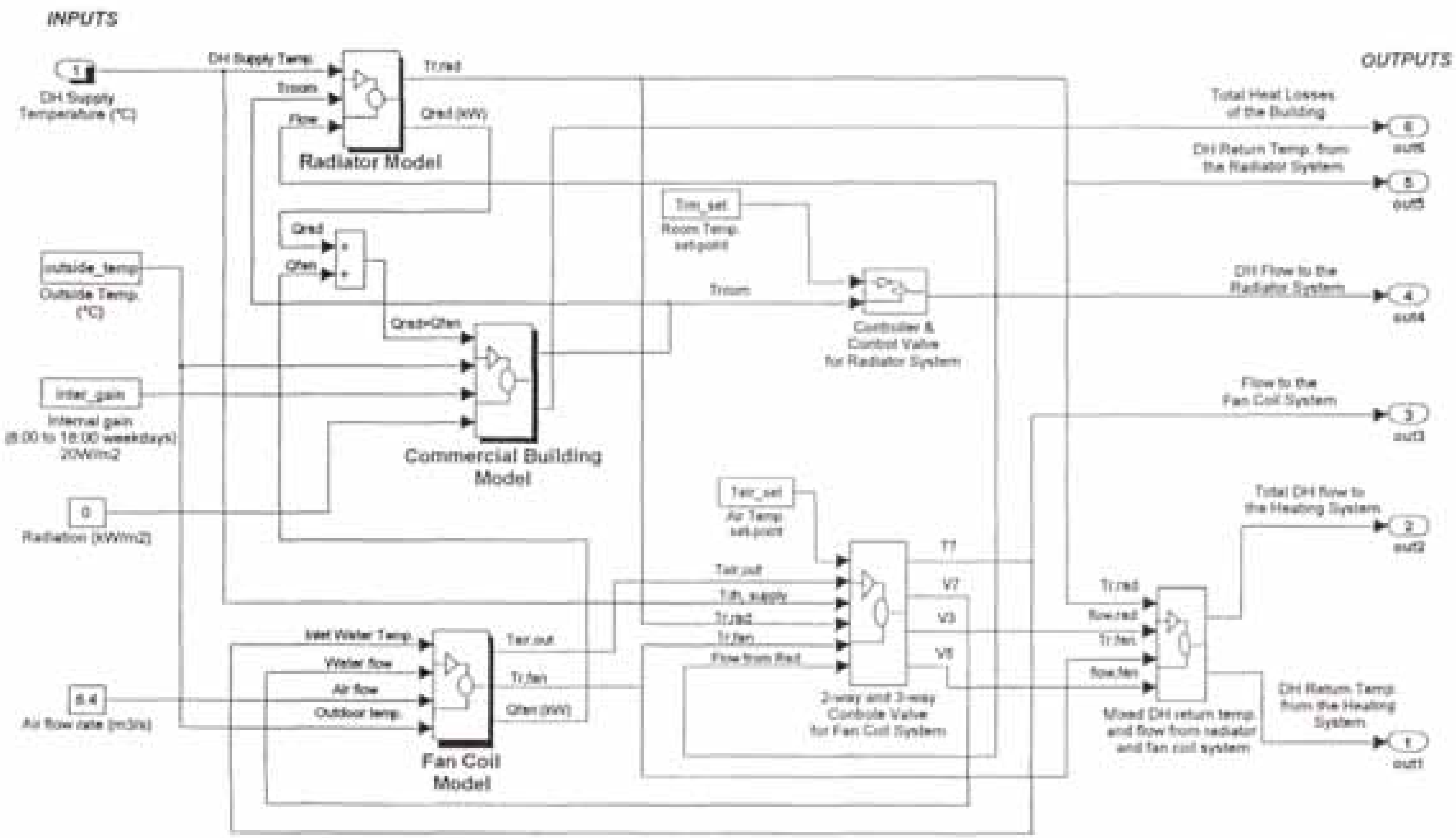

Fig. A.1.5 SIMULINK Block Diagram for a Directly-Connected Heating System for the Commercial Building.

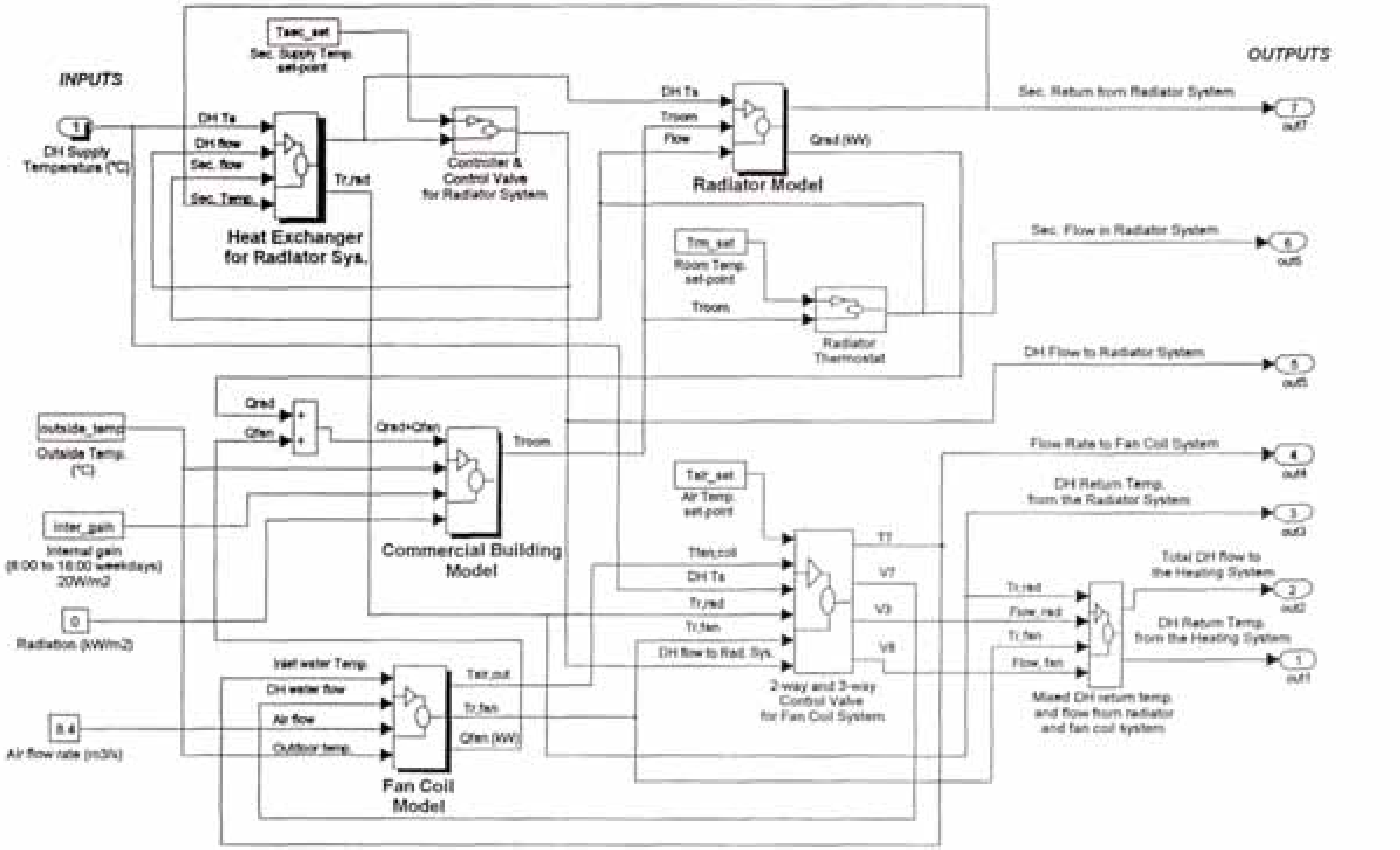

Fig. A.1.6 *SIMULINK Block Diagram for an Indirectly-Connected Heating System for the Commercial Building.*

A.2 Dynamic Models for Components Used in Building Heating Systems

To perform the SIMULINK simulations of building heating systems, dynamic models of the components that make up the heating systems were developed. These dynamic models for buildings, radiators, fan coils, plate heat exchangers, temperature sensors, controllers, actuators and control valves are described in detail in this section.

The simpler components such as temperature sensors, controllers and control valves were specified directly by a simple transfer function or SIMULINK built-in block. The more complex components such as radiators, plate heat exchangers and fan coils were developed based on general thermodynamic relations and previous work of Grétarsson et al. (1991), Hjorthol (1990), Hjorthol (1992) and Johnson (c.f. Volla et al. (1996)).

The outputs of models for the more complex components were verified by data obtained from a DH heat transfer station at a school, from laboratory experiments, or verified by manufacturers' data.

A.2.1 Dynamic Building Model

In order to enable accurate simulation of a complete district heating system, the building model must respond to the steady-state and dynamic effects of weather conditions and building occupancy patterns in a realistic manner. The thermal characteristics of a building are a complex combination of the heat transfer functions of all the components that make up the building envelope. As a result, a high level of absolute accuracy in the heat loss factor can only be achieved by detailed specification of the building. Since the DH system optimization studies were based on changes to the heating systems while keeping the building envelope constant, high absolute accuracy in any given building model is not necessary and a number of simplifications have been incorporated to speed up the simulation process. The primary emphasis in development of the building model has been on incorporating all the transfer functions that may have a significant influence on the characteristics of the various buildings that make up a typical community.

Model description

To supply the reference parameters to the model it was necessary to have a user interface that allowed the building thermal components to be specified in a convenient, standardized format. Many commercial programs are available to calculate the steady-state loss parameters of a building based on the dimensions and specification. A program (HOT2000) that computes the primary energy consumption components on a monthly basis was used to calculate average heat loss factors, using regression methods.

The following heat loss and thermal mass parameters have been incorporated in the model:

1) Envelope losses, including walls, ceiling and windows. Under steady state conditions, these losses are proportional to the difference between average inside temperature and outside temperature. Under transient conditions, the model accounted for the effects of thermal storage in the mass of the building.

2) Building thermal mass. The interior building temperature is a variable, as a function of thermostat deadband, heating system delays, night setback, etc. The temperature recovery from night setback can impose large loads on the DH system, since the heating system will operate at full power even if outside temperature is not particularly low. The problem will be compounded if the primary control valve is oversized, resulting in excessive flow from the DH network and high return temperature. This is exemplified in a following example. However, it should be noted that night setback was not used in the present simulations.

Transient measurements were made in a typical Canadian wood-frame house as the furnace operated at full power. It was concluded that if the effects of thermal mass in the outside walls can be ignored, the building transient response can be approximated by two thermal time constants in series, with air as the only heat transfer mechanism between the thermal masses and to the outdoors. For large buildings this will have errors, but since all buildings used in the simulations were held at nominally steady temperatures the errors were assumed to be small. The model incorporated a parameter related to the efficiency with which the thermal mass is coupled to the air in the building. This feature partly compensated for the different methods by which thermal mass is incorporated into the construction of buildings.

The transient temperature measurements and simulations are shown in Fig. A.2.1

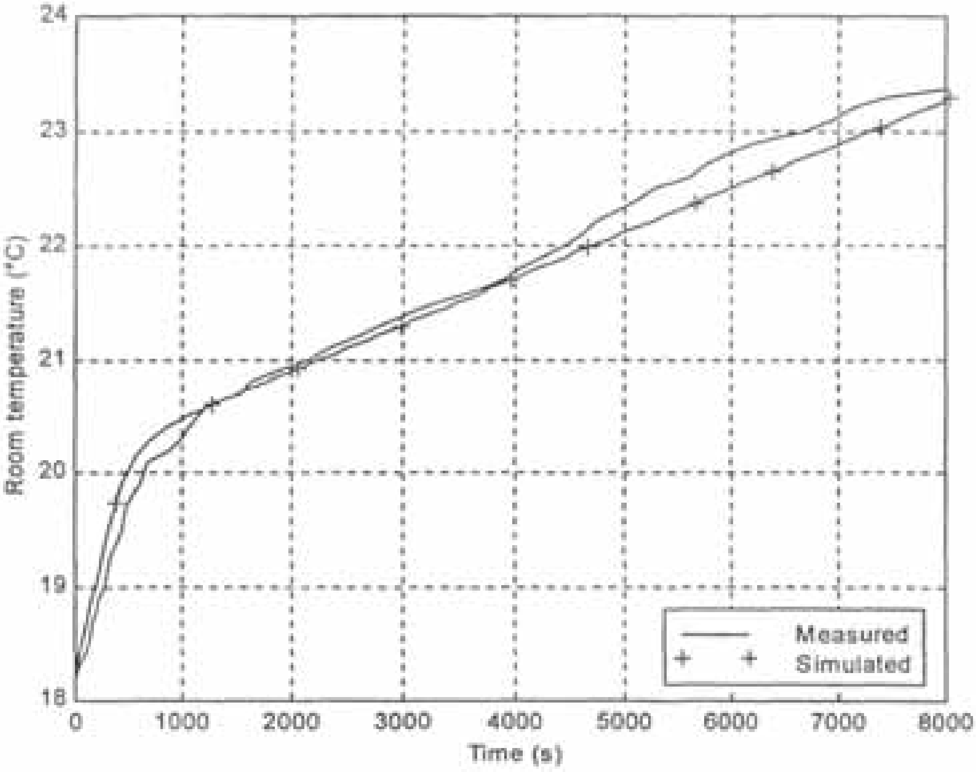

Fig. A.2.1 Measured and Simulated Building Response.

3) Ventilation losses. These losses consist of natural ventilation and/or forced ventilation. Forced ventilation heat loss, as in the case of the commercial building is a linear function of the temperature difference and mass flow rate. For the sake of simplicity, effects of varying humidity levels on the specific heat capacity have been ignored. For natural ventilation heat loss, options were included in the model to compute it as a nonlinear function of temperature difference.

If wind effects are ignored, according to Grimsrud et al (1981) the infiltration rate is given by:

$$Q = L\,(P_s\,\Delta T)^{1/2}$$

where:

L = the effective leakage area at 4 Pa, (m^2)
P_s = the stack effect parameter, ($m^2/°C\ s^2$)
ΔT = the indoor-outdoor temperature difference, (°C)

A rigorous calculation of natural ventilation requires measurements in the building to obtain the above parameters, or detailed knowledge of the construction methods. For simplicity in modeling the apartment and row-house buildings, values of estimated average yearly energy loss due to natural ventilation were calculated using the HOT2000 commercial program and a linear factor was added to the building heat loss coefficient. Estimates were done that indicated that this resulted in errors of less than three percent in the load on the DH system during any hour of the year.

4) Basement losses. The below-ground component of basement heat loss is a quasi-steady function of the long-term fluctuation of ground temperature around the building. Programs are available to calculate this, but they require detailed specification for accurate results. The building model has options for simulation of basement losses but since they were estimated to be relatively small for the buildings being modeled, these options were not incorporated.

The following building heat gains were considered in the model:

1) Building internal gains. Considerable amounts of heat are generated in buildings due to electrical equipment, lights, etc. The actual value will vary depending on time of day and day of the week. Standard design procedures are available to estimate the heat gain, based on definitions of building usage. The gains were pre-computed for our model and input as hourly data files.

2) Solar gains. The south, east and west windows will transmit solar energy at certain times of the day. The heat gain can be quite high during cold clear winter days, when the altitude of the sun is low.

The hourly solar radiation data is supplied in the form of global values on a horizontal surface. Since the solar elevation angle is continually changing, the computation of radiation on a vertical surface requires considerable amounts of data processing. The most efficient method is to pre-compute the values and then use a file to drive the simulation process by multiplying the radiation level by the window area and a transmittance factor. The transmittance factor normally ranges between 0.7 - 0.9, depending on the type of glass and number of glazings. For the current requirement, the radiation heat gains on the east and west surfaces were ignored.

SIMULINK model for buildings

The simplified block diagram of the building model is shown in Fig. A.2.2, with the detailed SIMULINK model in Fig. A.2.3.

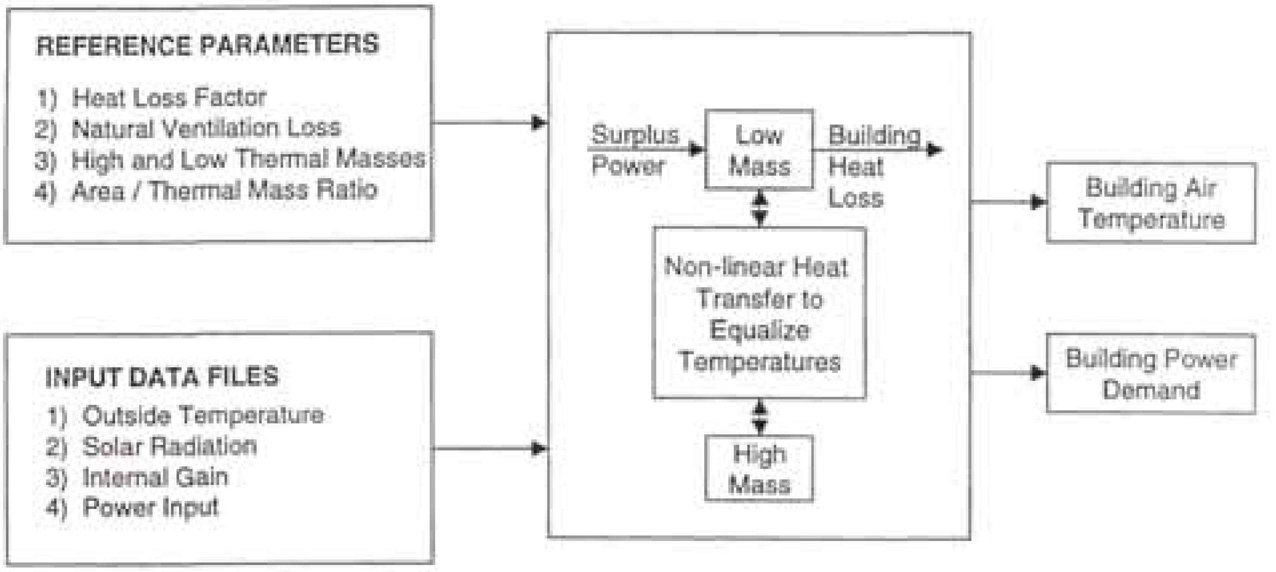

Fig. A.2.2 Simplified Building Model.

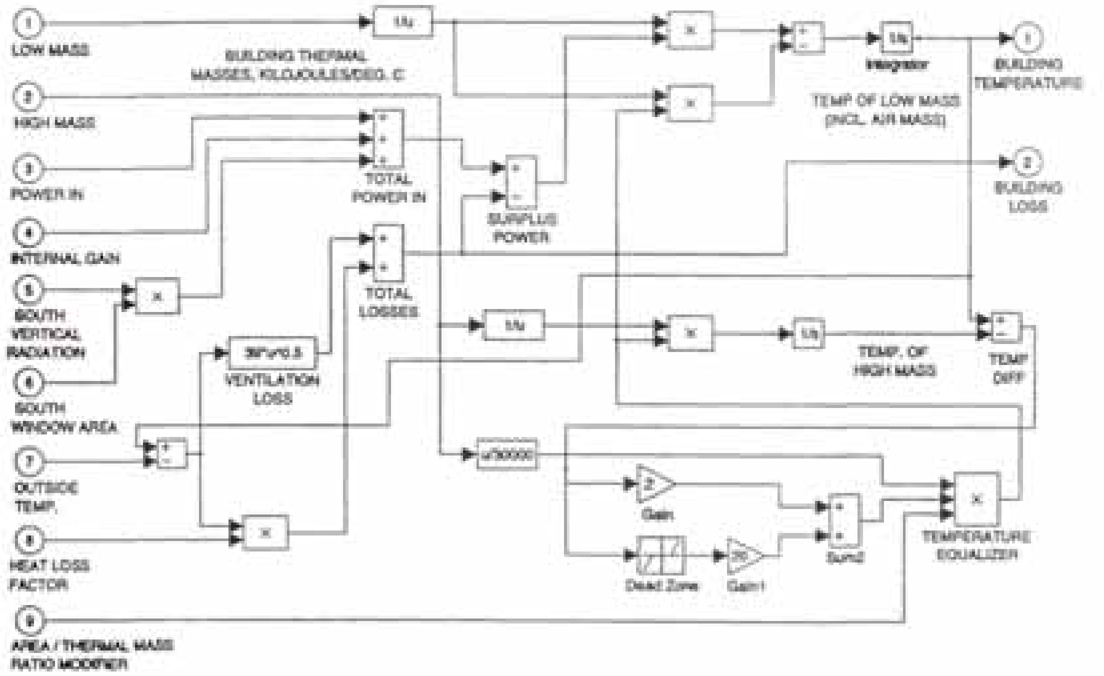

Fig. A.2.2 SIMULINK Building Model.

A key component of the building model is the temperature equalizer between the high and low thermal masses. The surplus power (input power minus losses) drives up the temperature of the low thermal mass, including air, at a rapid rate until a temperature difference of about 2.0°C between the two masses is reached. At this point the high thermal mass begins to absorb energy at a much higher rate (typically eight times faster), and the rate of temperature rise slows down in proportion. The inverse effect occurs as the building cools.

Validation of building model with dynamic data

The heating system of a school building of masonry and concrete construction was monitored for 40 days, covering periods between January 15 and March 12. DH flow and temperature measurements were taken at five-minute intervals. The outside temperature varied from +11°C to -24°C, and the interior building temperature varied from 19°C during weekdays to 13°C at night and during weekends. Sunny and cloudy periods were included as were periods of full occupancy and no occupancy, such as on weekends. From the data, estimates could be made regarding the effects of occupancy gain, solar gain and thermal mass.

Using the measured data, the model parameters were brought into agreement with the measurements. As shown in Fig. A.2.4, the simulation of the recovery cycle from night setback closely tracked the measurements. After the night setback was initiated, the building heating system "coasted" for over an hour while the stored energy was depleted, even though the outside temperature was dropping rapidly. Following this, there was considerable error between the simulated and measured data. From examination of the outside temperature function, it is obvious that the building heating system controller was acting in a nonlinear fashion. The heating system power level rose to a much higher level than would be required by the outside temperature. This was most likely caused by a delay between the average temperature of the building and the temperature seen by the control system sensor. A propagation delay function can be readily incorporated in the model to simulate this effect. Ideally, the actual school control system should use some form of derivative control to avoid the power surge.

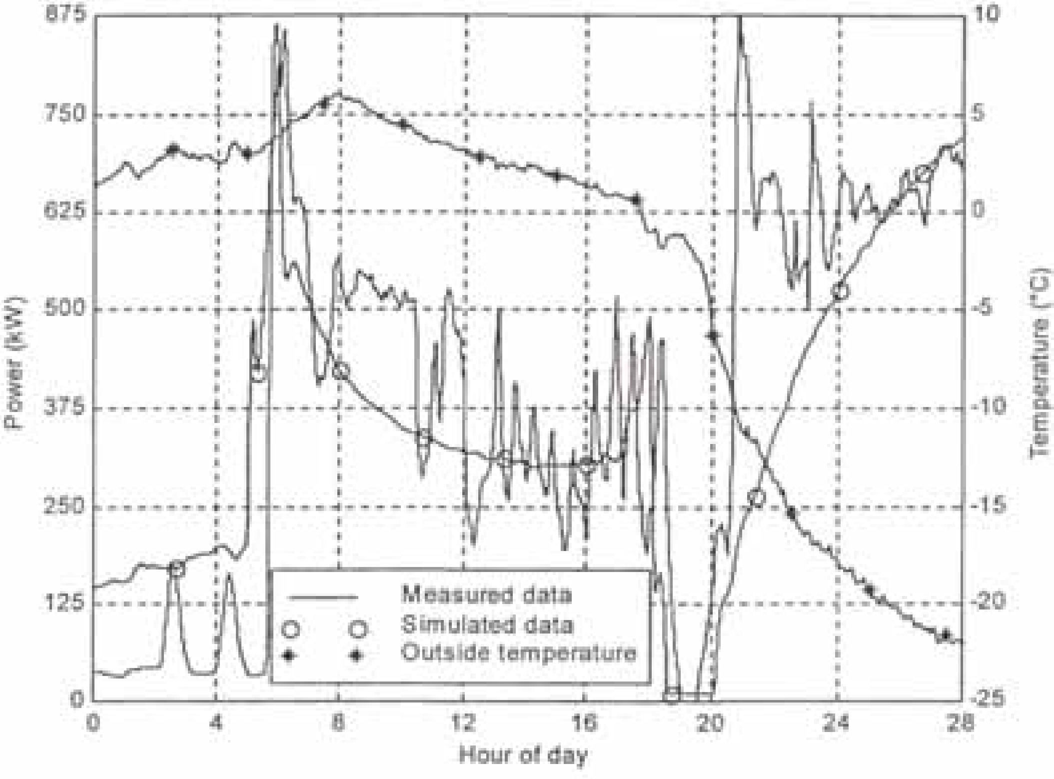

Fig. A.2.4 Measured and Simulated Building Power Demand.

A.2.2 Plate Radiator Model

Plate radiators were used for space heating in the building systems. The radiator model was based on general heat transfer theory and previous work by Grétarsson (1991) and Hjorthol (1992).

To simplify the mathematical treatment, the following assumptions were made:

- Uniform temperature in each element
- No heat conduction in the direction of water flow
- No heat conduction in the horizontal direction of the radiator plates
- Negligible temperature gradient in the radiator plate wall
- No fouling

Mathematical description of the model

The radiator is divided into a number of elements in the flow direction in the model (c.f. Fig. A.2.5), and the energy balance for each of these elements results in a first order differential equation. The heat transfer from the radiator to the surrounding space is by free convection and radiation from the outside surface area.

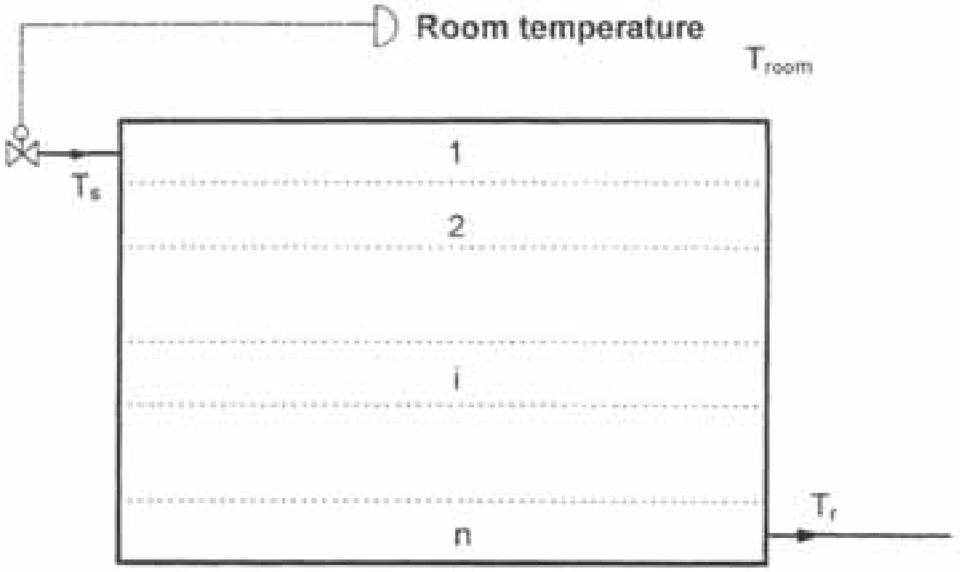

Figure A.2.5. Diagram of a Plate Radiator.

General energy balance equation:

$$\frac{C_{rad}}{n}\frac{\partial T_w(i)}{\partial t} = f_w \rho_w Cp_w (T_w(i-1) - T_w(i)) - h_{rc}(i)\frac{A_{rc}}{n}(T_{rs}(i) - T_{room})$$
$$- \varepsilon\sigma\frac{A_{rs}}{n}((273 + T_{rs}(i))^4 - (273 + T_{room})^4)$$

where

A_{rc}	-	total convection heat transfer area, m^2
A_{rs}	-	total outside surface area, m^2
C_{rad}	-	total heat capacity of radiator, J/°C
Cp_w	-	specific heat capacity of water, J/kg·°C (temperature dependent)
f_w	-	volume flow rate of water, m^3/s
$h_{rc}(i)$	-	convection heat transfer coefficient in element i, $W/m^2 \cdot °C$
n	-	number of elements used in the radiator model
T_{room}	-	room temperature, °C
$T_{rs}(i)$	-	surface temperature in element i, °C
$T_w(i)$	-	water temperature in element i, °C
ε	-	emissivity
ρ_w	-	density of water, kg/m^3 (temperature dependent)
σ	-	Stefan-Boltzmann constant, 5.67×10^{-8} $W/m^2 \cdot {}^4K$

The radiator surface temperature was approximated as follows:

$$T_{rs}(i) = \frac{4.5 \cdot T_w(i) + 0.5 \cdot T_{room}}{5}$$

Convection heat transfer coefficient

The overall convection heat transfer coefficient h_{rc} is the resistance summation of the convection coefficient between the water and the inside radiator wall, the convection coefficient between the outside surface of the radiator and the ambient air, and the resistance of the radiator plate wall.

The thermal resistance from radiator water to inside radiator wall and thermal resistance of radiator wall are relatively small, and have been neglected in the radiator model. Empirical relations for free convection were used to determine the outside convection factor between the radiator wall and the ambient air in the room:

$$Nu = CGr^m \Pr^n$$

The parameters C, m and n are empirically evaluated. The product of Grashof number (Gr) and Prandtl number (Pr) is called the Rayleigh number (Ra) which sets the transition between laminar and turbulent air flow across the vertical radiator wall. The convection heat transfer coefficient of element i, $h_{rc}(i)$, is therefore calculated by:

$$h_{rc}(\mathrm{i}) = \frac{k_a}{l_{rad}(i)} \cdot 0.10 \cdot (Gr \cdot \Pr)^{0.333} \qquad (10^9 < Ra < 10^{13}) \text{ Holman (1976)}$$

$$h_{rc}(\mathrm{i}) = \frac{k_a}{l_{rad}(i)} \cdot 0.59 \cdot (Gr \cdot \Pr)^{0.25} \qquad (10^4 < Ra < 10^9) \text{ Holman (1976)}$$

$$h_{rc}(\mathrm{i}) = \frac{k_a}{l_{rad}(i)} \cdot (1 + \frac{0.67(Gr \cdot \Pr)^{0.25}}{(1 + (\frac{0.492}{\Pr})^{0.563})^{0.444}}) \qquad (Ra < 10^4) \qquad \text{Zhu (1987)}$$

where

k_a - heat conductivity of ambient air, W/m·°C (temperature dependent)
$l_{rad}(i)$ - characteristic length (i.e. height to the top of (i)th element), m

The Grashof number is defined as:

$$Gr = \frac{g\beta\Delta T(i) l_{rad}{}^3(i)}{\nu^2}$$

where:

g - gravitational constant, m/s^2
β - heat expansion coefficient, 1/°K
ΔT(i) - logarithmic mean temperature difference at element i, °C
ν - kinematic viscosity, m^2/s (temperature dependent)

The above equations are empirical relations developed for vertical isothermal surfaces. When the convection coefficient is calculated the elements below the one considered were assumed to be at the same temperature. Grétarsson et al. (1991) investigated isolated cases for high temperature difference across the radiator. He found that this assumption caused a maximum 10% error in the convection coefficient.

Figure A.2.6 shows the inputs and outputs of the radiator model in SIMULINK.

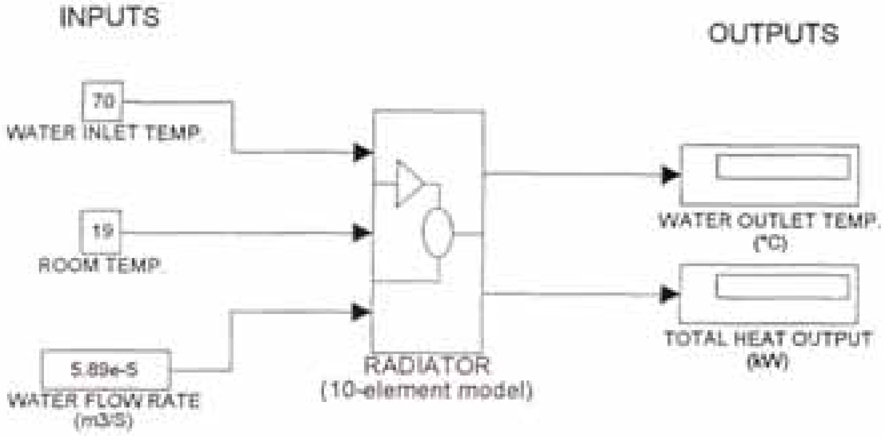

Fig. A.2.6 Radiator Model Input and Output Parameters.

Model verification

A steady-state verification of the radiator model was performed by simulating the outlet temperature and heat output from the radiator and comparing the results to the technical data obtained from the manufacturer's catalogue. Because no measurements were available for the dynamic performance of the radiator, dynamic model verification was not carried out.

The radiator model was verified using several sizes of THOR panel radiators of the model EURA. The manufacturer's catalogue included technical data needed in the simulations, such as inlet and outlet water temperature, heat output at various inlet temperature and flow levels, size of the radiators, heat transfer area, etc. The THOR panel radiators are designed for 90/70°C operation, and are produced in heights of 300, 450, 550, 650 and 850 mm with lengths between 400 to 3000 mm. The THOR panel radiators model EURA 10 (single panel without fins) with a length of 1000 mm and a height of 300, 450, 550, 650 and 850 mm were chosen for model verification.

Paulsen (1991) studied the effect of the number of vertical increments on the numerical simulation. He found that, for three very common radiator types, 10 elements are an appropriate division. Therefore, that number of divisions was used in our simulations.

Table A.2.1 shows the simulated radiator outlet temperature (T_{rc}) and heat output (Q_c), heat output according to catalogue (Q_o) and relative error between these two at various inlet temperature levels. The first column (temp.) shows the nominal inlet and outlet water temperatures provided by manufacturer's catalogue. The room temperature was constant at 20°C. The emissivity, ε, was 0.8.

Table A.2.1 Simulated Radiator Outlet Temperatures and Heat Outputs, Heat Outputs According to Manufacturer's Data and Relative Error of Heat Output at Various Inlet Temperature Levels.

	H=300 mm	L=1000 mm			H=450 mm	L=1000 mm			H=550 mm	L=1000 mm		
Temp.	Trc	Qc	Qo	error (%)	Trc	Qc	Qo	error (%)	Trc	Qc	Qo	error (%)
90/70	70.73	445	462	-3.68	69.80	640	646	-0.93	69.80	777	769	1.04
85/75	75.40	452	469	-3.62	75.00	654	652	0.31	74.80	792	773	2.46
80/60	60.60	354	365	-3.01	60.07	510	511	-0.20	59.78	616	609	1.15
80/40	41.00	238	245	-2.86	40.68	343	349	-1.72	40.50	415	420	-1.19
70/55	55.40	292	300	-2.67	54.94	421	419	0.48	54.68	509	498	2.21
60/40	40.23	182	186	-2.15	39.91	262	261	0.38	39.70	317	312	1.60
55/45	45.07	192	195	-1.54	44.81	277	272	1.84	44.58	335	321	4.36
	H=650 mm	L=1000 mm			H=850 mm	L=1000 mm						
Temp.	Trc	Qc	Qo	error (%)	Trc	Qc	Qo	error (%)				
90/70	69.50	915	892	2.58	69.50	1163	1132	2.74				
85/75	74.60	934	894	4.47	74.50	1187	1130	5.04				
80/60	59.50	725	706	2.69	59.50	922	900	2.44				
80/40	40.40	489	494	-1.01	40.73	629	640	-1.72				
70/55	54.42	598	576	3.82	54.43	762	734	3.81				
60/40	39.46	372	362	2.76	39.63	476	467	1.93				
55/45	44.39	394	371	6.20	44.42	502	474	5.91				

Trc is calculated radiator outlet temperature (Deg. C), Qc is calculated radiator heat output (W)
Qo (W) is radiator heat output according to manufacture's catalog.

It appears that the simulated radiator outlet temperatures and heat outputs are in fairly good agreement with the manufacturer's data. The relative error is within ± 6.20% and the larger errors occur at lower supply temperatures. The error may result from the simplification of the model and the empirical expression of the convection heat transfer coefficients. The results indicate that the radiator model gives acceptable accuracy.

THOR plate radiators with a height of 0.85m were used in the simulations. The radiator heat transfer area was enlarged simply by increasing its length.

A.2.3 Fan Coil Model

The fan coil, also called ventilation air coil, model was based on previous work done by Hjorthol (1992) and Johnson et al. (c.f. Volla et al. (1996)). A 3-cell model using basic energy equations was used in the CHESS program, c.f. Hjorthol (1992) and Volla et al. (1996), to simulate the fan coil. Johnson, at the University of Saskatchewan (U of S), validated the CHESS model by comparing its results to a steady state model developed at U of S. The steady state model was verified by measured data and showed that the uncertainties of the simulation were less than 5%.

The U of S model calculates the input values required in the CHESS model, such as air side heat transfer area, air volume, fin volume, tube volume, etc., for a given fan coil based on its detailed geometric data. The CHESS model and the steady state model have a good agreement if correct input values are introduced, otherwise errors up to 50% can occur in the overall heat transfer coefficient, see Part III of Rolla et al. (1996).

In the present study, the mathematical description of the model was based on general energy balance equations for water, tube wall/fin and air for each element. The input data to the model, such as air side heat transfer area, air volume, fin volume, tube volume, collar resistance, wall resistance, air side heat transfer coefficient and fin coefficient, were calculated using the U of S simulation program.

Figure A.2.7 shows the diagram of a 4-row, 4-pass fan coil which was used in the commercial building heating systems. Three cells were used in the fan coil length direction. Since the tube has four passes, there is a total of 12 elements in the model.

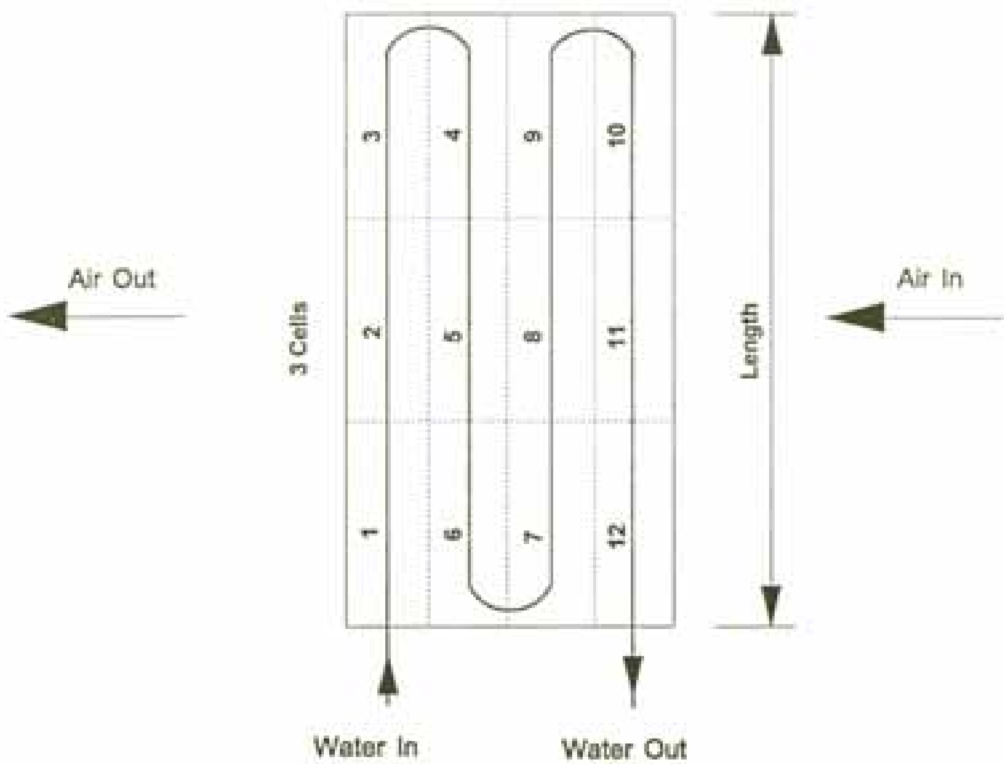

Fig. A.2.7 Diagram of a 4-Row, 4-Pass Fan Coil.

The following assumptions were made to simplify the model descriptions:

- Uniform temperature in each element
- No heat conduction in the water or air flow direction
- No fouling

Mathematical description of the model

General energy balance equation for water:

$$\frac{\partial(\rho_w Cp_w V_w T_w(i))}{\partial t} = f_w \rho_w Cp_w (T_w(i-1) - T_w(i)) - h_w A_w (T_{w,m}(i) - T_t(i))$$

General energy balance equation for air:

$$\frac{\partial(\rho_a Cp_a V_a T_a(i))}{\partial t} = f_a \rho_a Cp_a (T_{a,in}(i) - T_{a,out}(i)) - h_a A_a (T_{a,m}(i) - T_t(i))$$

General energy balance for tube wall and fin:

$$\frac{\partial(\rho_t Cp_t V_t T_t(i))}{\partial t} = h_w A_w (T_{w,m}(i) - T_t(i)) + h_a A_a (T_{a,m}(i) - T_t(i))$$

where $T_{a,in}$ (i) and $T_{a,out}$ (i) are the inlet and outlet air temperature at element i, and

$$T_{w,m}(i) = \frac{T_w(i-1) + T_w(i)}{2}$$

$$T_{a,m}(i) = \frac{T_{a,in}(i) + T_{a,out}(i)}{2}$$

The water side heat transfer area for each element was calculated by:

$$A_w = \frac{\pi D_t L_t N_t}{n}$$

where:

D_t = tube inner diameter, m
L_t = total tube length, m
N_t = total number of straight tubes per row (in vertical direction)
n = number of elements used in the model

The volume of water in each element is given by:

$$V_w = \frac{\frac{\pi}{4} D_t^2 L_t N_t}{n}$$

As mentioned previously, the air side heat transfer area A_a and air volume of each element V_a were calculated by the U of S model.

Heat transfer coefficients

The water side heat transfer coefficient was calculated from a typical dimensionless convection heat transfer equation:

$$Nu = \frac{h_w D_i}{\lambda_w} = C \, \mathrm{Re}^m \, \mathrm{Pr}^n$$

The Reynolds number is flow and temperature dependent while the Pr number is temperature dependent. The constant parameters C, m and n were empirically evaluated.

The air side effective heat transfer coefficient, including fin collar and fin wall, is calculated by:

$$\frac{1}{h_a} = (R_{collar} + R_{wall})A_a + \frac{1}{h_{air}\eta_{fin}}$$

The resistance of the collar R_{collar} and the wall R_{wall}, and fin efficiency η_{fin} can be calculated by the steady state model. The heat transfer coefficient of the air side h_{air} was approximated from the equation below:

$$h_{air} = h_{air,nom}\left(\frac{f_a}{f_{a,nom}}\right)^m$$

where:

$f_{air,nom}$ = air flow rate corresponding to the nominal air side heat transfer coefficient, m^2/s
f_a = actual air flow rate, m^2/s
$h_{air,nom}$ = air side heat transfer coefficient at nominal air flow rate, $W/m^2\ °C$. It can be calculated by the U of S model.
m = exponent correlating the change in heat transfer coefficient with the change in air flow rate.

Figure A.2.8 shows the input-output parameters of the fan coil model.

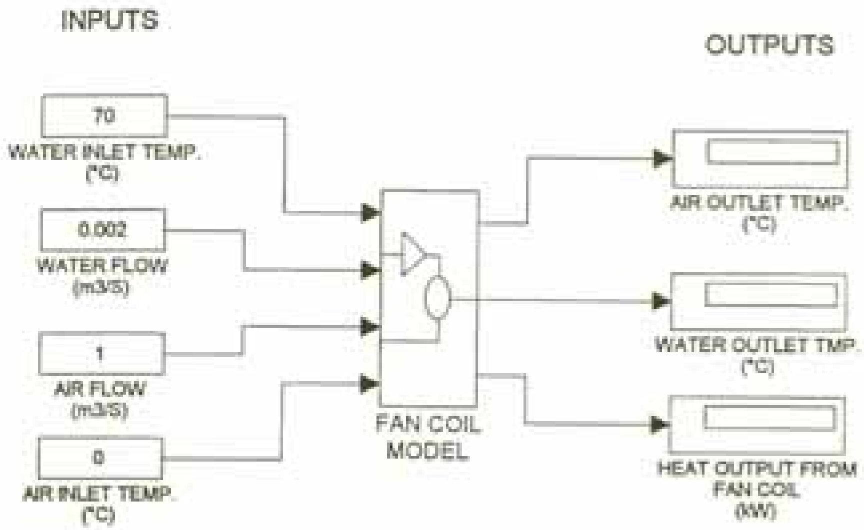

Fig. A.2.8 Fan Coil Model Input-Output Parameters.

Model Verification

The verification of the fan coil model was carried out by comparing the results from the SIMULINK model and the U of S steady state model. As stated by Johnson (see Volla et al. (1996)), the uncertainties of the steady state model were less than 5%.

A 4-row, 4-pass fan coil (see Fig. A.2.7 for the diagram) with 7 tubes per row was simulated by the SIMULINK model and the U of S model. The following equations were applied in the fan coil model to calculate the water side heat transfer coefficient:

$$Nu = 0.023\,\mathrm{Re}^{0.83}\,\mathrm{Pr}^{0.33} \qquad (\mathrm{Re} \geq 4200)$$
$$Nu = 1.86\,\mathrm{Re}^{0.33}\,\mathrm{Pr}^{0.33} \qquad (\mathrm{Re} < 4200)$$

The first equation was used for fully developed turbulent flow. As pointed out in Incropera (1996), this equation is easily applied, however errors as large as 25% may result from its use. Such errors may be reduced to less than 10% through the use of more recent, but generally more complex correlations, such as the correlation proposed by Gnielinski (1976). The Gnielinski form was adopted in the U of S steady state model. A comparison of these two equations was made, and it was found that the difference in Nusselt number was less than 15% at high Reynolds numbers (Re>20,000) and within 25% at lower Reynolds numbers. For the present study, however, the simple form shown above was deemed satisfactory.

The nominal air flow rate in the fan coil was assumed to be 1.5 m^3/s. By varying the air flow rate, the corresponding air side heat transfer coefficient was obtained from the U of S model.

Then the exponent, m, was evaluated. It was found that the average exponent value for the simulated fan coil was 0.7, i.e:

$$h_{air} = h_{air,nom}\left(\frac{f_a}{f_{a,nom}}\right)^{0.7}$$

Table A.2.2 shows the air and water outlet temperatures simulated by the SIMULINK model and the U of S model. The deviation of heat output shown in the table was calculated by:

$$Deviation\ (\%) = \frac{T_{a,out(SIMULINK)} - T_{a,out(U\ of\ S)}}{T_{a,out(U\ of\ S)} - T_{a,in}} * 100 \qquad \text{(Air Side)}$$

$$Deviation\ (\%) = \frac{T_{w,out(SIMULINK)} - T_{w,out(U\ of\ S)}}{T_{w,in} - T_{w,out(U\ of\ S)}} * 100 \qquad \text{(Water Side)}$$

Table A.2.2 Comparison of Simulation Results of the SIMULINK and U of S Model.

Inlet Temp. (°C)) (T_a / T_w)	Air Outlet Temp. (°C)		Water Outlet Temp. (°C)		Deviation (%)	
	U of S	SIMULINK	U of S	SIMULINK	Air Side	Water Side
-35 / 80	42.27	39.44	60.02	58.69	-3.66	6.66
-35 / 70	34.84	32.26	51.79	50.65	-3.69	6.26
-15 / 80	50.29	48.62	63.87	62.84	-2.56	6.39
-15 / 70	42.87	41.37	55.60	54.72	-2.59	6.11
0 / 80	55.85	54.80	66.63	65.82	-1.88	6.06
0 / 70	48.43	47.51	58.33	57.65	-1.90	5.83
10 / 80	59.35	58.63	68.42	67.74	-1.46	5.87
10 / 70	51.93	51.30	60.10	59.54	-1.50	5.66
* Air flow f_a=1.5 m^3/s, Water flow f_w=0.0017 m^3/s						
Flow Rate (m^3/s) (f_a / f_w)	Air Outlet Temp. (°C)		Water Outlet Temp. (°C)		Deviation (%)	
	U of S	SIMULINK	U of S	SIMULINK	Air Side	Water Side
1.50/0.00255	45.26	43.70	60.06	59.41	-2.59	6.54
1.50/0.00085	36.24	34.97	44.00	42.79	-2.48	4.65
2.25/0.0017	33.04	33.41	51.66	50.16	0.77	8.18
0.75/0.0017	55.85	52.95	61.50	60.88	-4.09	7.29
2.25/0.00255	35.88	36.33	57.13	56.00	0.88	8.78
0.75/0.00085	52.07	49.08	53.70	58.07	-4.46	5.64
0.38/0.00043	59.51	55.55	52.42	51.16	-5.31	7.17
* Air inlet temperature T_a=-15°C, Water inlet temperature T_w=70°C						

The comparison shows that the deviation between the two models was within ±5.31% on the air side and below 9% on the water side. The errors result mainly from the simple heat transfer coefficient correlation used in the SIMULINK model. However, the errors are within the range of acceptability. The results are accurate enough for the case studies of this project.

Experimental Model Validation

Fan coils are available in many different configurations and corresponding simulation models must be constructed for each case. A small residential size coil was purchased and a SIMULINK model developed to match its characteristics. The coil was also instrumented and installed in a wind tunnel to determine its heat transfer characteristics under different operating conditions. The water flow arrangement was as simple as possible, with one continuous path.

The coil parameters are:

Overall dimensions	0.38 x 0.38 m
Number of rows	2
Number of tubes per row	10
Number of water flow circuits	1

A simple diagram of the coil is shown in Fig. A.2.9. The interconnection of the cells is shown in Fig. A.2.10.

As a result of the single water flow circuit with staggered tubes, there will be a lateral gradient in the air stream as it goes through the coil. This gradient has an impact on the temperature of the air approaching the second row of tubes. The equivalent inlet air temperature on a second row tube will be a weighted function of the exit air temperatures of the first row tubes above and below it as well as the ambient air temperature coming directly between the first row tubes. In our fan coil model, the first row tube exit temperatures were weighted at 20% each, with the ambient air weighted at 60%.

Each straight tube section is one cell or computational element in the model. This leads to the use of 20 elements in the model, which may be more than is required for acceptable accuracy. Since the water flow alternates between the front and back rows, an advantage of the single tube cell is that the interaction between the front and back row is easier to compute. If it were found necessary to speed up the simulation by reducing the number of elements, this model can be used as a reference to check the accuracy of the simplified model.

The heat transfer characters of the air side of the coil were based on the U of S model, c.f. Volla et al. (1996), and these parameters were incorporated into the SIMULINK model.

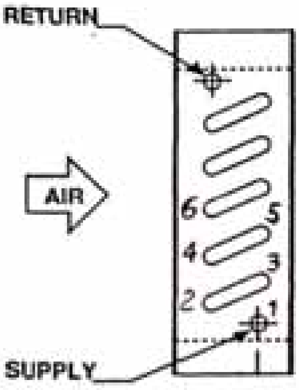

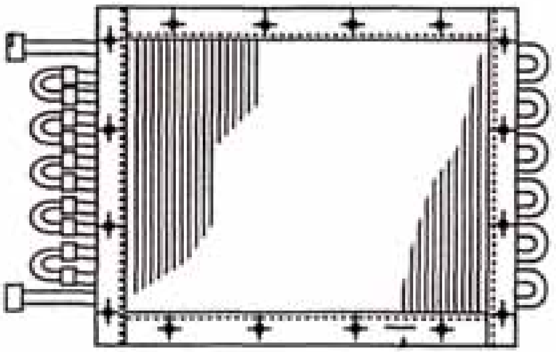

Fig. A.2.9 Definition of Elements and Flows in Fan Coil.

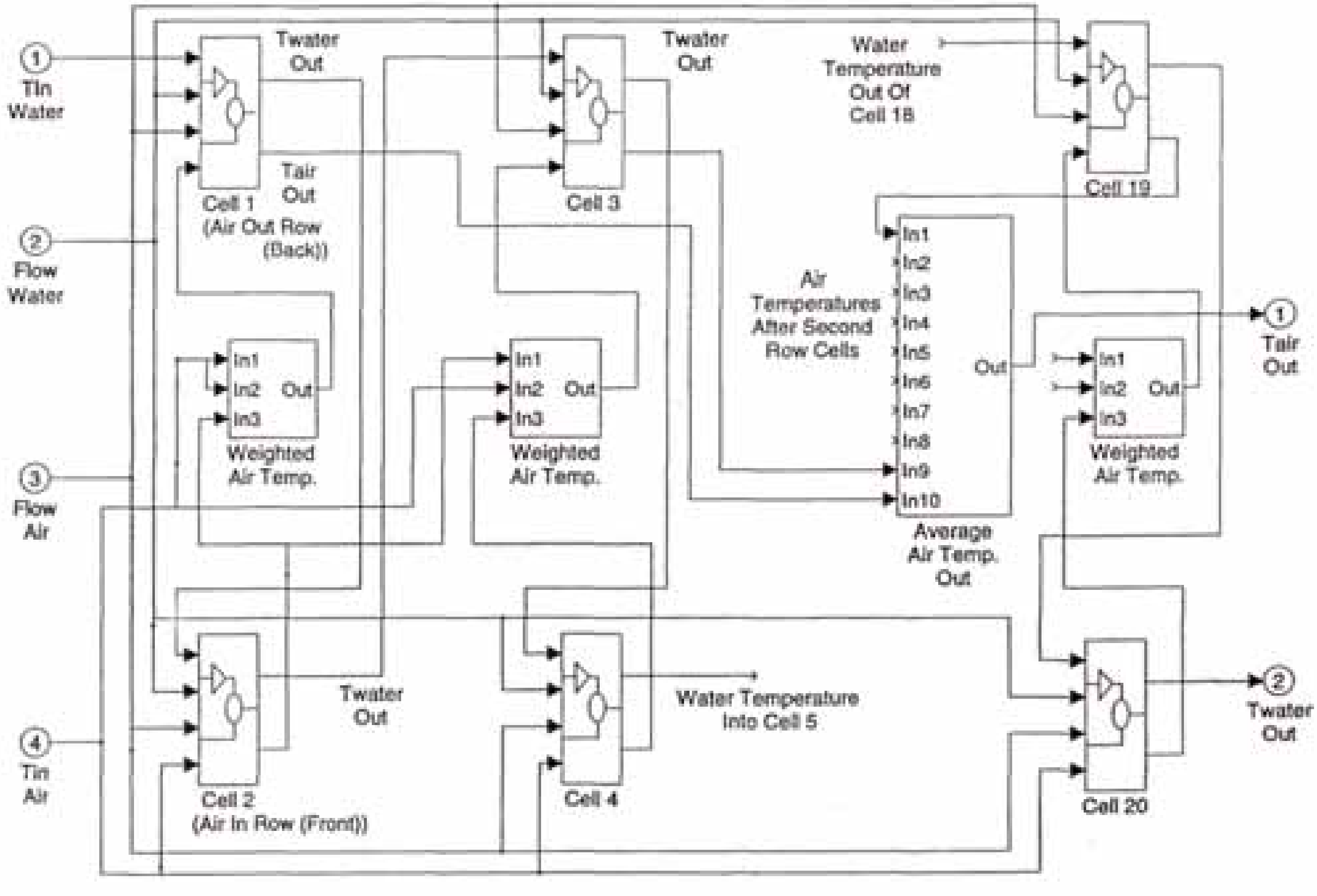

Fig. A.2.10 Interconnection of Elements in Fan Coil Model.

In order to establish the relative magnitude of the various thermal impedances in the model, it was operated at the following conditions:

Airflow velocity	1.0 m/s
Inlet air temperature	20°C
Water flow rate	$0.06 * 10^{-3}$ m^3/s
Inlet water temperature	50°C

The heat transfer parameters in the model were computed in Element 10 to give an indication of the average conditions in the model. There are four thermal impedance components:

Location	Thermal Impedance	% of Total
Liquid side	0.0171 °C/W	15.6 %
Collar resistance	0.00642 °C/W	5.9 %
Tube wall resistance	7.0×10^{-5} °C/W	0.06 %
Air side, incl. fin efficiency	0.0859 °C/W	78.4 %

The largest component of thermal impedance was on the air side. The tube wall resistance was negligible in this design, but this parameter was included in the model.

With the same temperature conditions of 50°C and 20°C for the inlet water and air temperature, computations were done using both the manufacturer's design software and the SIMULINK model. Both the water and air flow rates were varied over a range of about three to one. The results are shown in Fig. A.2.11. At the higher values of air flow velocity, the two results are in close agreement, with errors of less than 6%. At the lowest air flow rate the maximum errors are about 9%. The exponent that controls the variation of air side heat transfer coefficient in the SIMULINK model was set to 0.6. A slightly higher value of this exponent would reduce the errors at low air velocities.

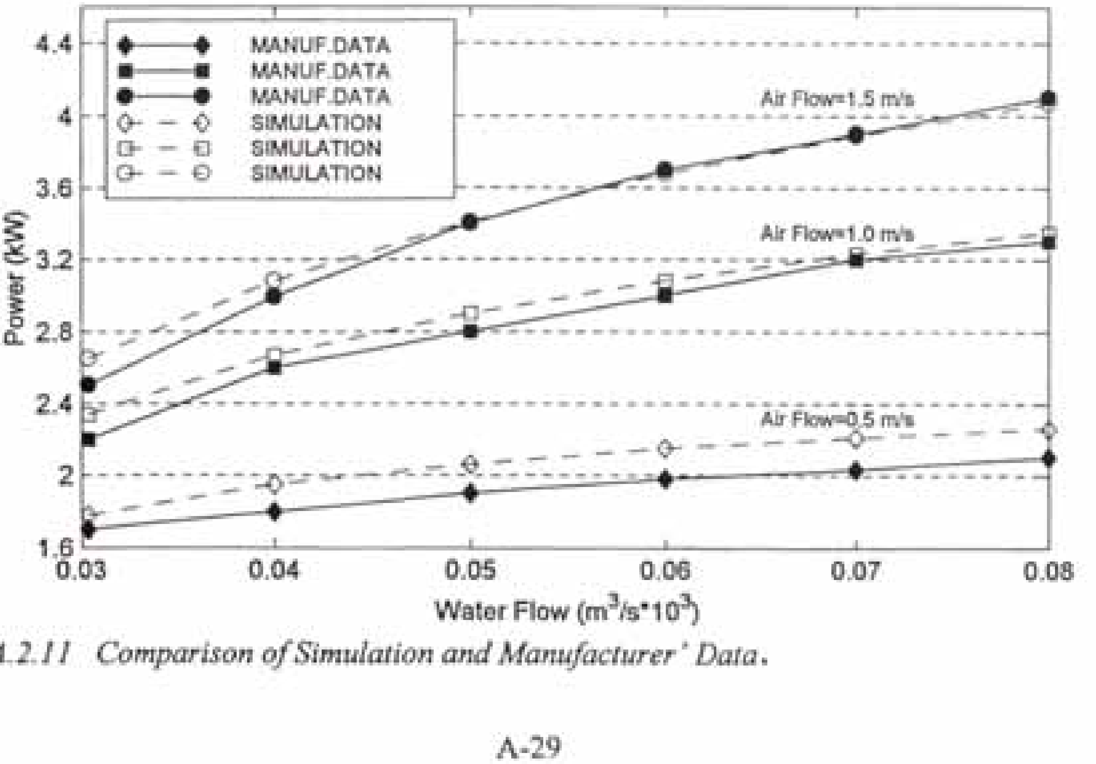

Fig. A.2.11 Comparison of Simulation and Manufacturer' Data.

A wind tunnel type duct was constructed to match the dimensions of the coil. The fan was located on the suction side of the coil, two metres downstream. A 30 cm section of duct was located on the intake side of the coil.

Air Flow Measurements

A vane anemometer was calibrated to an accuracy of 4.0%. The inlet air stream was measured at a plane 15 cm into the inlet duct. Nine points were sampled in three rows. Blockage corrections were applied. The area covered by the measurements was about 53% of the duct area. The averaged flow velocity in the corners of the duct was within 12% of the centre velocity for the higher flow, and within 16% for the low flows.

Temperature Measurements

The water inlet/outlet temperatures were taken with platinum RTDs, matched to 0.1°C, using four-wire measurements. The air temperature was measured with type T thermocouples. These were checked against an RTD at 25°C and agreed within 0.2°C. A single thermocouple was located in the centre of the inlet duct and an array of five thermocouples was located 30 cm downstream of the coil.

Test Conditions and Measurement Results

Airflow velocity	1.1 to 1.5 m/s
Inlet air temperature	24°C
Water flow rate	$0.043*10^{-3}$ to $0.061*10^{-3}$ m^3/s
Inlet water temperature	62°C

Since the inlet air and water temperatures could drift by about half a degree during the course of the experiment, it was difficult to establish when transients had become negligible after a change in water flow rate. To verify this, a second set of measurements was made at the same nominal operating points, with the water flow rate being changed in the opposite direction.

The results are shown in Fig. A.2.12, where the errors in the measurements are compared to the manufacturer's data. Results of simulations at the same operating points are also shown.

The measured values were low by 5.5 to 7.0%. There is a systematic error, most likely due to errors in air velocity measurements. The average of the exit air temperatures was within one degree of the manufacturer's value.

The results of the SIMULINK model were typically within 1.0% of the manufacturer's data, with one value at 2.9% error.

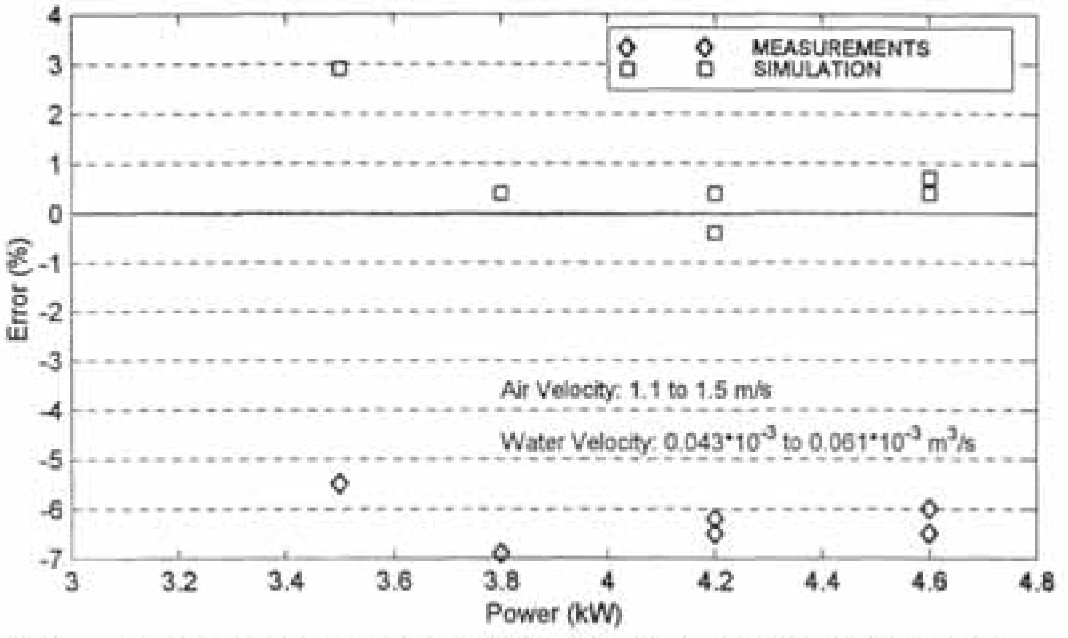

Fig. A.2.12 Measured and Simulated Error with Respect to Manufacturer's Data.

A.2.4 Plate Heat Exchanger Model

Plate heat exchangers were used for the DHW heating, and for separating the district heating water from the radiator circulation water in the indirectly connected space heating systems. The heat exchanger consists of a series of parallel plates. Figure A.2.13 shows a diagram of the plate heat exchanger.

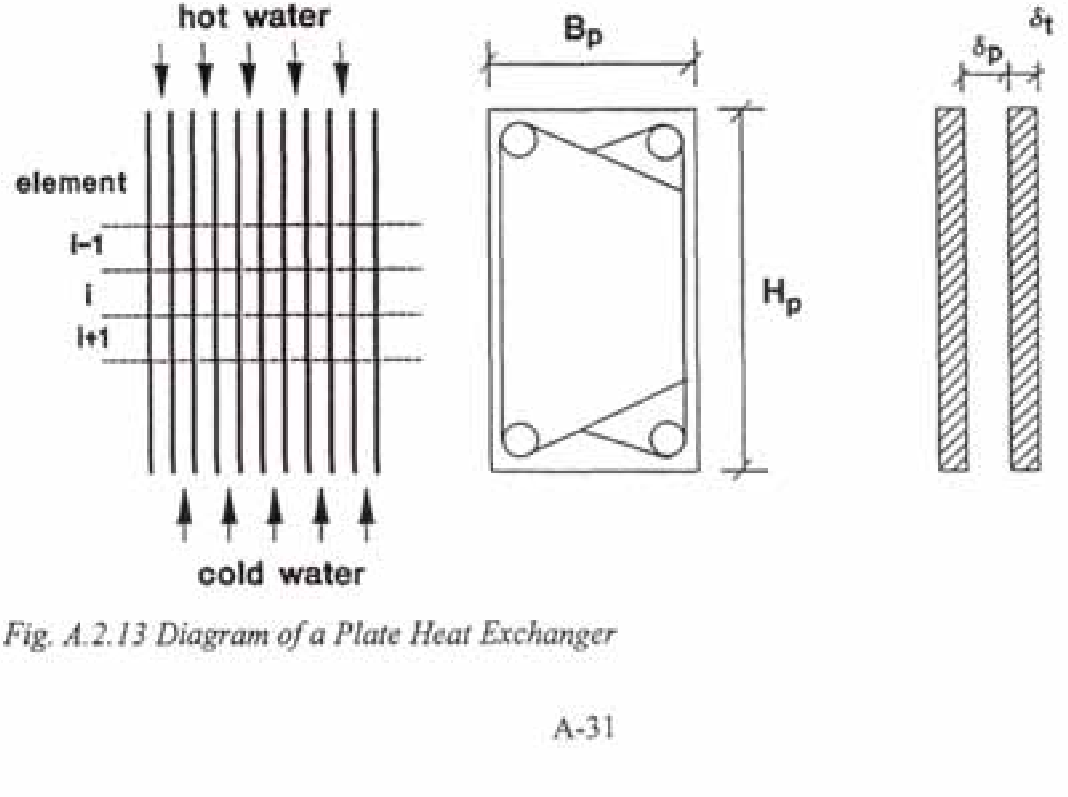

Fig. A.2.13 Diagram of a Plate Heat Exchanger

The model was based on general thermodynamic principles and previous work done by Gummérus (1990) and Hjorthol (1990). The assumptions used to simplify the mathematical description of the model were the same as those applied by Hjorthol (1990).

Mathematical description of the model

General energy balance equation of the hot water side for element i:

$$\frac{\partial(\rho_{hw}Cp_{hw}V_{hw}T_{hw}(i))}{\partial t} = f_{hw}\rho_{hw}Cp_{hw}(T_{hw}(i-1)-T_{hw}(i)) \\ -h_{hw}A_{hw}(T_{hw,m}(i)-T_{t}(i))$$

General energy balance equation of the cold water side for element i:

$$\frac{\partial(\rho_{cw}Cp_{cw}V_{cw}T_{cw}(i))}{\partial t} = f_{cw}\rho_{cw}Cp_{cw}(T_{cw}(i+1)-T_{cw}(i)) \\ -h_{cw}A_{cw}(T_{cw,m}(i)-T_{t}(i))$$

General energy balance equation of the plate wall for element i:

$$\frac{\partial(\rho_{t}Cp_{t}V_{t}T_{t}(i))}{\partial t} = h_{hw}A_{hw}(T_{hw,m}(i)-T_{t}(i))+h_{cw}A_{cw}(T_{cw,m}(i)-T_{t}(i))$$

where:

$$T_{hw,m}(i) = \frac{T_{hw}(i-1)+T_{hw}(i)}{2}$$

$$T_{cw,m}(i) = \frac{T_{cw}(i)+T_{cw}(i+1)}{2}$$

The symbols used in the above equations are shown in the nomenclature.

The heat transfer area of the hot water side and cold water side in each element is calculated by:

$$A_{hw} = A_{cw} = \frac{B_p H_p S N_p}{n}$$

The volume of the hot water and cold water in each element is determined by:

$$V_{hw} = V_{cw} = \frac{B_p \delta_p H_p S N_p}{2n}$$

The volume of the plate wall in each element is calculated by:

$$V_t = \frac{B_p H_p \delta_p N_p}{n}$$

where n is the number of elements used in the model, δ_t is the plate wall thickness and S is the plate shape factor.

Heat transfer coefficient

The heat transfer coefficients of the hot water side (h_{hw}) and of the cold water side (h_{cw}) are calculated from the typical dimensionless heat transfer equation:

$$Nu = \frac{h_w D_e}{\lambda_w} = C\,\mathrm{Re}^m\,\mathrm{Pr}^n$$

The parameters C, m and n are empirically evaluated. As stated in Slünder et al. (1983), it is impossible to give specific, accurate equations due to the great variation in plate performance.

Figure A.2.14 shows the inputs and outputs of the plate heat exchanger model in SIMULINK.

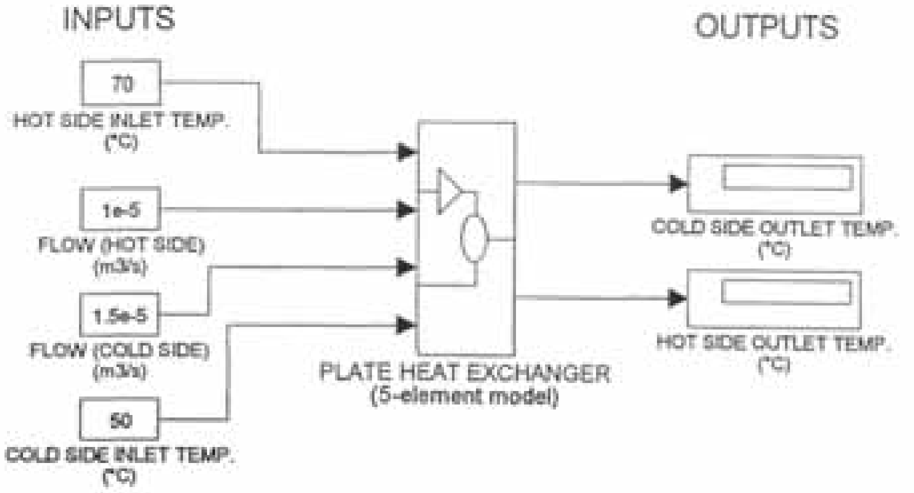

Fig. A.2.14 Plate heat Exchanger Input-Output Parameters,

Model Verification

Hjorthol (1990) has performed dynamic model verifications for a plate heat exchanger model similar to the one used in this report. He compared the simulations and measurements on an Alfa Laval heat exchanger (type CBH25 with 20 plates). Hjorthol (1990) found that the average temperature deviation was 2.1% on the cold side and was 0.5% on the hot water side. The parameters used for calculating the heat transfer coefficient in the simulation were 0.47, 0.63 and 0.39 for C, m and n respectively.

In the current study, Alfa Laval plate heat exchangers, type CB25 (similar to the one studied by Hjorthol (1990)), were used in the building heating systems of the apartment building and the row-house. Alfa Laval plate heat exchangers, type M6-FG, were used in the commercial building heating systems.

Static simulation results were compared to the data supplied by the manufacturer. Table A.2.3. shows the heat exchanger outlet temperatures and the overall heat transfer coefficients ("UA") obtained from the manufacturer ("A.L.") and from the simulation ("Simu"). The deviations of the outlet temperatures and "UA" are also shown in Table A.2.3. As stated previously, the parameters C, m and n used in the dimensionless heat transfer equation were empirically evaluated. The parameter values depend on the geometry of the plate. In the current simulations of type CB25 plate heat exchangers, values of C=0.46, m=0.63 and n=0.39 were used. Slightly different values were applied for type M6-FG (i.e. C=0.44, m=0.63 and n=0.39). Five elements were used in the model.

Table A.2.3 Comparison of Heat Exchanger Outlet Temperatures and Overall Heat Transfer Coefficients (UA) Provided by the Manufacturer (A.L.) and the Simulation (Simu).

Flow (l/s)	Hot Side Temp. (°C)				Cold Side Temp. (°C)				UA (W/°C)		
		Outlet		Devi.		Outlet		Devi.			Devi.
Hot / Cold	Inlet	A.L.	Simu	(%)	Inlet	A.L.	Simu	(%)	A.L.	Simu	(%)
CB25 (2-pass)											
0.25 / 0.25 (25 plates)	70	50.50	50.40	-0.51	45	64.50	64.56	0.31	6295	6463	2.67
0.14 / 0.14 (25 plates)	70	49.47	49.55	0.39	45	65.53	65.41	-0.58	4517	4479	-0.85
0.04 / 0.04 (25 plates)	70	39.26	39.39	0.42	35	65.74	65.56	-0.59	2055	1981	-3.59
M6-FG (1-pass)											
6.25 / 7.79 (62 plates)	80	54.80	54.55	0.99	50	69.90	70.36	2.31	90850	94830	4.40
4.15 / 5.17 (43 plates)	80	54.80	54.47	1.31	50	70.00	70.43	2.15	60280	63620	5.54

It appears from Table A.2.3 that the manufacturer's data and the SIMULINK predictions are comparable. The maximum temperature deviation was 1.31% on the hot side and 2.31% on the cold side. The maximum deviation in the overall heat transfer coefficient was 5.54%. This may result from the simplification of the model and lack of accurate geometry data of the heat exchangers.

A.2.5 Temperature Sensor Model

The temperature sensors can be modeled in many different ways. In Hjorthol (1990), three alternative solutions for modeling temperature sensors are given. The first is a model which only uses the sensor time constant; the second is a model which uses both time constant and pure time delay of the sensor; and the third is a discretized model which continuously calculates both the sensor time constant and the time delay. The third method can fit the process curve exactly, but requires exact knowledge of sensor geometry which is not always known. The second method gives satisfactory results and is especially applicable for sensors installed in sensor pockets where time delay is more pronounced. It was found that the first method with a fixed time constant describes the sensor performance in an acceptable manner, especially for thin sensors where the time delay is relatively small.

The first method was adopted in this study. The Transfer Function block in SIMULINK was applied directly to model the temperature sensor. The time constant of the temperature sensor was defined in the parameter "denominator".

A.2.6 Controller Model

Controllers consist of mathematical transformations of signals which will be fed to actuators. Input signals to a controller are induced by temperature sensors in the temperature control system. The control algorithms are of various types. In DH heat transfer stations PI or PID controllers are very common. Proportional controllers are also found in practice.

Although there is a standard block for a PID controller in SIMULINK, in this study proportional controllers were selected to regulate the flow rate in the building heating systems.

A.2.7 Actuator Model

The actuator is the engine which actually moves the control valve plug. The actuator speed and direction are determined by the control signal from the controller and the actuator dead band.

The SIMULINK "Rate Limiter" block was directly applied to model the actuator performance. The actuator dead band was not considered in the model.

A.2.8 Control Valve Model (2-port)

A control valve is the component governing the flow rate through a heat exchanger, radiator, etc. The characteristic of the valve $f_v(z)$ presents the manner that volume flow through the valves varies with stem position, and is defined by:

$$f_v(z) = \frac{f}{f_{max}}$$

Where f is volume flow rate through the control valve and f_{max} is the volume flow rate when valve is fully open.

The volume flow rate through the valve can be calculated by:

$$f = K_{vs} f_v(z) \sqrt{\Delta P_v \frac{\rho_o}{\rho_1}}$$

where:

K_{vs} = volume flow rate through fully open valve at 20°C and 1 bar, m^3/h
ΔP_v = pressure difference over the valve, bar
ρ_o = density of water at 20°C, kg/m^3
ρ_1 = density of water at actual temperature, kg/m^3

In the present study, it was assumed that all the control valves have a quadratic characteristic, i.e.:

$$f_v(z) = (1 - \frac{1}{R})z^2 + \frac{1}{R}$$

where

R = control ratio of the valve, i.e. the ratio between the maximum and minimum controllable flow rate at 1bar and 20°C.
z = valve position (0 = fully closed, 1 = fully open).

By assuming a constant density and a relatively high valve control ratio, the volume flow rate through the control valve then was simplified to the following expression:

$$f = K_{vs} \sqrt{\Delta P_v} z^2$$

It was also assumed that the pressure difference ΔP_v was constant. In physical systems, this is achieved by installing a pressure-difference regulator across the control valve.

A.2.9 Three-way Control Valve Model

The heating systems for the commercial building have a serial connection of the return water flow from the radiator system to the ventilation air heating coil (fan coil system). A three-way control valve is used in this serial connection. The flow in the fan coil system is regulated by a controller with the ventilation outlet air temperature as a control parameter. The three-way control valve model is based on previous work of Volla et al. (1996). Figure A.2.15 shows a detailed diagram of the three-way valve connection.

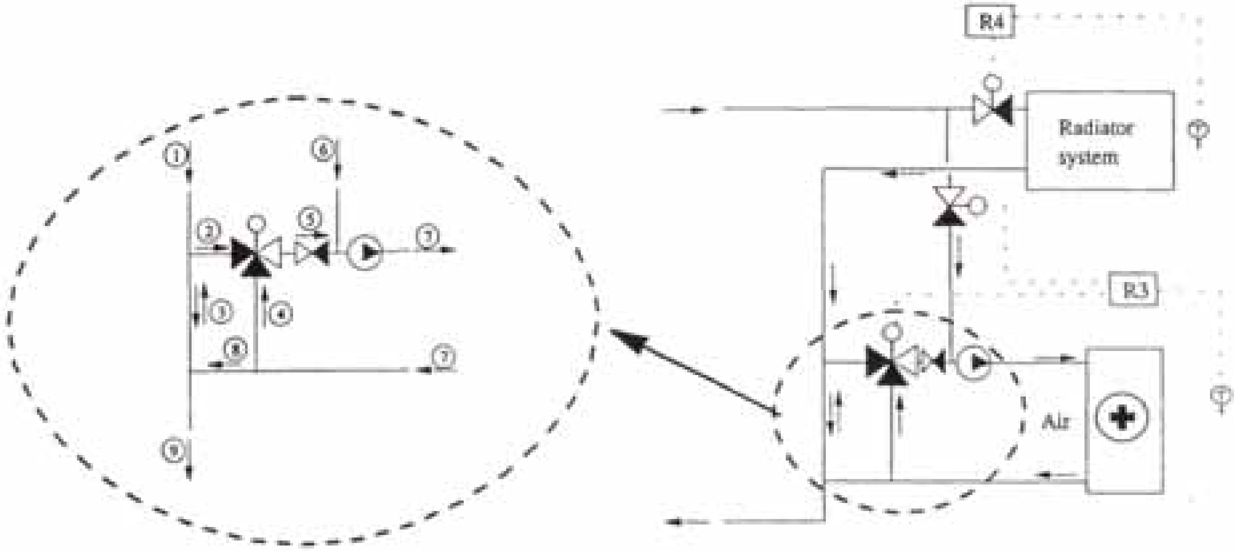

Fig. A.2.15 Three-way Valve Connection for the Radiator System and the Fan Coil System in Commercial Building Heating System. From Volla et al. (1996).

There are three operational modes for the fan coil heating system:

1. Serial connection of radiator system and fan coil system, where all of the water to the fan coil is supplied by the three-way mixing valve.

2. Mixed serial and parallel connection, where the water to the fan coil system is supplied by both the two-way and three-way valves. This occurs when the water from the radiator system alone is no longer sufficient to heat the ventilation air to the required temperature.

3. Parallel connection of radiator and fan coil system, where the total water to the fan coil system is supplied by the DH water. The return water from the radiator system bypasses the fan coil circuit.

Referring to Figure A.2.15, it was assumed that in operation modes 1 and 2, flow 7 in the fan coil circuit is determined by the circulation pump. It was also assumed that this flow was constant (f_{fan_cir}). In operation mode 3, the flow through the two-way valve f_6 has displaced flow 5, and the system works as a parallel connection. A further increase in flow 6 results in increase of flow 7, flow 8 and flow 9.

The flow through the three-way valve was defined by:

$$f_5 = f_{fan\_cir} - f_6 \qquad \text{(mode 1 and mode 2)}$$
$$f_5 = 0 \qquad (\text{mode } 3,\ f_6 > f_{fan\_cir})$$

The flow (f_2) through the control port of the three-way valve was calculated by:

$$f_2 = f_{v,3-way}(z) * f_5$$

where $f_{v,3-way}(z)$ is defined by the valve position and valve characteristic.

The flow (f_4) through the bypass port of the three-way valve was determined by:

$$f_4 = f_5 - f_2$$

The flow through the fan coil f_7 was given by:

$$f_7 = f_6 + f_5$$

where flow 6 was determined by the 2-way control valve characteristic and its position.

Flow 3 was either a bypass of the superfluous radiator flow (positive) or added to flow 2 (negative):

$$f_3 = f_1 - f_2$$

The flow returned from the fan coil system was:

$$f_8 = f_7 - f_4$$

The total flow return to the network was derived from:

$$f_9 = f_3 + f_8$$

As stated by Volla et al. (1996), the 3-way valve model can simulate the flow in the serial and parallel modes, as well as in the transition mode. However, the simplified approach to describe the changing pressure conditions in mixed mode operation may result in a small deviation between the calculated and observed valve position. For the current study, this simple model was deemed satisfactory.

A.2.10 Summary

The dynamic models for buildings, radiators, fan coils, plate heat exchangers, temperature sensors, controllers, actuators and control valves have been described in this section. Detailed model verifications have been carried out for buildings, radiators, fan coils and plate heat exchangers.

The outputs of the building model were compared to the data obtained from a DH heat transfer station at a school. The simulated power is in fairly good agreement with the measured one.

THOR plate radiators were selected to verify the radiator model. The simulated radiator outlet temperatures and heat outputs were compared with data obtained from the manufacturer's catalogue. The relative error was within ±6.2%. The results indicate that the radiator model gives acceptable accuracy.

The verification of the fan coil model was carried out by comparing the outlet temperatures from the SIMULINK model and from the steady state model developed by the University of Saskatchewan. The comparison shows that for a 4-row, 4-pass fan coil, the deviation between the two models was within ±5.3% on the air side and below 9% on the water side. The errors result mainly from the simple heat transfer coefficient correlation used in the SIMULINK model.

Laboratory tests were carried out for a small residential size fan coil. The heat outputs obtained from the measurements and the SIMULINK model were compared to those calculated by the manufacturer's steady state model. The results show that the measured values were 5.5 to 7% lower than the manufacturer's data. These were most likely due to errors in air velocity measurements.

The plate heat exchanger model was verified by comparing the outlet temperatures from the SIMULINK model to the outlet temperatures obtained from an Alfa Laval heat exchanger. The comparisons show that the maximum temperature deviation was 1.3% on the hot side and 2.3% on the cold side. The maximum deviation in the overall heat transfer coefficient was below 5.5%.

References

Grétarsson, S., Valdimarsson, P. and Jónsson, V. (1991): *"Heat Transfer Modelling of a Plate Radiator for District Heating Applications"*, International Journal of Energy Research, Vol. 15, pp.301-315, 1991.

Grimsrud, D. T., Sherman, M. H., Sonderegger, R. C. (1981): *"Infiltration Measurements in Audit and Retrofit Programs"*, Energy & Environment Division, Lawrence Berkeley Laboratory, University of California, Report No. LBL-12221, April 1981.

Gummérus, P. (1990): *"Analysis of Conventional District Heating House Stations"*, Ph.D Dissertation, Chalmers Technical University, Göteborg, Sweden, 1990. ISBN 91-7032-467-0.

Hjorthol, E. M. (1990): *"Optimization of Design Values in District Heating Substations by System Simulation"*, Ph.D Dissertation, Norwegian Institute of Technology, Trondheim, Norway, November 1990. ISBN 82-7199-230-2.

Hjorthol, E. M. and Ulseth, R. (1992): *"Consumer Heating System Simulation"*, IEA District and Cooling Project Report published by NOVEM, Sittard, The Netherlands, 1992.
ISBN 90-72130-32-4.

Holman, J.P. (1976): *"Heat Transfer"*, McGraw-Hill Book Company, 1976.
ISBN 0-07-029598-0.

Incropera, Frank P. and DeWitt, David P. (1996): *"Fundamentals of Heat and Mass Transfer"*, John Wiley & Sons, Inc., Fourth Edition, 1996. ISBN 0-471-30460-3.

Paulsen, O. (1991): *"Test of Small Gas Fired Boilers with Continuous Computer Simulated Load"*, Report on European Workshop Concerning Interaction between Heat Generators/Heating Systems and Buildings - Annual Efficiency for Domestic Boilers, Danish Technological Institute, June 1991.

Slünder, E.U. et al. (1983): *"Heat Exchanger Design Handbook"*, VDI-Verlag, 1983.

Volla, R., Ulseth, R. et al. (1996): *"Efficient Substations and Installations"*, SINTEF, the Norwegian Institute of Technology, IEA District Heating and Cooling Project Report published by NOVEM, Sittard, The Netherlands, 1996. ISBN 90-72130-88-X.

Zhu, P. (1987): *"Heat Exchanger and Calculation"*, Qinghua University, 1987.
ISSN 15235.290. (In Chinese).

Nomenclature

A_a	-	air side heat transfer area	m^2
A_{cw}	-	heat transfer area of the cold water side in plate heat exchanger	m^2
A_{hw}	-	heat transfer area of the hot water side in plate heat exchanger	m^2
A_{rc}	-	radiator convection heat transfer area	m^2
A_{rs}	-	radiator outside surface area	m^2
A_w	-	water side heat transfer area	m^2
B_p	-	width of plates in plate heat exchanger	m
C	-	constant used in the dimensionless heat transfer equations	
Cp_a	-	specific heat capacity of air	J/kg·°C
Cp_t	-	specific heat capacity of tube wall/plate wall	J/kg·°C
Cp_w	-	specific heat capacity of water	J/kg·°C
C_{rad}	-	total heat capacity of the radiator	J/°C
D_e	-	equivalent diameter	m
D_i	-	tube inner diameter	m
f	-	volumetric flow rate	m^3/s
f_a	-	actual air flow rate	m^3/s
$f_{air,nom}$	-	nominal air flow rate	m^3/s
f_{cw}	-	cold water flow rate in plate heat exchanger	m^3/s
f_{hw}	-	hot water flow rate in plate heat exchanger	m^3/s
fv(z)	-	valve characteristic	
f_w	-	volumetric flow rate of water	m^3/s
g	-	gravitational constant	m/s^2
Gr	-	Grashof number	
h_a	-	heat transfer coefficient at air side	W/ m^2·°C
h_{air}	-	air side heat transfer coefficient at actual air flow rate	W/m^2·°C
$h_{air,nom}$	-	air side heat transfer coefficient at nominal air flow rate	W/m^2·°C
h_{rc}	-	radiator convection heat transfer coefficient	W/ m^2·°C
h_{cw}	-	heat transfer coefficient at cold water side	W/ m^2·°C
h_{hw}	-	heat transfer coefficient at hot water side	W/ m^2·°C
h_w	-	heat transfer coefficient at water side	W/ m^2·°C
Hp	-	height of the plates in plate heat exchanger	m
k_a	-	thermal conductivity of ambient air	W/ m·°C
K_{vs}	-	volume flow rate through fully open valve at 20°C and 1 bar	m^3/h
L	-	effective leakage area	m^2
l_{rad}	-	characteristic length of radiator	m
L_t	-	total tube length of fan coil	m
m	-	exponent used in the dimensionless heat transfer equations	
n	-	exponent used in the dimensionless heat transfer equations	
n	-	number of elements	
Np	-	number of plates in plate heat exchanger	
N_t	-	total number of straight tubes per row of fan coils	
Nu	-	Nusselt number	
Pr	-	Prandtl number	
Ps	-	stack parameter	m^2/°C·s^2
Q	-	building infiltration rate	m^3/s

R	control ratio of the valve, i.e. the ratio between the maximum and minimum controllable flow rate at 1 bar and 20°C	
Ra	Rayleigh number	
R_{collar}	thermal resistance of fan coil collar	$m^2 \cdot °C/W$
Re	Reynolds number	
R_{wall}	thermal resistance of the tube wall	$m^2 \cdot °C/W$
S	shape factor of the plates in plate heat exchanger	
T_a	air temperature	°C
T_{cw}	cold side water temperature	°C
T_{hw}	hot side water temperature	°C
T_{room}	room temperature	°C
T_{rs}	radiator surface temperature	°C
T_t	temperature of tube wall/plate wall	°C
T_w	water temperature	°C
V_a	volume of air	m^3
V_{cw}	volume of hot water in plate heat exchanger	m^3
V_{hw}	volume of cold water in plate heat exchanger	m^3
V_t	volume of tube wall/plate wall	m^3
V_w	volume of water	m^3
z	valve position	
β	thermal expansion coefficient	1/K
δp	distance between plates	m
δt	thickness of plates	m
ε	emissivity	
η_{fin}	fan coil fin efficiency	
λ_w	thermal conductivity of water	$W/ m \cdot °C$
ν	kinematic viscosity	m^2/s
ρ_o	density of water at 20°C	kg/ m^3
ρ_1	density of water at actual temperature	kg/m^3
ρ_a	density of air	kg/ m^3
ρ_t	density of tube wall/plate wall	kg/ m^3
ρ_w	density of water	kg/ m^3
σ	Stefan-Boltzmann constant	$W/ m^2 \cdot K^4$
ΔPv	pressure difference over valve	bar
ΔT	indoor-outdoor temperature difference in the building model	°C
ΔT	logarithmic mean temperature difference,	°C

IEA District Heating and Cooling

Optimisation of Operating Temperatures and an Appraisal of the benefits of Low Temperature District Heating

Published by
Netherlands Agency for Energy and the Environment

Mailing address: P.O. Box 17, 6130 AA Sittard, the Netherlands
Street address: Swentiboldstraat 21, Sittard
Telephone: +31 46 4202020
Telefax: +31 46 4528260
Internet: www.novem.org
Internet: www.iea-dhc.org

1999: T1

ISBN-90-5748-010-7